

**JPL Publication 09-19**



# **NASA 2008 HypIRI Whitepaper and Workshop Report**

*HypIRI Group*

Prepared for  
**National Aeronautics and  
Space Administration**

by

**Jet Propulsion Laboratory  
California Institute of Technology  
Pasadena, California**

**May 2009**

---



**JPL Publication 09-19**

# **NASA 2008 HypSIIRI Whitepaper and Workshop Report**

*HypSIIRI Group*



Prepared for  
**National Aeronautics and  
Space Administration**

by

**Jet Propulsion Laboratory  
California Institute of Technology  
Pasadena, California**

---

**May 2009**

The work described in this publication was performed at a number of organizations, including the Jet Propulsion Laboratory, California Institute of Technology, under a contract with the National Aeronautics and Space Administration (NASA). Compiling and publication support was provided by the Jet Propulsion Laboratory, California Institute of Technology under a contract with NASA.

Reference herein to any specific commercial product, process, or service by trade name, trademark, manufacturer, or otherwise, does not constitute or imply its endorsement by the United States Government, or the Jet Propulsion Laboratory, California Institute of Technology.

Copyright 2009. All rights reserved.

## Abstract

From October 21-23, 2008, NASA held a three-day workshop to consider the Hyperspectral Infrared Imager (HyspIRI) mission recommended for implementation by the 2007 report from the U.S. National Research Council Earth Science and Applications from Space: National Imperatives for the Next Decade and Beyond, also known as the Earth Science Decadal Survey. The open workshop provided a forum to present the initial observational requirements for the mission and assess its anticipated impact on scientific and operational applications as well as obtain feedback from the broader scientific community on the mission concept.

The workshop participants concluded the HyspIRI mission would provide a significant new capability to study ecosystems and natural hazards at spatial scales relevant to human resource use. In addition, participants confirmed that the proposed instrument designs could meet the measurement requirements and be implemented through the use of current technology.

The workshop participants, like the Decadal Survey itself, strongly endorsed the need for the HyspIRI mission and felt the mission, as defined, would accomplish the intended science.

## Document Contacts

Many researchers provided Inputs for this workshop report. Readers seeking more information about particular details and contacting researchers in certain areas may access that information through the following two individuals.

- Simon J. Hook  
MS 183-503  
Jet Propulsion Laboratory  
4800 Oak Grove Dr.  
Pasadena, CA 91109  
Email: [Simon.J.Hook@jpl.nasa.gov](mailto:Simon.J.Hook@jpl.nasa.gov)  
Office: (818) 354-0974  
Fax: (818) 354-5148
- Bogdan V. Oaida  
MS 301-165  
Jet Propulsion Laboratory  
4800 Oak Grove Dr.  
Pasadena, CA 91109  
Email: [Bogdan.Oaida@jpl.nasa.gov](mailto:Bogdan.Oaida@jpl.nasa.gov)  
Office: (818) 354-5517  
Mobile: (626) 375-5398  
Fax: (818) 393-9815

## Preface

In 2004, the National Aeronautics and Space Administration (NASA), the National Oceanic and Atmospheric Administration (NOAA), and the U.S. Geological Survey (USGS) requested the National Research Council (NRC) identify and prioritize the satellite platforms and associated observational capabilities that should be launched and operated over the next decade for Earth observation. In addition to providing information for the purpose of addressing scientific questions, the committee identified the need to ensure that the measurements helped benefit society and provide policymakers with the necessary information to make informed decisions on future policies affecting the Earth.

The resulting NRC study *Earth Science and Applications from Space: National Imperatives for the Next Decade and Beyond*, also known as the Earth Science Decadal Survey, (NRC, 2007) recommended launching 15 missions in three time phases. These three time phases are referred to as Tier 1, Tier 2, and Tier 3, respectively. The Hyperspectral Infrared Imager (HypIRI) mission is one of the Tier 2 missions recommended for launch in the 2013–2016 timeframe. This global survey mission provides an unprecedented capability to assess how ecosystems respond to natural and human-induced changes. It will help us assess the status of biodiversity around the world and the role of different biological communities on land and within inland water bodies, as well as coastal zones and at reduced resolution in the ocean. Furthermore, it will help identify natural hazards; in particular volcanic eruptions and any associated precursor activity, and it will map the mineralogical composition of the land surface. The mission will advance our scientific understanding of how the Earth is changing as well as provide valuable societal benefit, in particular, in understanding and tracking dynamic events such as volcanoes and wildfires.

The HypIRI mission includes two instruments: a visible shortwave infrared (VSWIR) imaging spectrometer operating between 0.38 and 2.5  $\mu\text{m}$  at a spatial scale of 60 m with a swath width of 145 km and a boresighted thermal infrared (TIR) multispectral scanner operating between 4 and 12  $\mu\text{m}$  at a spatial scale of 60 m with a swath width of 600 km. The VSWIR and TIR instruments have revisit times of 19 and 5 days, respectively. Several of the other Tier 1 and Tier 2 missions provide complementary measurements for use with HypIRI data, in particular, the DESDynI, ACE, ICESat-II, and GEO-CAPE Decadal Survey missions each of which addresses very different spatial scales compared to the local and landscape scales observable with HypIRI. While the synergy between HypIRI and other sensors, including those on operational satellites, benefits all missions and would support relevant scientific endeavors, the ability of HypIRI to achieve its primary mission goals is not dependent on data from these other instruments.

This report documents a NASA-sponsored three-day workshop held in Monrovia, California, in October 2008 to refine the scientific questions, objectives, and requirements of the HypIRI mission and to identify priority near-term investments to mature the HypIRI concept towards a possible Mission Concept Review (MCR) at the end of 2009. Initially, some background on the NRC Decadal Survey is provided, and this is followed by a discussion of the science, measurement requirements, instrument requirements, and associated mission activities as presented and discussed at the workshop, along with recommendations for future activities.

## Executive Summary

NASA held a three-day workshop on October 21–23, 2008 to consider the Hyperspectral Infrared Imager (HyspIRI) mission recommended for implementation by the 2007 NRC Earth Science Decadal Survey (DS, 2007). The workshop was open to the research community as well as members of other communities with an interest in the HyspIRI mission. It provided a forum for the HyspIRI Science Study Group (SSG) to present their initial observational requirements and assess the anticipated impact of HyspIRI on their scientific and operational applications and obtain feedback from the broader scientific community.

As part of the ongoing preparatory studies for the HyspIRI mission, the SSG has developed sets of measurement requirements tied to addressing a particular set of science questions. These requirements together with those already provided by the Decadal Survey formed the basis for the overall instrument and mission requirements presented at the workshop. Workshop participants evaluated the instrument and mission requirements in the context of the science questions, and they identified ancillary measurements that might be required to address these questions. Breakout sessions provided a forum for participants to review the science questions, as well as measurement requirements, and to suggest additional opportunities for enhanced science or applications that might be achieved through synergies with other planned missions and/or with augmentations to the current mission.

Several key conclusions resulted from the workshop:

- HyspIRI provides a unique capability to address a set of specific scientific questions about local and global ecosystems, habitats, biodiversity, and hazards and their response to anthropogenic or natural changes.
- HyspIRI will help integrate terrestrial and aquatic (inland, coastal, and oceanic) ecosystem studies, and allow assessments at spatial scales relevant to resource use by humans.
- The instrument design is capable of meeting the scientific measurement requirements.
- There is a stable set of instrument measurement requirements for HyspIRI, and these requirements are traceable to the science questions for the mission.
- Significant heritage exists from both a design and risk-reduction standpoint for both instruments. This heritage includes missions such as the Moon Mineralogy Mapper and the Advanced Spaceborne Thermal Emission and Reflection Radiometer as well as the associated algorithms to deliver the Level 0 through Level 2 data products.
- There do not appear to be any significant technology “show stoppers,” and the mission is ready for implementation at the earliest opportunity.
- HyspIRI complements measurements from the DESDynI, ACE, and GEO-CAPE missions, each of which addresses very different spatial scales compared to the local and landscape scales observable with HyspIRI.

The research community, like the Decadal Survey, strongly endorsed the need for the HyspIRI mission. There was a strong consensus that the HyspIRI mission, as defined, would accomplish the intended science.

## Contents

<b>Abstract</b> .....		<b>iii</b>
<b>Document Contacts</b> .....		<b>iii</b>
<b>1 Introduction</b> .....		<b>1-1</b>
1.1 The Decadal Survey .....		1-1
1.2 The HyspIRI Workshop.....		1-1
<b>2 Science and Societal Benefits</b> .....		<b>2-1</b>
2.1 Overarching Thematic Topics.....		2-1
2.1.1 VQ1 - Pattern and Spatial Distribution of Ecosystems .....		2-1
2.1.2 VQ2 - Ecosystem Function, Physiology and Seasonal Activity .....		2-4
2.1.3 VQ3 - Biogeochemical Cycles .....		2-5
2.1.4 VQ4 - Ecosystem Response to Disturbance.....		2-6
2.1.5 VQ5 - Ecosystems and Human Well-being .....		2-7
2.1.6 VQ6 - Surface and Shallow-Water Bottom Composition .....		2-10
2.1.7 TQ1 - Volcanoes and Earthquakes.....		2-10
2.1.8 TQ2 - Wildfires .....		2-12
2.1.9 TQ3 - Water Use and Availability .....		2-13
2.1.10 TQ4 - Human Health and Urbanization .....		2-14
2.1.11 TQ5 - Earth Surface Composition and Change.....		2-15
2.1.12 CQ1 - Coastal, Ocean, and Inland-Aquatic Environments .....		2-16
2.1.13 CQ2 - Wildfires .....		2-18
2.1.14 CQ3 - Volcanoes .....		2-18
2.1.15 CQ4 - Ecosystem Function and Diversity .....		2-20
2.1.16 CQ5 - Land Surface Composition and Change .....		2-21
2.1.17 CQ6 - Human Health and Urbanization .....		2-22
2.2 Science Traceability Matrices.....		2-23
<b>3 Measurement Requirements</b> .....		<b>3-1</b>
3.1 VSWIR Instrument .....		3-1
3.2 TIR Instrument.....		3-1
<b>4 Mission Concept</b> .....		<b>4-1</b>
<b>5 Data Products and Algorithms</b> .....		<b>5-1</b>
<b>6 Synergies</b> .....		<b>6-1</b>
6.1 VSWIR/TIR Instruments .....		6-1
6.2 Other Missions and Programs .....		6-1
<b>7 Conclusions and Recommendations</b> .....		<b>7-1</b>
<b>8 References</b> .....		<b>8-1</b>
<b>9 Appendices</b> .....		<b>9-1</b>
Appendix A – Acronyms .....		9-1
Appendix B - Workshop Agenda.....		9-4
Appendix C – List of Participants.....		9-6
Appendix D – Science-Traceability Matrices.....		9-9

## Figures

- Figure 1: Species-level map of the Santa Ynez Front Range mapped using 20-m AVIRIS data. (Adapted from Dennison and Roberts, 2003a) ..... 2-4
- Figure 2: Presence of *Microcystis* bloom in the Sacramento-San Joaquin delta captured in hyperspectral imagery June 2007. .... 2-4
- Figure 3: Canopy Nitrogen, Carbon Assimilation, and Albedo in Temperate and Boreal Forests (Ollinger et al. 2008) 2-6
- Figure 4: Maps of canopy cover, nitrogen and water (panels to the left) derived from imaging spectroscopy were used to map highly invasive trees (upper right; red) in a Hawaiian rainforest. A biogeochemical model then showed increased nitrogen gas fluxes from the soils beneath the invader (Asner and Vitousek 2005). .... 2-7
- Figure 5: Watershed-scale ecosystem responses to disturbance. Disturbance is measured using MODIS imagery (X-axis) and Landsat (panel C), illustrating an inverse response stream nitrogen (A) and foliar nitrogen (B), as derived from Hyperion. (McNeil et al. (2007). .... 2-8
- Figure 6: Map of surface rock and soil mineralogy at Cuprite, NV using solar reflected imaging spectroscopy measurements from 380 to 2500 nm. (Left: AVIRIS image cube, Center: 1 micron region minerals, Right: 2 micron region minerals) (Swayze et al. 2003)..... 2-10
- Figure 7: (a) ASTER night-time multispectral TIR image of Augustine Volcano showing hot pyroclastic flow deposits (bright in TIR) and eruption plume. Colors indicate spectral variations between materials entrained in plume. Magenta indicates mixtures of water droplets (steam) and silicate ash; red, yellow, and orange indicate mixtures of ash and SO<sub>2</sub>. (b) SO<sub>2</sub> map derived from ASTER TIR data. (c) Thermal infrared anomaly associated with the M6.4 Zarand, Iran earthquake of Feb. 22, 2005, as derived from night-time Advanced Very High Resolution Radiometer (AVHRR) images recorded prior to this event (after Saraf et al. 2008). The excess IR intensity emitted from the epicentral region (presented in yellow-orange colors), and 10K temperature increase, are proposed to be indicators of the build-up of stress at the hypocenter. Lower right: Location of the epicenter (star) relative to the region of maximum uplift (red: 25 cm) and subsidence (blue: 17 cm) from Interferometric Synthetic Aperture Radar (InSAR) data. .... 2-11
- Figure 8: False-color ASTER image of a large fire in southern Africa, acquired on 17 August 2001, with the 2.4, 1.6, and 0.5  $\mu\text{m}$  bands shown as red, green, and blue, respectively. With this color scheme the actively burning fire front appears yellow to red, previously-burned areas appear black, and unburned vegetation appears green. The specialized 4-micron channel of the HypSIRI thermal sensor will not exhibit the saturation-induced blooming apparent along the more intense portions of the flaming front in this scene. .... 2-12
- Figure 9: Multi-scale ET maps for 1 July 2002 produced with the ALEXI/DisALEXI surface energy balance models (Anderson, et al. 2007) using surface temperature data from aircraft (30-m resolution), Landsat-7 ETM+ (60m), Terra MODIS (1-km), GOES Imager (5-km) and GOES Sounder (10-km) instruments. The continental-scale ET map is a 14-day composite of clear-sky model estimates. .... 2-13
- Figure 10: Landsat TM data of the Atlanta, GA metropolitan area showing urban extent in gray (bottom) and corresponding surface thermal responses (top) (Quattrochi et al. 2009) ..... 2-15
- Figure 11: HypSIRI-like image for the area around Lake Mead, Nevada. Three TIR bands are processed with a decorrelation stretch algorithm and displayed in red, green and blue, respectively (from Hook et al. 2005). ... 2-16
- Figure 12: Weight-specific absorption coefficients ( $\text{m}^2 \text{mg}^{-1}$ ) derived for the major pigment types found in marine phytoplankton (from Bidigare et al. 1989). .... 2-17
- Figure 13: Top panel: Retrieved fire temperature (in kelvins) from an AVIRIS scene spanning a portion of the large Southern California Fire Complex from October 2003. Bottom panel: False color SWIR-NIR-red composite of the original AVIRIS scene. (Dennison et al. 2006). .... 2-18
- Figure 14: Hyperion SWIR image of Erta Ale volcano, Ethiopia, showing the active lava lake. Hyperspectral VSWIR and TIR data will allow the cooling rate and gas flux from the lake to be determined. Right: model of cooling and degassing-driven magma convection within an open system volcano. The heat and gas flux data are important boundary conditions for determining magma ascent dynamics and circulation within the conduit (adapted from Frances et al. 1993). .... 2-19
- Figure 15: Map of *Bromus tectorum* (Cheatgrass) generated using imaging spectrometry. Cheatgrass spreads through a combination of disturbance and strategic use of soil moisture. It alters fire regimes, promoting its spread while early germination of Cheatgrass enables it to produce seed in advance of native plants while reducing available water for competitors. (Noujdina and Ustin 2008). .... 2-20

Figure 16: False color composite HypsIRI simulated image of Grand Canyon, Arizona derived from TIR (red band - quartz-rich rocks), SWIR (green band - clay and muscovite-rich rocks; blue band - carbonate-rich rocks), and VNIR (dark green - green vegetation) data.....2-21

Figure 17: Temperature and albedo measurements for the Atlanta, GA central business district as derived from multispectral aircraft data (Quattrochi et al. 2009).....2-23

Figure 18: Process for developing the Science-Traceability Matrixes. ....2-23

Figure 19: HypsIRI-VSWIR Key Signal-to-Noise and Uniformity Requirements. ....3-1

Figure 20: Number of image acquisitions in 19 days. ....4-1

Figure 21: Illustration of the Sun illumination at the winter solstice.....4-1

## Tables

Table 1: Overarching Thematic Science Questions.....2-2

Table 2: VQ1 Thematic Subquestions .....2-3

Table 3: VQ2 Thematic Subquestions .....2-5

Table 4: VQ3 Thematic Sub Questions .....2-5

Table 5: VQ4 Thematic Subquestions .....2-6

Table 6: VQ5 Thematic Sub Questions .....2-8

Table 7: VQ6 Thematic Sub Questions .....2-10

Table 8: TQ1 Thematic Subquestions .....2-11

Table 9: TQ2 Thematic Subquestions .....2-13

Table 10: TQ3 Thematic Subquestions .....2-14

Table 11: TQ4 Thematic Subquestions .....2-15

Table 12: TQ5 Thematic Subquestions .....2-15

Table 13: CQ1 Thematic Subquestions .....2-17

Table 14: CQ2 Thematic Subquestions .....2-18

Table 15: CQ3 Thematic Subquestions .....2-19

Table 16: CQ4 Thematic Subquestions .....2-21

Table 17: CQ5 Thematic Subquestions .....2-22

Table 18: CQ6 Thematic Subquestions .....2-22

Table 19: VSWIR Measurement Characteristics .....3-2

Table 20: TIR Measurement Characteristics .....3-3

Table 21: HypsIRI Data Volume, includes illumination constraints for VSWIR, compression and overhead. ....4-2

## 1 Introduction

### 1.1 The Decadal Survey

In 2004, NASA, NOAA, and the USGS commissioned the National Research Council to conduct a Decadal Survey (DS) for Earth science and applications from Space. The 2007 report from that survey is titled: *Earth Science and Applications from Space: National Imperatives for the Next Decade and Beyond*. The objective of the survey was to generate consensus recommendations from the Earth and environmental science and applications communities regarding an integrated approach to future space-based and ancillary observations.

The NRC appointed a committee to undertake the Decadal Survey. The committee participated in—and synthesized work from—seven thematically organized study panels:

- 1) Earth-science applications and societal benefits;
- 2) Land-use change, ecosystem dynamics, and biodiversity;
- 3) Weather;
- 4) Climate variability and change;
- 5) Water resources and the global hydrologic cycle;
- 6) Human health and security and
- 7) Solid-Earth hazards, resources, and dynamics.

Each of these thematic areas identified key science measurements, justified these measurements, and recommended a small number of missions. The Decadal Survey committee consolidated the recommendations from each theme into a short list of prioritized missions. Included in this list as a high priority was the Hyperspectral Infrared Imager (HyspIRI) mission, which would provide global observations of multiple key surface attributes at local and landscape spatial scales

(tens of meters to hundreds of kilometers) for a wide array of Earth-system studies, including integrating assessments of local and landscape changes key to understanding biodiversity in both terrestrial and aquatic (inland, coastal, and oceanic) ecosystems, measuring the condition and types of vegetation on the Earth's surface, and changes in the mineralogical composition of the surface in order to understand the distribution of geologic materials. The mission would help map volcanic gases and surface temperatures, which were identified as indicators of impending volcanic hazards, as well as plume ejecta which pose risks to aircraft and people and property downwind.

The committee recommended that HyspIRI be launched in the 2013–2016 timeframe and include a hyperspectral visible-shortwave infrared (VSWIR) imaging spectrometer and a multispectral thermal infrared (TIR) scanner. The mission would provide global coverage from low Earth orbit with a high temporal frequency, especially in the case of the TIR instrument, which would have a revisit time of 6 days or less.

The NRC Decadal Survey participants recognized that both instruments had strong spaceborne heritage through the Hyperion Instrument on the Earth Observing-1 (EO-1) platform, the Moon Mineralogy Mapper (M3) instrument on the Chandrayaan-1 platform and the Advanced Spaceborne Thermal Emission and Reflection Radiometer (ASTER) instrument on the Terra platform.

### 1.2 The HyspIRI Workshop

The HyspIRI workshop was held on October 21–23, 2008 in Monrovia, California and was open to all interested parties (US and international). The goals of the workshop were to confirm and clarify the science requirements for the HyspIRI mission and to

provide an open forum for community participation in early planning activities. The agenda sought to introduce participants to the Decadal Survey and associated activities at NASA Headquarters and then provide the measurement requirements for HypsIRI. Next, a series of science presentations and breakout groups on the HypsIRI science questions and associated science traceability matrices led to the refinement of the science traceability matrices, which directly link the science questions to instrument and mission requirements. There were also presentations on technology needs and partnership opportunities and discussions of next steps (see Appendix B for the workshop Agenda). Approximately 150 people participated in the workshop from academia and industry including several international participants from Australia, Canada, Japan, and Europe. Presentations given by NASA and academia addressed key aspects of the mission with additional time for open discussion when appropriate. All the oral presentations can be found on the HypsIRI website at: <http://hyspiri.jpl.nasa.gov>. All workshop participants were encouraged to discuss and refine the mission science goals and methods to maximize the scientific return from the data.

The morning of the first day, the workshop focused on providing background information on the Decadal Survey and NASA's approach to the HypsIRI mission, followed by descriptions of the measurement requirements provided by the Decadal Survey and subsequently reviewed by the HypsIRI Science Study Group (SSG). The SSG is a group of scientists assembled in advance of the workshop by NASA to represent the scientific community and domestic agencies interested in HypsIRI data including the NASA centers. Terrestrial and marine ecologists, geologists, and atmospheric scientists participated in this group. They refined the measurement requirements laid out

in the Decadal Survey to ensure they represented the needs of the scientific community. Doing so involved developing a set of science questions for the two instruments (VSWIR and TIR) and an associated set of science traceability matrices (STMs). The STMs trace each measurement requirement back to a science question(s).

In the late morning and afternoon of the first day, presentations and breakouts focused on the VSWIR instrument. The breakouts worked through both the science questions and the STMs to make sure they were clearly articulated.

The second day began with a discussion of potential airborne precursor activities for HypsIRI. The goal of these discussions was to identify how best to put together simulated HypsIRI data from airborne instrument data, which could subsequently be used for algorithm development. Later that day, participants reviewed the science questions and STMs for the TIR instrument. Again, work focused on ensuring the TIR science questions were clearly articulated and the measurement requirements understood. The end of the second day saw a series of presentations on the potential for advanced technologies to optimize the HypsIRI mission. Of particular interest was inclusion of a direct broadcast system on HypsIRI together with an Intelligent Payload Module, which would allow the download of selected bands and band combinations in near realtime.

The third day of the workshop included a review of the science questions and traceability matrixes for the combined science questions. The combined science questions are questions requiring the use of data from both instruments (VSWIR and TIR). The participants felt these questions were particularly interesting and offered a clear demonstration of synergies arising from,

acquiring data from both instruments simultaneously.

In the afternoon of the last day, participants revisited the measurement requirements for both VSWIR and TIR instruments in light of discussions on previous days and highlighted those areas requiring further study. They noted that both sets of instrument requirements were mature and well matched to the science the instruments would address. Potential opportunities for domestic and international partnerships were the subject of another talk that afternoon. Several agencies expressed interest in the mission, ranging from roles in the distribution of the data products to upgrading foreign ground stations for additional downlink capability. The workshop's final presentation focused on next steps and is described in the subsequent section on conclusions and recommendations.

The remainder of this report is organized as follows. Section 2 presents the science behind the mission and provides top-level questions followed by overarching thematic questions and thematic sub-questions (Table 1 through Table 18 contain these questions).

The subsections address the science underlying these questions. The Science section includes the STMs, which focus on the more detailed sub-level questions. (Appendix D contains the STMs.) Section 3 discusses the measurement requirements that grow from the STMs and the framework provided by the Decadal Survey. Section 4 outlines the Mission Concept, in particular the baseline operations concept. Section 5 provides a preliminary discussion of the expected data products and algorithms. Section 6 explores synergies with other instruments and partnerships. This section is expected to expand as the HypsIRI mission and other Decadal Survey missions mature. Finally, Section 7 provides a set of conclusions and recommendations based on the workshop. A series of appendices offer a list of acronyms, the workshop agenda, a list of workshop participants, and the STMs.



## 2 Science and Societal Benefits

The HypsIRI mission is science driven. In other words, one can trace back the measurement requirements for the mission to a particular science question. HypsIRI has three top-level science questions related to 1) Ecosystem function and composition, 2) Volcanoes and natural hazards, and 3) Surface composition and the sustainable management of natural resources. The NRC Decadal Survey called out these three areas. The top-level science questions for the HypsIRI mission are:

### **Ecosystem function and composition**

What is the global distribution and status of terrestrial and coastal-aquatic ecosystems and how are they changing?

### **Volcanoes and natural hazards**

How do volcanoes, fires, and other natural hazards behave; and do they provide precursor signals that can be used to predict future activity?

### **Surface composition and sustainable management of natural resources**

What is the composition of the land surface and coastal shallow water regions, and how can they be managed to support natural and human-induced change?

These questions provide a scientific framework for the HypsIRI mission. NASA appointed the HypsIRI Science Study Group (SSG) to refine and expand these questions to a level of detail that was sufficient to define the measurement requirements for the HypsIRI mission. In 2007, the first SSGs were formed, and there was a separate SSG for each instrument (VSWIR and TIR). These groups were then merged in 2008, their overall membership re-assessed, and the HypsIRI SSG formed.

The SSG developed a more detailed set of overarching thematic questions that

were separated into three groups. The first two groups deal with overarching questions that may be addressed by only one of the two instruments. The third group requires data from both instruments. All three groups may require supporting measurements from other instruments, whether spaceborne, airborne, or ground. The three question groups are referred to as the 1) VSWIR questions (VQ), 2) TIR questions (TQ) and 3) Combined questions (CQ), respectively (Table 1). Within each of these overarching thematic questions, there are a set of thematic subquestions, and it is these subquestions that provide the necessary detail to understand the measurement requirements (Table 2 through Table 18). Section 2.1 below provides a summary of the science behind each of the overarching thematic questions.

## **2.1 Overarching Thematic Topics**

### **2.1.1 VQ1 - Pattern and Spatial Distribution of Ecosystems**

Terrestrial and aquatic ecosystems represent an assemblage of biological and non-biological components and the complex interactions among them, including cycles and/or exchanges of energy, nutrients, and other resources. The biological components span multiple trophic levels and range from single-celled microbial organisms to higher order organisms, including vegetation in forests and grasslands, and in coastal and other aquatic environments, as well as animals. In many ecosystems, a dominant or keystone species is critical in how that system functions. Because of their abundance and geographic extent, plant or phytoplankton communities provide distinct characteristics to habitats and ecosystems, and these are visible from great distances, including from space.

**Table 1: Overarching Thematic Science Questions**

Question #	Area	Question	Lead and Co-Lead
VQ1	Pattern and Spatial Distribution of Ecosystems and their Components	What is the global spatial pattern of ecosystem and diversity distributions, and how do ecosystems differ in their composition or biodiversity?	Roberts, Middleton
VQ2	Ecosystem Function, Physiology, and Seasonal Activity	What are the seasonal expressions and cycles for terrestrial and aquatic ecosystems, functional groups, and diagnostic species? How are these being altered by changes in climate, land use, and disturbance?	Gamon
VQ3	Biogeochemical Cycles	How are the biogeochemical cycles that sustain life on Earth being altered/disrupted by natural and human-induced environmental change? How do these changes affect the composition and health of ecosystems, and what are the feedbacks with other components of the Earth system?	Ollinger
VQ4	Changes in and Responses to Disturbance	How are disturbance regimes changing, and how do these changes affect the ecosystem processes that support life on Earth?	Asner, Knox
VQ5	Ecosystem and Human Health	How do changes in ecosystem composition and function affect human health, resource use, and resource management?	Townsend, Glass
VQ6	Earth Surface and Shallow-Water Substrate Composition	What is the land surface soil/rock and shallow-water substrate composition?	Green, Dierssen
TQ1	Volcanoes and Earthquakes	How can we help predict and mitigate earthquake and volcanic hazards through detection of transient thermal phenomena?	Abrams, Freund
TQ2	Wildfires	What is the impact of global biomass burning on the terrestrial biosphere and atmosphere, and how is this impact changing over time?	Giglio
TQ3	Water Use and Availability	How is consumptive use of global freshwater supplies responding to changes in climate and demand, and what are the implications for sustainable management of water resources?	Anderson, Allen
TQ4	Urbanization and Human Health	How does urbanization affect the local, regional, and global environment? Can we characterize this effect to help mitigate its impact on human health and welfare?	Quattrochi, Glass
TQ5	Surface Composition and Change	What is the composition and temperature of the exposed surface of the Earth? How do these factors change over time and affect land use and habitability?	Prakash, Mars
CQ1	Coastal, ocean, and inland aquatic environments	How do inland, coastal, and open-ocean aquatic ecosystems change due to local and regional thermal climate, land-use change, and other factors?	Muller-Karger,
CQ2	Wildfires	How are fires and vegetation composition coupled?	Giglio,
CQ3	Volcanoes	Do volcanoes signal impending eruptions through changes in the temperature of the ground, rates of gas and aerosol emission, temperature and composition of crater lakes, or health and extent of vegetation cover?	Wright, Realmuto
CQ4	Ecosystem Function and Diversity	How do species, functional type, and biodiversity composition within ecosystems influence the energy, water, and biogeochemical cycles under varying climatic conditions?	Roberts, Anderson
CQ5	Land surface composition and change	What is the composition of the exposed terrestrial surface of the Earth, and how does it respond to anthropogenic and non anthropogenic drivers?	Mars, Prakash
CQ6	Human Health and Urbanization	How do patterns of human environmental and infectious diseases respond to leading environmental changes, particularly to urban growth and change and the associated impacts of urbanization?	Quattrochi, Glass

In diverse ecosystems, often suites of plant or phytoplankton species can be organized into assemblages of organisms with similar form and function, defined as plant functional types (PFTs) or functional groups (FGs). Dominant vegetation types or PFTs that capture the major features of an ecosystem are often amenable to detection via remote sensing.

The distribution of terrestrial and aquatic ecosystems across the Earth is largely controlled by climate, modified by surface elevation, substrate, oceanic and atmospheric circulation, and a number of other factors. Anthropogenic disturbance, primarily in the form of land-cover conversion and, at larger scales, climate change has imposed increasing pressures on Earth's ecosystems. Remote sensing represents perhaps the only viable approach for mapping the current distribution of these ecosystems globally, monitoring their status and improving our understanding of feedbacks among modern ecosystems, climate and disturbance.

At the finest scales, spectral reflectance is largely governed by the concentration of pigments (primarily chlorophylls and carotenoids), important biochemicals (such as cellulose, lignin, starch and water), and the arrangement of internal structures (Gates et al., 1965; Curran 1989) and surface features (waxes and hairs). Scaling up to plant canopies on land or assemblages of marine organisms, spectral reflectance is governed by the arrangement of components (branches, leaves, and trunks on land, and depth and density in a marine environment) and the manner in which multiple scattering and shadowing modify reflectance (Asner, 1998; Hochberg and Atkinson, 2003; Roberts et al., 2004). To the extent that fine-scale chemistry and anatomy and coarser scale structure uniquely define a species or PFT/FG, remote sensing can map the distribution of these organisms and be

used to monitor their response to disturbance and environmental change.

Unique seasonal changes in biochemistry and structure offer additional leverage for discriminating individual species.

**Table 2: VQ1 Thematic Subquestions**

ID	Question
VQ1a	How are ecosystems organized within different biomes associated with temperate, tropical, and boreal zones; and how are these changing?
VQ1b	How do similar ecosystems differ in size, species composition, fractional cover and biodiversity across terrestrial and aquatic biomes and on different continents?
VQ1c	What is the current spatial distribution of ecosystems, functional groups, or key species within major biomes including agriculture, and how are these being altered by climate variability, human uses, and other factors?
VQ1d	What are the extent and impact of invasive species in terrestrial and aquatic ecosystems?
VQ1e	What is the spatial structure and species distribution in a phytoplankton blooms?
VQ1f	How do changes in coastal morphology and surface composition impact coastal ecosystem composition, diversity and function?

Within a region, the unique spectral signatures of plants have been used to discriminate and map dominant plant species and PFTs. Dennison and Roberts (2003a), used the Airborne Visible Infrared Imaging Spectrometer (AVIRIS) to map dominant plant species in the fire prone Front range of the Santa Ynez Mountains (Figure 1). The ability to discriminate plant species was also found to depend significantly on season of acquisition, defined in this area by a change in soil water balance (Dennison and Roberts, 2003b).

Comparisons between broadband sensors, Hyperion and high fidelity AVIRIS data, demonstrated significant improvements in species-level discrimination using imaging spectrometry. The link between spectroscopy, biochemistry, and biodiversity may also be expressed in the spectral diversity within an ecosystem. For example, Carlson et al. (2007) demonstrated a strong link between field-

measured species diversity in Hawaii and spectral diversity mapped using AVIRIS.

HypSIRI, as a high-fidelity imaging spectrometer with a 19-day repeat pass, has the potential for dramatically improving our ability to identify PFTs/FGs, quantify species diversity, discriminate plant and phytoplankton species, and map their distribution in terrestrial and coastal environments.

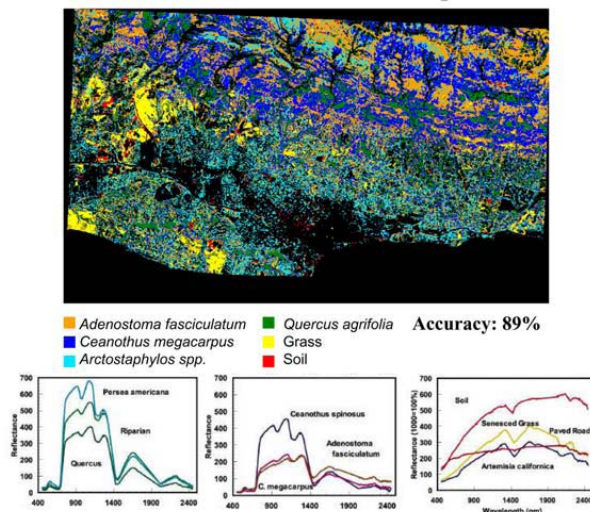


**Figure 1: Species-level map of the Santa Ynez Front Range mapped using 20-m AVIRIS data. (Adapted from Dennison and Roberts, 2003a)**

**2.1.2 VQ2 - Ecosystem Function, Physiology and Seasonal Activity**

Vegetation dynamics express themselves across a wide range of time scales from diurnal to inter-annual. Although we well understand broad phenological patterns such as leaf emergence, more subtle patterns of vegetation activity reflecting underlying physiological dynamics are less well known and require the unique hyperspectral capabilities and frequent repeat cycles provided by HypSIRI. Improved assessment of vegetation pigment levels can improve models of carbon exchange and identify periods of stress and reduced photosynthetic activity. For example, xanthophyll cycle

pigments, chlorophyll/carotenoid ratios, or anthocyanin levels—all indicators of physiological state—can only be characterized by the fine spectral resolution provided by hyperspectral sensors (Ustin et al. 2004). Similarly, narrow water-absorption features provide subtle indicators of water content and evapotranspiration (Serrano et al. 2002, Fuentes et al. 2006, Claudio et al. 2006), key physiological variables critical to surface energy balance and climate regulation. Furthermore, expressions of physiological dynamics and biochemistry vary across species and functional types, and provide novel ways to characterize biological diversity from remote sensing (Gamon et al. 2005, Carlson et al. 2007), particularly when combined with frequent repeat cycles that capture key phenological events (such as leaf out, flowering, and senescence). This combination of numerous cycles with narrow spectral bands will also be useful in capturing certain short-lived or rapidly changing phenomena including algal blooms (Figure 2), outbreaks of pathogens or insect infestations (Pontius et al. 2005), or invasive weedy species (Noujdina and Ustin 2008), which can have significant economic or public health consequences (e.g., Kallio et al. (2001) used hyperspectral data to track seasonal changes in water quality in Finnish lakes).

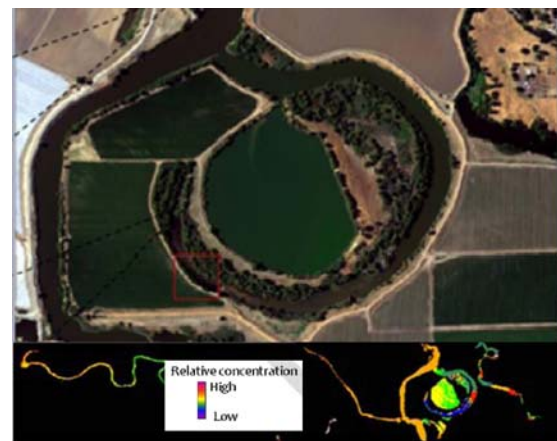


**Figure 2: Presence of Microcystis bloom in the Sacramento-San Joaquin delta captured in hyperspectral imagery June 2007.**

With the spatial and temporal resolution provided by HypsIRI, subtle differences in phenology and physiology associated with dynamic environmental conditions or microsites can be captured (Gamon et al. 1993, Garcia and Ustin 2001, Zarco-Tejada et al. 2005a, b) providing clear benefits to resource managers in many disciplines including forestry, agriculture, and water-quality management.

**Table 3: VQ2 Thematic Subquestions**

ID	Question
VQ2a	How are these being altered by changes in climate, land use, and disturbance?
VQ2b	How are seasonal patterns of ecosystem function being affected by climate change?
VQ2c	How do changes in phenology affect productivity, carbon sequestration, and hydrological processes across ecosystems and agriculture?
VQ2d	How do environmental stresses affect the seasonality of the physiological function of water and carbon exchanges within ecosystems?
VQ2e	What is the seasonality and environmental impact of algal blooms in shallow water environments?

### 2.1.3 VQ3 - Biogeochemical Cycles

The biogeochemical cycles of C, H, O, N, P, S, and dozens of other elements sustain life on Earth, are central to human well-being and are at the core of some of our most pressing environmental concerns. As these elements travel between the atmosphere, biosphere, hydrosphere, and lithosphere, they shape the composition and productivity of ecosystems, they influence the climate regulating properties of the atmosphere, and they affect the quantity and quality of water supplies. Because human livelihood has long been tied to the production of food, fiber, and energy, our activities have had particularly profound effects on cycles of carbon, nitrogen, and water. Issues such as climate change, nitrogen deposition, coastal eutrophication, groundwater contamination, and erosion represent human alterations of these basic biogeochemical cycles (Vitousek et al. 1997).

The HypsIRI instrument stands to advance our understanding of biogeochemical cycling in a number of important ways. Nutrient cycling patterns in both terrestrial and aquatic ecosystems can influence the growth and distribution of species as well as the morphology and chemistry of their tissues (e.g., LeBauer and Treseder 2008, Wright et al. 2004, Reich et al. 2006). Several decades of work with laboratory and aircraft instruments have demonstrated repeatedly that many of these vegetation features can be detected through analysis of high-quality imaging spectrometer data. Examples include the detection of leaf pigments in both terrestrial and aquatic plants (e.g., Asner 1998, Gitelson et al. 2007, Thomas et al. 2008), vegetation chemical constituents such as nitrogen, lignin, and cellulose (Wessman et al. 1988, Roberts et al. 1997, Serrano et al. 2002, Ollinger and Smith 2005) and invasive plants that cause distinct changes in the biogeochemistry of their surroundings (Asner and Vitousek 2005).

**Table 4: VQ3 Thematic Sub Questions**

ID	Question
VQ3a	How do changes in climate and atmospheric processes affect the physiology and biogeochemistry of ecosystems?
VQ3b	What are the consequences of uses of land and coastal systems, such as urbanization and resource extraction, for the carbon cycle, nutrient fluxes, and biodiversity?
VQ3c	What are the consequences of increasing nitrogen deposition for carbon cycling and biodiversity in terrestrial and coastal ecosystems?
VQ3d	How do changes in hydrology, pollutant inputs, and sediment transport affect freshwater and coastal marine ecosystems?
VQ3e	How do changing water balances affect carbon storage by terrestrial ecosystems?
VQ3f	What are the key interactions between biogeochemical cycles and the composition and diversity of ecosystems?
VQ3e	How do changes in biogeochemical processes feed back to climate and other components of the Earth system?

Because the plant traits being detected play key roles in processes such as carbon assimilation, biomass production, litterfall,

and decomposition, these capabilities have led to substantial improvements in our understanding of biogeochemical properties such as soil nitrogen cycling (Ollinger et al. 2002), algal production and exchanges of carbon and water between the land and atmosphere (e.g., Ustin et al. 2004, Fuentes et al. 2006). The principal limitation of these methods to date has been the spatial extent, frequency, and reliability of data acquisition.

Overcoming the limitations of current sensors will be critical for our ability to integrate field-based knowledge of biogeochemistry with climate research and Earth-system modeling. As an example, recent research with AVIRIS and eddy-covariance tower data revealed a coupling of carbon assimilation and vegetation shortwave albedo that is mediated by nitrogen concentrations in vegetation canopies (Figure 3).

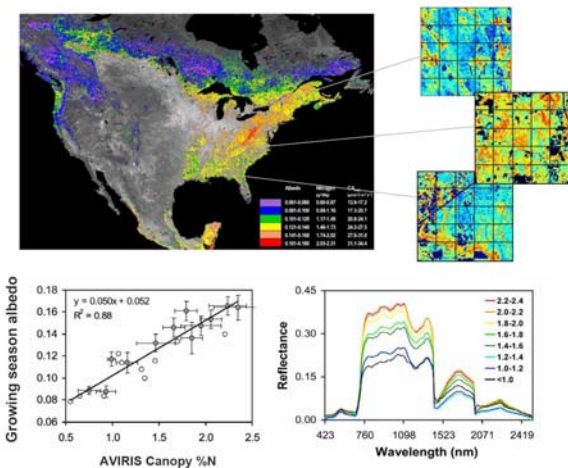


**Figure 3: Canopy Nitrogen, Carbon Assimilation, and Albedo in Temperate and Boreal Forests (Ollinger et al. 2008)**

This suggests a feedback in the climate system that models do not presently capture, in part because the relevant global data sets are not available from available sensors. Data from HypsIRI would solve this problem by providing the ideal spectral data for mapping both canopy nitrogen and, given its full

spectral coverage, total shortwave surface albedo.

The advent of HypsIRI as an orbital sensor will mark a substantial leap forward for the biogeochemical sciences. It is for this reason that organizations such as the Scientific Organization on Problems of the Environment (SCOPE) have identified hyperspectral technologies as being a key part of future studies of element cycling (Ollinger et al. 2003, Mellilo et al. 2003).

**2.1.4 VQ4 - Ecosystem Response to Disturbance**

Ecological disturbance plays a central role in shaping the Earth system. Disturbances (such as extreme weather events, fire, forest thinning or dieback, rangeland degradation, insect and pathogen outbreaks, and invasive species) affect vegetation biochemical and physiological processes with cascading effects on whole ecosystems. Similar effects take place based on disturbances to aquatic ecosystems, such as sediment re-suspension, nutrient input, or storm events, among many others. These and other disturbances often occur incrementally at spatial scales that fall well within the pixel size of current global satellite sensors.

**Table 5: VQ4 Thematic Subquestions**

ID	Question
VQ4a	How do patterns of disturbance vary and change over time within and across ecosystems?
VQ4b	What are the trends in disturbance regimes, compared with previous regional and global observations?
VQ4c	How do climate changes affect disturbances such as fire and insect damage?
VQ4d	How do climate change, pollution, and disturbance alter the vulnerability of ecosystems to invasive species?
VQ4e	What are the effects of disturbances on productivity, water resources, and other ecosystem functions and services?
VQ4f	How do changes in human uses of ecosystems affect their vulnerability to disturbance and extreme events?

Since disturbance often involves changes in vegetation function (physiology and biochemistry) and composition (e.g., the spread of introduced species) that may not be detectable with conventional satellite approaches, detection and quantification often requires the full spectral signatures available from imaging spectroscopy.

HyspIRI's high-fidelity imaging spectrometer will facilitate the study of ecological processes in disturbed areas at a level not possible with current satellite sensors.

HyspIRI will directly address a range of ecological disturbance-response questions central to predictions of future global change. For example, invasive species are considered a major driver of ecological change worldwide. Biological invasions can go unnoticed due to their often subtle impacts on vegetation structure. However, the chemical and physiological effects of invasion can be measured with imaging spectroscopy, as shown using the updated AVIRIS sensor (Figure 4)

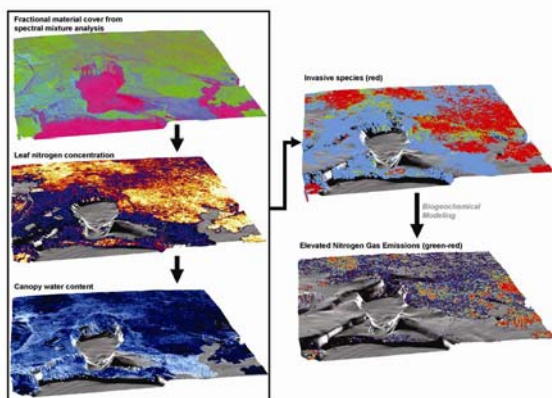


**Figure 4:** Maps of canopy cover, nitrogen and water (panels to the left) derived from imaging spectroscopy were used to map highly invasive trees (upper right; red) in a Hawaiian rainforest. A biogeochemical model then showed increased nitrogen gas fluxes from the soils beneath the invader (Asner and Vitousek 2005).

Combining multiple plant properties derived from reflectance spectra provided a

means to map invasives in a Hawaiian rainforest. The primary invader was a nitrogen-fixing tree species that raised nutrient flow throughout the ecosystem, as shown in the modeling results using AVIRIS-derived data products. HyspIRI provides an unprecedented capability to examine the effect of similar disturbances in aquatic habitats.

### 2.1.5 VQ5 - Ecosystems and Human Well-being

Ecosystem condition affects the humans dependent on those ecosystems for life and livelihood. For example, measurements of ecosystem condition derived from hyperspectral imagery can provide important insights into how ecosystem health is related to water quality, and by extension to human health. Similarly, hyperspectral data have been demonstrated to be effective for mapping the presence of invasive or undesirable plant species, which in turn affect the production of natural resources for human use by displacing desirable species with species of comparably lower value. Additional linkages from ecosystem to human condition include the monitoring of changes to ecosystems that may influence disease spread, resource availability, and resource quality. In border areas and areas with high human population densities, such information may provide insights into underlying causes of social, economic, or political conflict. Therefore, measurements of ecosystem condition from HyspIRI provide the potential to better characterize relationships between ecosystem health and human well-being.

The Group on Earth Observations (GEO) Remote Sensing of Water Quality Workshop in Geneva, Switzerland in 2007 stated that an ideal hyperspectral water quality sensor would have a range of 0.35 to 2.4  $\mu\text{m}$  and a spectral resolution of 5–10 nm, which fits well with the HyspIRI VSWIR capability. At these wavelengths and spectral resolutions, key water quality characteristics can be

observed, such as chlorophyll concentration to monitor eutrophication of in-land and coastal water and to determine plankton species type—or possibly the presence of harmful algal blooms (HABs) (Ritchie et al. 2003) as demonstrated by Kutser (2004). Hyperspectral data can also be used to measure directly water quality parameters that relate to nitrogen and phosphorus concentration, chlorophyll-a, colored dissolved organic matter (CDOM), particulate matter and tripton (Giardino et al. 2007, Brando and Dekker 2003, Thiemann and Kaufmann 2002, Fraser 1998), all of which have a bearing on the provision of clean water, water treatment, and hazards to human and animal health. Thus, the hyperspectral imaging capability of HypsIRI can be used to monitor seasonal changes in coastal and in-land waters for human health risks and potential threats to aquatic resources that could have economic impacts (e.g., reduced fish stocks safe for human consumption) and adversely affect the availability of potable water and food.

**Table 6: VQ5 Thematic Sub Questions**

ID	Question
VQ5a	How do changes in ecosystem composition and function affect the spread of infectious diseases and the organisms that transmit them?
VQ5b	How will changes in pollution and biogeochemical cycling alter water quality?
VQ5c	How are changes in ecosystem distribution and productivity linked to resource use, and resource management?
VQ5d	How will changes in climate and pollution affect the health and productivity of aquatic and agricultural resources?
VQ5d	What are the economic and human health consequences associated with the spread of invasive species?
VQ5e	How does the spatial pattern of policy, environmental management, and economic conditions correlate with the state and changes in ecosystem function and composition?
VQ5f	What are the impacts of flooding and sea level rise on ecosystems, human health, and security?

Furthermore, changes in watershed ecosystems can be tied to changes in water quality. The ability of hyperspectral data to

detect foliar nutrient concentrations has been well documented (Martin et al. 2008). Recently McNeil et al. (2007) showed that disturbance to forests leads to concurrent declines in foliar nutrient quality (measured using Hyperion) and nutrient export to watersheds (measured in situ) that was manifested in declines in downstream water quality disturbed relative to undisturbed watersheds (Figure 5).

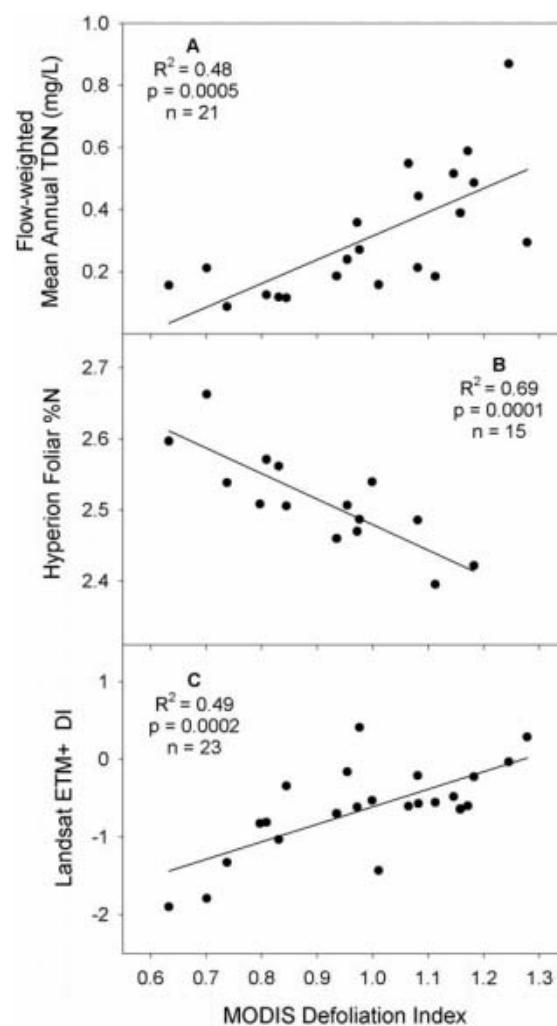


**Figure 5: Watershed-scale ecosystem responses to disturbance. Disturbance is measured using MODIS imagery (X-axis) and Landsat (panel C), illustrating an inverse response stream nitrogen (A) and foliar nitrogen (B), as derived from Hyperion. (McNeil et al. (2007).**

This points to functional relationships between ecosystem processes and water quality that affect both the availability of clean water for human use, and decisions that resource managers must make with respect to landscape management and water treatment. Hyperspectral imagery is also effective for the detection of other ecosystem changes resulting from flooding (Ip et al. 2006) and saltwater intrusion.

The detection of stress to vegetation from pests and pathogens also represents an important application of hyperspectral imagery with implications for human well-being. In forested ecosystems, Pontius et al. (2005) recently demonstrated the use of AVIRIS imagery to detect early signs of decline in hemlocks as a consequence of infestation by the hemlock woolly adelgid. Hemlock is a valuable species ecologically, economically, and for recreation, meaning that detection of hemlock decline can provide resource managers with opportunities for mitigation response prior to high levels of mortality. Additional studies have also demonstrated the capacity of hyperspectral data to detect plant decline from pathogens affecting economically important species like eucalypts (Stone et al. 2001), pines (Coops et al. 2003), ash (Pontius et al. 2008) and California oaks (Pu et al. 2008), as well forests in general (Treitz and Howarth 1999). Applications to agricultural systems are also widespread, as hyperspectral imagery can provide measures of growth/yield status (Datt et al. 2003), nutrient status (Haboudane et al. 2002, Strachan et al. 2002), and stress (Zarco-Tejada et al. 2005b), and has potential applications for food safety (Kim et al. 2001). Other work has demonstrated the ability of EO-1 Hyperion to detect sugarcane “orange rust” (Apan et al. 2004) as well as fungal diseases in wheat.

Non-native plant species pose a significant threat to ecosystems worldwide. In many areas, invasive plants displace native

species that are depended upon for food, fiber, or ecosystem services such as nutrient retention. Replacement by non-native species may have effects not just on the function, composition, and structure of the native ecosystems (e.g., fauna), but also on the human societies that use these ecosystems. Hyperspectral imagery has been demonstrated to be effective at discriminating invasive species (often resulting from differing nutrient assimilation strategies) in US western coastal habitats (Underwood et al. 2003 and 2006, and Rosso et al. 2005, Judd et al. 2007, Sadro et al. 2007), US eastern coastal habitats (Bachmann et al. 2002), and other wetlands (Hirano et al. 2003, Jollineau and Howarth 2008), as well as specific invasives such as common reed, *Phragmites communis*, formerly *P. australis* (Pengra et al. 2007), leafy splurge in central and western North America (Glenn et al. 2005), Chinese tallow (Ramsey et al. 2005a, Ramsey et al. 2005b), tamarix (Anderson et al. 2005, Pu et al. 2008), and the invasive nitrogen-fixer *Myrica faya* in Hawaii (Asner et al. 2006, Asner and Vitousek 2005). Detection of invasives may be critical to assessing significant changes in ecosystem level nutrient and water availability (Asner and Vitousek 2005). Hyperspectral imagery has also proven effective for discriminating increases in liana dominance of tropical and subtropical forests (Foster et al. 2008, Kalacska et al. 2007, Sanchez-Azofeifa and Castro-Esau, 2004), as liana abundance has been demonstrated to be increasing as a consequence of global change (Phillips et al. 2002). Loss of habitat, as well as of free-standing forests could lead to significant economic strains on societies dependent on these forests. Furthermore, invasives can possibly pose an increased threat to human safety and property. In wetlands, the invasive *Phragmites communis* has been identified as producing more fuel for wildfires around human habitations than native species and

could hamper mosquito control (Marks et al. 1994).

Because of the importance of ecosystem resources to human society, it is expected that information that can be derived from HypsIRI on vegetation stress, invasive species, and other factors relevant to water and food quality and human health will prove valuable for detecting seasonal trends in ecosystems and natural resources that might result in significant declines in human well-being. Data from HypsIRI may provide the opportunity to develop management options to reduce impacts on human societies.

**2.1.6 VQ6 - Surface and Shallow-Water Bottom Composition**

The surface composition within exposed rock and soils of a wide range of materials is revealed in the solar reflected light spectroscopic signature from 400 to 2500 nm. Figure 6 shows the mapping of iron oxide, clay, carbonate, and other minerals in the desert region of Cuprite, Nevada. HypsIRI will be able to measure the surface composition of those areas with 75% or less vegetation cover, which occur seasonally over 30% of the land surface of the Earth. These HypsIRI measurements will enable new research opportunities for mineral and hydrocarbon resource investigation and emplacement understanding as called for in the Decadal Survey.

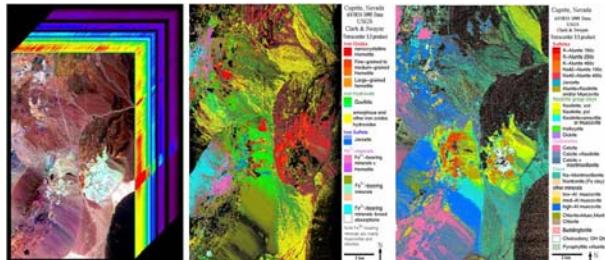


Figure 6: Map of surface rock and soil mineralogy at Cuprite, NV using solar reflected imaging spectroscopy measurements from 380 to 2500 nm. (Left: AVIRIS image cube, Center: 1 micron region minerals, Right: 2 micron region minerals) (Swayze et al. 2003)

With reasonable water clarity in the shallow-coastal and inland water regions, the bottom composition may be derived with imaging spectroscopy measurements in the region from 380 to 800 nm. A high fraction of the world's population lives in close proximity to these shallow water regions. Measurement by HypsIRI globally and seasonally of the composition and change of these environments will support understanding of their condition and associated resources and hazards. HypsIRI will be an important tool with which to assess coastal bathymetry as well as water quality, and the distribution of different benthic habitats such as coral reefs, algae, sand, and other geological components. The mission will help assess their relationship to land processes or disturbance, and how they change seasonally or over longer time scales.

Table 7: VQ6 Thematic Sub Questions

ID	Question
VQ6a	What is the distribution of the primary minerals and mineral groups on the exposed terrestrial surface?
VQ6b	What is the surface composition (sand, rock, mud, coral, algae, etc.) of the shallow-water regions of the Earth?
VQ6c	How can measurements of rock and soil composition be used to understand and mitigate hazards?

Understanding of the detailed surface mineralogy of rocks and soils allows improved understanding and potential mitigation of a range of natural and anthropogenic hazards. The HypsIRI VSWIR, like AVIRIS measurements, should help discover unmapped earthquake faults, natural and anthropogenic asbestos, acid mine drainage, expanding clay soils, and other surface hazard zones.

**2.1.7 TQ1 - Volcanoes and Earthquakes**

Volcanic eruptions and earthquakes yearly affect millions of lives, causing thousands of deaths, and billions of dollars in property damage. The restless earth provides

premonitory clues of impending disasters; thermal infrared images acquired by HypsIRI will allow us to monitor these transient thermal phenomena. Together with modeling, we will advance our capability to one day predict some natural disasters.

TIR data will allow us to measure changes in SO<sub>2</sub> emissions. Frequent coverage by HypsIRI will allow us to better monitor changes in tropospheric emissions, a capability not offered by existing moderate (~1 km) resolution instruments. Measuring SO<sub>2</sub> gives us information about a volcano’s plumbing system, and state of pressurization of sub-surface magma reservoirs. Multispectral TIR data will allow the identification of the mixture of ash, SO<sub>2</sub>, and water vapor in eruptive plumes, providing improved hazards warnings for aviation safety. These capabilities are illustrated in Figure 7 (a and b).

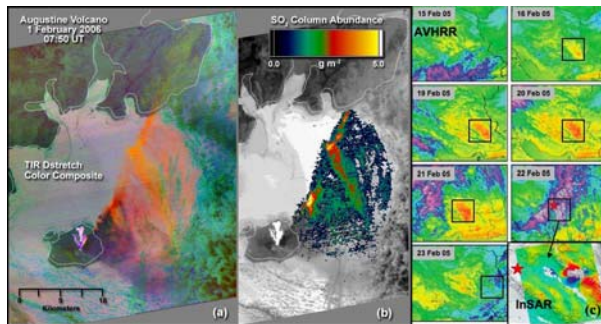


**Figure 7:** (a) ASTER night-time multispectral TIR image of Augustine Volcano showing hot pyroclastic flow deposits (bright in TIR) and eruption plume. Colors indicate spectral variations between materials entrained in plume. Magenta indicates mixtures of water droplets (steam) and silicate ash; red, yellow, and orange indicate mixtures of ash and SO<sub>2</sub>. (b) SO<sub>2</sub> map derived from ASTER TIR data. (c) Thermal infrared anomaly associated with the M6.4 Zarand, Iran earthquake of Feb. 22, 2005, as derived from night-time Advanced Very High Resolution Radiometer (AVHRR) images recorded prior to this event (after Saraf et al. 2008). The excess IR intensity emitted from the epicentral region (presented in yellow-orange colors), and 10K temperature increase, are proposed to be indicators of the build-up of stress at the hypocenter. Lower right: Location of the epicenter (star) relative to the region of maximum uplift (red: 25 cm) and

subsidence (blue: 17 cm) from Interferometric Synthetic Aperture Radar (InSAR) data.

Changing high temperature phenomena include crater lakes, fumaroles, lava lakes, and dome growth. All of these volcanic phenomena are surface manifestations of dynamic sub-surface events occurring within a volcano’s plumbing system. Thermal observations of active lava flows allow effusion rates to be estimated, and these can be used to drive numerical models that forecast lava flow hazards. Thermal observations of dome growth provide clues to upward movement of magma within a volcano, and can also signal blockages of the main conduit. Together, these are possible precursors signaling potential eruptions. Adequate monitoring of these features requires HypsIRI’s high spatial resolution, frequent observational re-visits, and proper spectral resolution.

**Table 8: TQ1 Thematic Subquestions**

ID	Question
TQ1a	Do volcanoes signal impending eruptions through changes in surface temperature or gas emission rates, and are such changes unique to specific types of eruptions?
TQ1b	What do changes in the rate of lava effusion tell us about the maximum lengths that lava flows can attain, and the likely duration of lava flow-forming eruptions?
TQ1c	What do the transient thermal infrared anomalies that may precede earthquakes tell us about changes in the geophysical properties of the crust?
TQ1d	What are the characteristic dispersal patterns and residence times for volcanic ash clouds, and how long do such clouds remain a threat to aviation?

Research has suggested that some earthquakes may be preceded by thermal infrared anomalies observable from satellites (Ouzounov and Freund, 2004). The anomalies have been noted to precede earthquakes by days to weeks and were associated with earthquakes M>5 and focal depths generally no deeper than 35 km, occasionally down to 50 km in earthquakes related to subduction zones (Figure 7). There may be a relationship between the observed increased IR flux and

tectonic stress and/or processes in the atmosphere. Possible causes may be warming by greenhouse gas release over the epicentral region, changes in latent heat due to an increase of soil moisture and evaporation rate, or a quantum-mechanically driven process arising from the radiative decay of vibrationally excited states of atoms at the Earth surface that result from the recombination of electronic charge carriers stress-activated deep below, at hypocentral depth.

### 2.1.8 TQ2 - Wildfires

Both naturally occurring wildfire and biomass burning associated with human land-use activities have come to be recognized as having an important role in regional and global climate change. There consequently exists a substantial need for timely, global fire information acquired with satellite-based sensors. While some existing (e.g., MODIS) and planned (e.g., VIIRS) instruments currently provide (or will provide) such information at coarse spatial resolution ( $\sim 1$  km), the availability of robust, high-resolution fire information is extremely limited. While ASTER, for example, has yielded high resolution fire imagery (Figure 8), the sensor lacks the radiometric capabilities necessary to reliably map or characterize many flaming fires and most smoldering fires (Giglio et al. 2008).

In conjunction with its long-wave infrared channels, the specialized 4- $\mu\text{m}$  channel of the HypSPIRI thermal sensor will fill this void and permit reliable detection of fires at much higher spatial resolution than other current or planned sensors. The unprecedented sensitivity will enable the detection and characterization of small, often land-use-related fires that remain undetected by lower resolution sensors. The 4- $\mu\text{m}$  channel will also permit direct retrieval of the instantaneous rate of energy released by the fire (i.e., fire radiative power - FRP), a

quantity of interest because it is proportional to the rate of fuel combustion and thus supplies useful (and otherwise inaccessible) information about both fire intensity and the rate of emission of trace gases and aerosols (Kaufman et al., 1998; Ichoku and Kaufman, 2005).

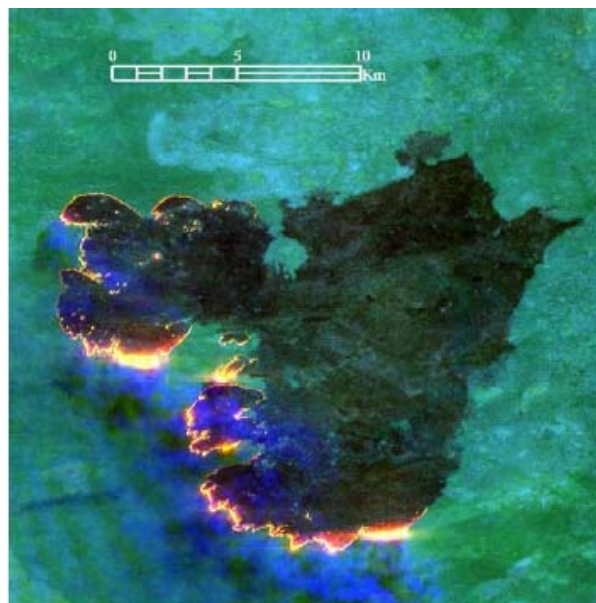


**Figure 8:** False-color ASTER image of a large fire in southern Africa, acquired on 17 August 2001, with the 2.4, 1.6, and 0.5  $\mu\text{m}$  bands shown as red, green, and blue, respectively. With this color scheme the actively burning fire front appears yellow to red, previously-burned areas appear black, and unburned vegetation appears green. The specialized 4-micron channel of the HypSPIRI thermal sensor will not exhibit the saturation-induced blooming apparent along the more intense portions of the flaming front in this scene.

While at present only the Terra and Aqua MODIS sensors, and more recently the Spinning Enhanced Visible and Infrared Imager (SEVIRI) on-board the Meteosat-8 geostationary satellite, can provide radiative power observations over very large spatial scales, they do so at comparatively coarse spatial resolution (1 km and 4.8 km, respectively). The larger fractional area of active burning within the higher resolution HypSPIRI pixels will allow for more accurate FRP retrievals. In addition, HypSPIRI will provide improved spatial and temporal

coverage than ASTER, needed for more detailed studies of fire regimes.

**Table 9: TQ2 Thematic Subquestions**

ID	Question
TQ2a	How are global fire regimes (fire location, type, frequency, and intensity) changing in response to changing climate and land use practices?
TQ2b	Is regional and local fire frequency changing?
TQ2c	What is the role of fire in global biogeochemical cycling, particularly trace gas emissions?
TQ2d	Are there regional feedbacks between fire and climate change?

**2.1.9 TQ3 - Water Use and Availability**

Given current trends in population growth and climate change, accurate monitoring of the Earth’s freshwater resources at field to global scales will become increasingly critical (DS 2007, WGA 2006, 2008). Land surface temperature (LST) is a valuable metric for estimating evapotranspiration (ET) and available water because varying soil moisture conditions yield distinctive thermal signatures: moisture deficiencies in the root zone lead to vegetation stress and elevated canopy temperatures, while depleted water in the soil surface layer causes the soil component of the scene to heat rapidly.

Several techniques have been developed to use TIR remote sensing data to generate accurate estimates of ET at multiple spatial scales (Figure 9; see also review by Kalma et al., 2008). Of particular utility are TIR data at “high” spatial resolution (100 m or finer), resolving natural and anthropogenic land-cover features important to local and regional water management: individual fields and irrigation pivots, riparian zones, canals and riverbeds, reservoirs, and other man-made hydrologic structures. With frequent revisit (< 7 days), high-resolution TIR imaging can provide accurate estimates of consumptive water use at the spatial scale of human management and time scale of vegetation growth, needed to monitor irrigation

withdrawals, estimate aquifer depletion, evaluate performance of irrigation systems, plan stream diversions for protection of endangered species, and estimate historical water use for negotiating water rights transfers (Allen et al. 2007).

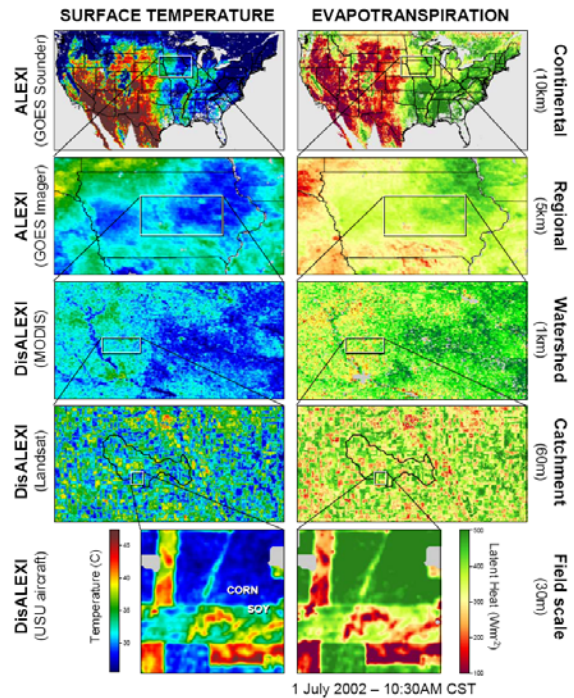


**Figure 9: Multi-scale ET maps for 1 July 2002 produced with the ALEXI/DisALEXI surface energy balance models (Anderson, et al. 2007) using surface temperature data from aircraft (30-m resolution), Landsat-7 ETM+ (60m), Terra MODIS (1-km), GOES Imager (5-km) and GOES Sounder (10-km) instruments. The continental-scale ET map is a 14-day composite of clear-sky model estimates.**

Climate change may lead to increased frequency of drought and flooding events, and accurate monitoring of extreme moisture conditions at high spatiotemporal resolution will be essential for effective targeted mitigation efforts. Comparisons between satellite-derived maps of actual evapotranspiration (ET) and potential evapotranspiration (PET) provide useful information about anomalously wet and dry conditions at the scale of imaging, without requiring any rainfall data (Anderson et al. 2007). While regional drought can be

reasonably assessed at low spatial resolution with data from ground-based precipitation networks, local information at sub-county and field scales is currently unavailable with uniform quality across the U.S., and can be very sparse in other parts of the world. Furthermore, satellite rainfall estimates are notoriously unreliable over many types of land surfaces. Thermal-based ET/PET maps provide a robust and high-resolution alternative to precipitation-based indices for global drought monitoring. For flood prediction, information about moisture conditions in narrow floodplain zones is critical. In many cases, these floodplains are not resolved at the MODIS TIR 1-km scale.

High-resolution maps of ET/PET, resolving individual fields, can also be used to remotely detect and quantify irrigated land area, an important input field required by land-surface models driving weather, water use, and climate models.

**Table 10: TQ3 Thematic Subquestions**

ID	Question
TQ3a	How is climate variability impacting the evaporative component of the global water cycle over natural and managed landscapes?
TQ3b	How can information about evapotranspiration and its relationship to land use/land-cover be used to facilitate better management of freshwater resources?
TQ3c	How can we improve early detection, mitigation, and impact assessment of droughts at local to global scales?
TQ3d	What is the current global irrigated acreage, how is it changing with time, and are these changes in a sustainable balance with regional water availability?
TQ3e	Can we increase food production in water-scarce agricultural regions while improving or sustaining water available for ecosystem function and other human uses?
TQ3f	How can improved accuracy in evapotranspiration imaging drive advances in science and understanding of the water cycle and hydrologic processes?

Local depressions in ET over irrigated land area, along with hyperspectral indicators of vegetation stress from HypspIRI, provide early signatures of increasing soil salinity that

can be used to map salinization onset at the global scale.

#### **2.1.10 TQ4 - Human Health and Urbanization**

Excess deaths occur during heat waves on days with higher-than-average temperatures and in places where summer temperatures vary more or where extreme heat is rare (e.g., Europe, northeastern U.S.). Exposure to excessive natural heat caused a reported 4,780 deaths during the period 1979-2002, and an additional 1,203 deaths had hyperthermia reported as a contributing factor (CDC, 2005). Urban heat islands (UHI) may increase heat-related impacts by raising air temperatures in cities approximately 1–6 °C over the surrounding suburban and rural areas due to absorption of heat by dark paved surfaces and buildings; lack of vegetation and trees; heat emitted from buildings, vehicles, and air conditioners; and reduced air flow around buildings (EPA, 2006). An example of the extent of the UHI in response to urban land covers is given in Figure 10. The figure shows Atlanta’s urban extent in gray (bottom) and corresponding thermal responses (top) as derived from Landsat TM data. Critical to understanding the extent, diurnal and energy balance characteristics of the UHI is having remote sensing data collected on a consistent basis at high spatial resolutions to enable modeling of the overall responses of the UHI to the spatial form of the city landscape for different urban environments around the world. Unfortunately, current satellite systems do not have adequate revisit times or multiple thermal spectral bands to provide the information needed to model UHI dynamics and its impact on humans and the adjacent environment. HypspIRI will have a return time, spectral characteristics, and nighttime viewing capabilities that will greatly enhance our knowledge of UHI’s form, spatial extent, and temporal characteristics for urban areas across the globe.

Additionally, HypsIRI will provide multispectral thermal IR at a high spatial resolution that is currently not available from other Earth-observation satellites for assessing how urbanization affects adjacent ecosystems.

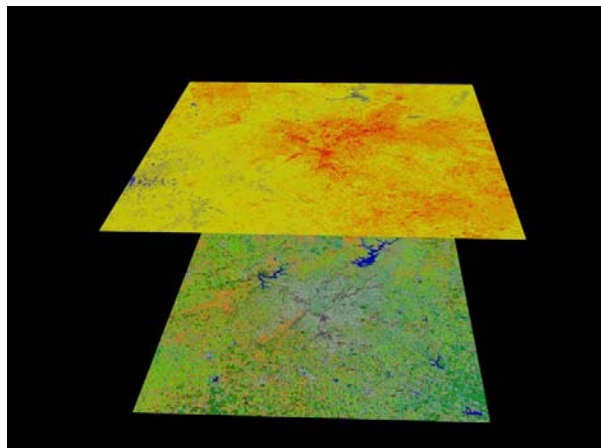


**Figure 10: Landsat TM data of the Atlanta, GA metropolitan area showing urban extent in gray (bottom) and corresponding surface thermal responses (top) (Quattrochi et al. 2009)**

**Table 11: TQ4 Thematic Subquestions**

ID	Question
TQ4a	How do changes in land cover and land use affect surface energy balance and the sustainability and productivity of natural and human ecosystems?
TQ4b	What are the dynamics, magnitude, and spatial form of the urban heat island (UHI) effect; how does it change from city to city; what are its temporal, diurnal, and nocturnal characteristics; and what are the regional impacts of the UHI on biophysical, climatic, and environmental processes?
TQ4c	How can the characteristics associated with environmentally related health effects, such as factors influencing heat stress on humans and surface temperatures that affect vector-borne and animal-borne diseases, be better resolved and measured?
TQ4d	How do horizontal and temporal scales of variation in heat flux and mixing relate to human health, human ecosystems, and urbanization?

For example, while urban and suburban landscapes covered about 45 million acres in the lower 48 states (about 2% of the land area) (John Heinz III Center for Science, Economics and the Environment, 2007), the amount of land area that is affected by urbanization continues to grow in the U.S. and around the world. The known affects of the

UHI on natural ecosystems concomitant with urban growth is extremely limited in the developed and developing world. HypsIRI will be able to provide data to assist in measuring and modeling thermal energy balance characteristics of biophysical systems that are, or will be, impacted by urban growth and the subsequent land cover/land use changes that accompany urbanization. HypsIRI will provide high spatial resolution TIR data with excellent revisit times to help us better model the affects of global urbanization on natural ecosystems on a continuous basis.

### 2.1.11 TQ5 - Earth Surface Composition and Change

The emitted energy from the exposed terrestrial surface of the Earth can be uniquely helpful in identifying rocks, minerals, and soils (Figure 11). Spaceborne measurements from HypsIRI will enable us to derive surface temperatures and emissivities for a variety of Earth's surfaces.

**Table 12: TQ5 Thematic Subquestions**

ID	Question
TQ5a	What is the spectrally observable mineralogy of the Earth's surface and how does this relate to geochemical and surficial processes?
TQ5b	What is the nature and extent of man-made disturbance of the Earth's surface associated with exploitation of renewable and non-renewable resources? How do these vary over time?
TQ5c	How do surface temperature anomalies relate to deeper thermal sources, such as hydrothermal systems, buried lava tubes, underground coal fires and engineering structures? How do changes in the surface temperatures relate to changing nature of the deep-seated heat source?
TQ5d	What is the spatial distribution pattern of Earth surface temperatures and emissivities, and how do these influence the Earth's heat budget?
TQ5e	What are the water surface-temperature distributions in coastal, ocean, and inland water bodies; how do they change; and how do they influence aquatic ecosystems?

Emissivity variations are particularly useful for mapping structures and areas of mineralization. For example different Si-O bonded structures vary in their interaction

with energy in the thermal infrared region (8-12  $\mu\text{m}$ ). Framework silicates, such as quartz and feldspar, show minimum emissivity at shorter wavelengths (8.5  $\mu\text{m}$ ). Silicates having sheet, chain, and isolated-tetrahedral structure show minimum emissivity at progressively longer wavelengths (Hunt 1980). This important property helps to discriminate the felsic and mafic rock composition remotely.

Between day and night, Earth surface composition remains the same, but temperature changes. Daytime and nighttime HypsIRI images will be used to map temperatures and extract further information about properties of the surface such as thermal inertia.

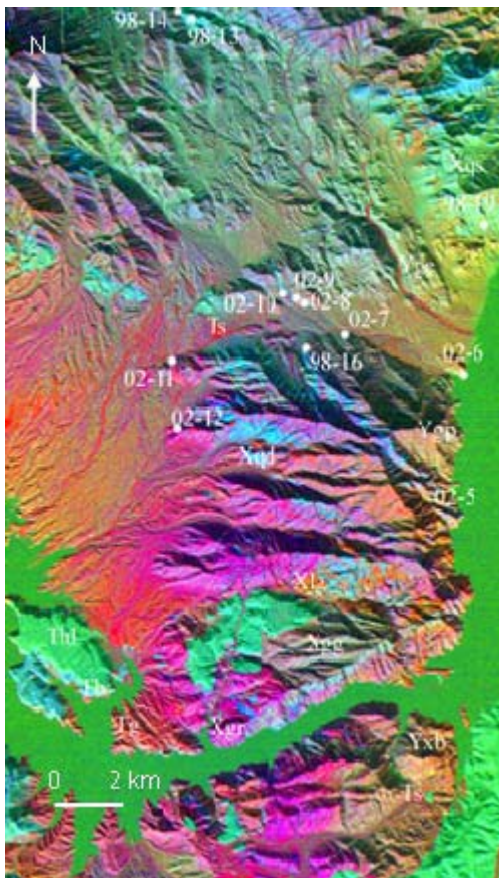


**Figure 11: HypsIRI-like image for the area around Lake Mead, Nevada. Three TIR bands are processed with a decorrelation stretch algorithm and displayed in red, green and blue, respectively (from Hook et al. 2005).**

Buried sources of high temperatures, (such as lava tubes, underground fires in coal seams and high temperature rocks) cause hot spots on the Earth's surface. The temperature profile across these hot spots holds clues to the depth of the heat source. Assuming that heat is conducting linearly in a semi-infinite medium, numerical modeling reveals that the shallower sources cause distinct thermal profiles, while deeper sources cause broad and more diffuse thermal profiles (Berthelote et al. 2008). HypsIRI data will be used to map temperature anomalies, extract thermal profiles, and numerically derive the depth of the hot sources.

### **2.1.12 CQ1 - Coastal, Ocean, and Inland-Aquatic Environments**

The oceans and inland-aquatic environments, including ice, play a critical role in Earth's climate through the hydrological cycle, and in supporting life and sustaining biodiversity on Earth. The oceans cover more than 70% of the Earth's surface, and about half of the globe's primary productivity occurs within them. More than \$1 trillion of the U.S.'s annual gross domestic product (GDP) is generated within the relatively narrow strip of land immediately adjacent to the coast (USCOP, 2004). Services provided by coastal ecosystems include purification of water through nutrient recycling, sediment storage, shoreline protection, and supplying habitat and food for migratory and resident animals, as well as humans. Aquatic habitats provide important biological and mineral resources for the pharmaceutical, oil, gas, and sand and gravel industries; and they support key tourism, fisheries, and maritime operations, including housing our ports. Yet we know little about the variety of coastal habitats and resources in them. Climate change, land subsidence, aerosol production, and sea-level rise complicate our understanding of the processes

of pollution, development, and structures that alter sediment flow.

Hyperspectral and high spatial resolution data from HypSPIRI will allow for better separation of phytoplankton pigments and phytoplankton FGs such as carbon exporters (diatoms), nitrogen fixers (*Trichodesmium* sp.), calcium carbonate producers (coccolithophores), and the microbial loop organisms (*Prochlorococcus* sp.). More spectral information helps improve the accuracy and diversity in retrievals of absorption and backscattering coefficients as well as other environmental properties through inversion algorithms, including effective discrimination of biogeochemical constituents of the water and seafloor (e.g., colored dissolved organic matter [CDOM], phytoplankton concentration and composition, suspended sediments, bottom type) and physical properties (e.g., temperature, bathymetry, light attenuation) (GEO 2007). HypSPIRI will enable better derivation of chlorophyll retrievals where other materials also change the color of water, such as inland and coastal and estuarine areas (Figure 12, Bidigare et al. 1989; Goodin et al. 1993; Kutser et al. 2006; Craig et al. 2006; Hu et al. 2005).

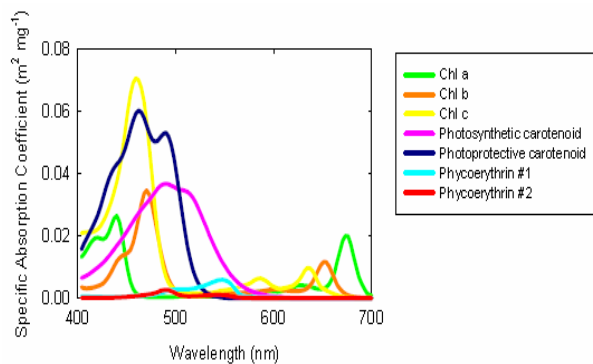


**Figure 12: Weight-specific absorption coefficients ( $m^2\ mg^{-1}$ ) derived for the major pigment types found in marine phytoplankton (from Bidigare et al. 1989).**

HypSPIRI also will help identify coral reef habitat with assessments of other bottom types (Hochberg and Atkinson, 2006, 2008), floating macroalgae (e.g., *Sargassum*; Gower

et al., 2006), the water column proper (Lee et al., 2007), and aquatic ice communities. HypSPIRI will be a critical tool to study habitats for marine life such as fish, turtles, and other marine organisms (GEO 2007), and to develop better coastal bathymetric charts. The infrared channels will help characterize physical conditions by measuring sea-surface temperature changes over small scales. And the potential for lower resolution global ocean images will allow accurate characterization of key ocean conditions away from land and coastal zones.

The data will augment our capabilities for atmospheric correction over turbid waters with bands between 670 nm and the short-wave infrared (SWIR) (Hu et al. 2000; Wang and Shi 2005), and allow the study of radiative properties of clouds, aerosols, snow, and ice over aquatic systems.

**Table 13: CQ1 Thematic Subquestions**

ID	Question
CQ1a	What are the feedbacks between climate and change in habitat structure, biogeochemical cycling, biodiversity, and ecosystem productivity of aquatic habitats, including ice-covered habitats? What are the ecological linkages of landscape-scale ocean-atmosphere interactions including the hydrologic cycle, aerosol production and transport, and cloud radiative forcing?
CQ1b	How are small-scale processes in water column, shallow benthic, and ice-covered habitats related to changes in functional community types (including harmful algal blooms and vector-borne diseases), productivity, and biogeochemical cycling (including material fluxes and water quality) at local scales?
CQ1c	How can these observations be used to guide the wise management of living marine and other aquatic resources?

The mission will contribute significantly to, and benefit from, efforts conducted through the National Science Foundation's ORION program, the coastal components of the Integrated Ocean Observing System (IOOS), the Climate Change Science Program (CCSP), and the Global Earth Observation System of Systems (GEOSS). The higher spatial and spectral

resolution will be of particular utility in coastal resource management applications.

### 2.1.13 CQ2 - Wildfires

While the HypsIRI thermal sensor will provide a greatly improved capability for detecting fires and characterizing their intensity (see TQ2), coupling the multispectral thermal data with hyperspectral VSWIR observations will significantly improve our understanding of the coupling between fires and vegetation and the associated trace-gas emissions. For example, HypsIRI's hyperspectral observations will allow precise mapping of vegetation at the level of individual species (e.g., Roberts et al. 1998). Furthermore, HypsIRI will permit reliable retrieval of fuel moisture (e.g., Serrano et al. 2002), a critically important factor that dictates a host of fire-related variables including fire danger, fire spread rate, and combustion completeness.

**Table 14: CQ2 Thematic Subquestions**

ID	Question
CQ2a	How do the timing, temperature, and frequency of fires affect long-term ecosystem health?
CQ2b	How do vegetation composition and fire temperature impact trace-gas emissions?
CQ2c	How do fires in coastal biomes affect terrestrial biogeochemical fluxes into estuarine and coastal waters and what is the subsequent biological response?
CQ2d	What are the feedbacks between fire temperature and frequency and vegetation composition and recovery?
CQ2e	How does vegetation composition influence wildfire severity?
CQ2f	On a watershed scale, what is the relationship of vegetation cover, clay-rich soils, and slope to frequency of debris flows?

In addition to improved fuel characterization, HypsIRI's hyperspectral observations will also provide detailed snapshots of the combustion process itself. Green (1996), for example, used ~150 channels of the hyperspectral AVIRIS to observe active fires in Brazil, and applied a two-temperature fire model to estimate average fire temperature

and sub-pixel fire area at 20-m spatial resolution. An improved endmember-library approach was subsequently developed by Dennison et al. (2006), allowing the retrieval of fire temperature and sub-pixel area, and background land cover (Figure 13).

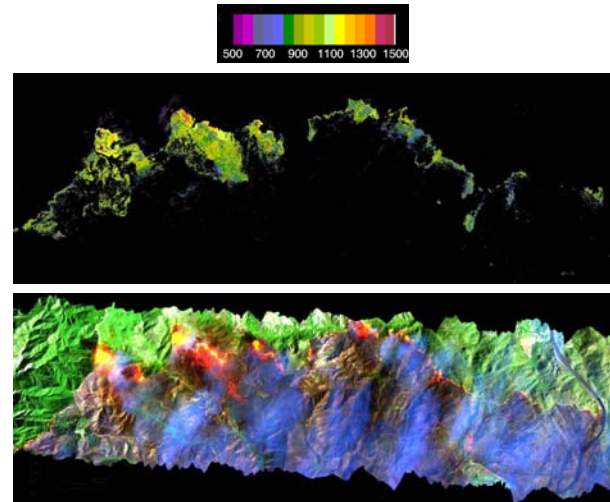


**Figure 13: Top panel: Retrieved fire temperature (in kelvins) from an AVIRIS scene spanning a portion of the large Southern California Fire Complex from October 2003. Bottom panel: False color SWIR-NIR-red composite of the original AVIRIS scene. (Dennison et al. 2006).**

Such information is necessary for producing accurate estimates of trace-gas fire emissions since the emission factor for a given species depends on the relative proportion of the flaming and smoldering stages.

### 2.1.14 CQ3 - Volcanoes

The replenishment of shallow magma reservoirs can herald a) the onset of an eruption at a previously inactive volcanic system or, b) significant changes in eruptive behavior at already active volcanoes. This magma brings with it volatiles (such as SO<sub>2</sub>) and thermal energy, both of which are ultimately released into the atmosphere. Satellite measurements of the heat and gas emitted by a volcano allow the mass of magma required to sustain the observed fluxes to be quantified (Francis et al., 1993). Determining magma budgets in this way provides information about how ascending

magma is partitioned between the surface (i.e., erupted) and the subsurface (i.e., intruded) as it circulates within the conduit (Figure 14).

Combined observations of cooling and degassing also provide insights into shallow-conduit processes that generate cyclic overpressures at silicic dome-forming volcanoes. Such cyclicity is increasingly recognized as characteristic of these dangerous volcanoes. In short, a permeable shallow conduit allows gas to escape freely, resulting in an elevated gas flux from the dome and an abundance of high temperature cracks on its surface.

Degassing-induced changes in permeability cause the upper conduit to seal, reducing gas flow (and, as a result, the abundance of hot fumaroles), and generating overpressures that result in an explosive eruption, after which the cycle begins anew (Oppenheimer *et al.*, 1993; Matthews *et al.*, 1997).



**Figure 14: Hyperion SWIR image of Erta Ale volcano, Ethiopia, showing the active lava lake. Hyperspectral VSWIR and TIR data will allow the cooling rate and gas flux from the lake to be determined. Right: model of cooling and degassing-driven magma convection within an open system volcano. The heat and gas flux data are important boundary conditions for determining magma ascent dynamics and circulation within the conduit (adapted from Frances *et al.* 1993).**

Space-based monitoring of dome-surface temperatures and degassing rates using VSWIR and TIR data will allow this cycle, and the transition between effusive and explosive phases, to be monitored, and may constitute a robust eruption precursor.

The surface temperature of an active lava flow controls the rate at which it cools and solidifies, and hence the distance from the vent at which it comes to a halt and the hazard it represents.

**Table 15: CQ3 Thematic Subquestions**

ID	Question
CQ3a	What do comparisons of thermal flux and SO <sub>2</sub> emission rates tell us about the volcanic mass fluxes and the dynamics of magma ascent?
CQ3b	Does pressurization of the shallow conduit produce periodic variations in SO <sub>2</sub> flux and lava-dome surface temperature patterns that may act as precursors to explosive eruptions?
CQ3c	Can measurements of the rate at which lava flows cool allow us to improve forecasts of lava flow hazards?
CQ3d	Do the temperature and composition of volcanic crater lakes change prior to eruptions?
CQ3e	Do changes in the health and extent of vegetation cover indicate changes in the release of heat, gas, and ash from crater regions?

Realistic parameterization of numerical lava-flow models relies on surface temperature data as a boundary condition for determining the rheology of the lava and its ability to flow. Remotely sensed data covering both the SWIR and TIR are necessary to constrain the non-linear mixture models required for the accurate determination of flow surface temperature (which is heterogeneous at the subpixel scale) and lava cooling rates from orbit (Wright and Flynn, 2003).

Precursory earthquakes and changes in temperature and element fluxes into volcanic crater lakes can increase lake turbidity, biological productivity, and the scattering properties of the water (Delmelle and Bernard, 2000). All have been known to result in changes in lake color. A combination of VSWIR and TIR data will allow us to monitor all aspects of volcanic crater lake variability (color and temperature) for signs of eruption.

### 2.1.15 CQ4 - Ecosystem Function and Diversity

Climate has a strong influence on the distribution of plant and animal species and associated biodiversity (MacDonald 2002). Numerous physiological and biochemical feedbacks exist between climate and ecosystems, where changing climate impacts the presence and functioning of organisms, which in turn modifies regional climate, either enhancing or buffering such changes. A good example of such a feedback is the impact of increased temperatures at higher latitudes, leading to northward expansion of boreal forest into tundra, or the migration of marine species from lower to higher latitudes. The migration of boreal forests enhanced surface temperatures due to lower conifer albedo (Hansen 2008), alterations in surface carbon and water fluxes (Smith et al. 2004), and changes in the incidence of fire (Kasischke and Stocks, 2000). One of the most pronounced indications of these high latitude changes has been an increase in the length of the growing season, readily observed from long-term satellite observations (Myneni et al., 1997). Similarly increased winter temperatures at higher elevations and latitudes facilitate the spread of forest pests, including bark beetles, leading to large-scale increases in forest mortality (Berg et al. 2006). Expansion of invasive plant species throughout the American southwest, such as cheat grass, illustrates numerous feedbacks between an organism and surface composition, modifying wildfire fuels, soil biogeochemistry, surface albedo and soil water balance, promoting further expansion of the invader (Noujdina and Ustin 2008: Figure 15).

Numerous research questions remain difficult to resolve due to limitations in current remote sensing capabilities. For example, changes in the amplitude of the normalized difference vegetation index (NDVI) at high latitudes attributed to enhanced growth could

also be explained by a change in ecosystems from conifer dominated to early successional aspen. No current sensor can simultaneously retrieve canopy temperature and quantify physiological or compositional changes in response to stress.

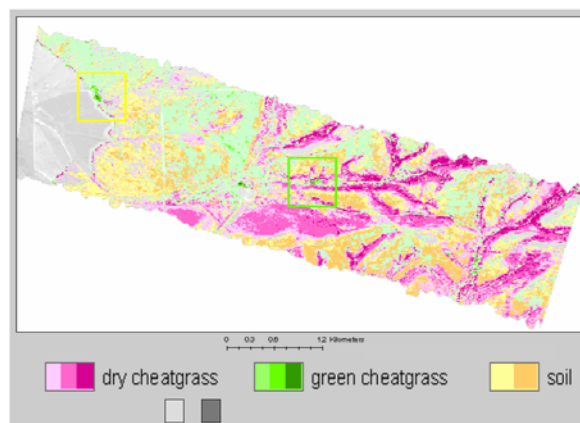


**Figure 15: Map of *Bromus tectorum* (Cheatgrass) generated using imaging spectrometry. Cheatgrass spreads through a combination of disturbance and strategic use of soil moisture. It alters fire regimes, promoting its spread while early germination of Cheatgrass enables it to produce seed in advance of native plants while reducing available water for competitors. (Noujdina and Ustin 2008).**

Together, the suite of instruments on HypsIRI should significantly improve our ability to partition the surface energy budget between latent and sensible heat and between soil and canopy contributions, combining hyperspectral characterizations of plant type, canopy structure, and surface residue cover with high spatiotemporal resolution measurements of surface temperature. Because access to water is a critical driver of plant species competition, HypsIRI will provide a unique opportunity to study in detail the response of plant populations to changes in moisture availability deduced from the TIR bands. HypsIRI will also provide improved measures of plant physiological function through simultaneous estimates of surface temperature and plant biochemistry, improved estimates of surface biophysical properties (e.g., albedo, crown mortality) and energy

balance, and improved discrimination of plant species and functional types.

The mission represents an important research tool to examine the changes in coastal and inland ecosystems as snow- and glacier-melting patterns change, affecting aquatic communities that receive the discharge.

**Table 16: CQ4 Thematic Subquestions**

ID	Question
CQ4a	How can we enhance phenological & stress characterization through synergy between reflective and emitted radiation with higher frequency temporal sampling?
CQ4b	How is energy partitioned between latent and sensible heat fluxes as a function of different plant types and fractional cover, and how does this impact hydrology?
CQ4c	How is physiological function affecting water and carbon exchange expressed at the ecosystem scale, especially seasonal down-regulation due to environmental stress factors?
CQ4d	What is the vegetation phenological response to seasonal and interannual changes in temperature and moisture due to climate change and how does this response vary at the community/species level?
CQ4e	What are the feedbacks between changes in canopy composition, mortality, and retrieved canopy temperatures resulting from disturbances (e.g., disease, moisture deficiency, insect attack, fire, land degradation, fragmentation) in natural and managed ecosystems?
CQ4f	How do climate-induced temperature and moisture changes impact the distribution and spread of invasive and native species?

### 2.1.16 CQ5 - Land Surface Composition and Change

Rocks, soils, and minerals exposed on the terrestrial surface of the Earth reflect and emit energy that can be measured from space. Spaceborne measurements from HypsIRI will obtain the surface reflectance and surface emissivity of the Earth's surface. The reflectance and emissivity information from rocks, soils, and vegetation exhibits diagnostic features at various wavelengths that provide a means for their remote discrimination and

identification. These features are caused by the interaction of electromagnetic energy with the atoms and molecules that make up the material. For example different Si-O bonded structures vary in their interaction with thermal infrared light (8–12  $\mu\text{m}$ ). Collectively, the Si-O spectral features in the thermal infrared are referred to as the reststrahlen band. Reststrahlen bands are diagnostic of silicate minerals such as quartz and can be used to map quartz and silica-rich rocks (Figure 16).

Molecular vibrational processes of Al-O-H,  $\text{CO}_3$ , MgO-H, and H-O-H produce absorption features in the 2.0 to 2.5  $\mu\text{m}$  region that can be used to map clay, carbonate, amphiboles, and evaporite minerals. (Hunt, 1977). Ferrous and ferric iron, typical in many rocks and soils, has electronic optical absorption features in the 0.5 to 1.85  $\mu\text{m}$  region. Thus, HypsIRI VNIR, SWIR, and TIR data will be used to map the composition of the surface of the Earth.

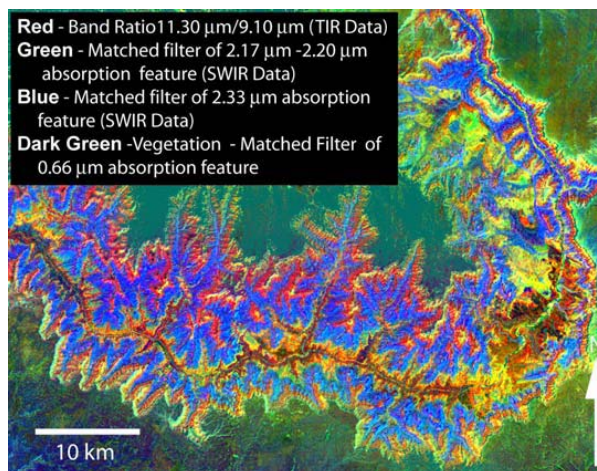


**Figure 16: False color composite HypsIRI simulated image of Grand Canyon, Arizona derived from TIR (red band - quartz-rich rocks), SWIR (green band - clay and muscovite-rich rocks; blue band - carbonate-rich rocks), and VNIR (dark green - green vegetation) data.**

Hydrothermal systems have produced many of the world's economic deposits of metallic ores. Different types of hydrothermal systems

produce different types of minerals and mineral distributions. For example, porphyry copper hydrothermal systems produce elliptical to circular halos of altered minerals such as kaolinite, alunite, sericite, and quartz (Lowell and Guilbert, 1970).

**Table 17: CQ5 Thematic Subquestions**

ID	Question
CQ5a	How does the surface mineralogy and soil composition relate to the plant physiology and function on the terrestrial surface of the Earth?
CQ5b	How is the composition of exposed terrestrial surface responding to anthropogenic and non anthropogenic drivers (desertification, weathering, and disturbance [e.g., logging, mining])?
CQ5c	How do types and distributions of altered rocks define regional trends in hydrothermal fluid flow for magmatic arcs and tectonic basins, better define hydrothermal deposit models, and assist in the discovery of new economic deposits?
CQ5d	How do regional trends of minerals and shale thermal maturity within basins better define depositional models and assist in the discovery of new hydrocarbon reserves?
CQ5e	How do changes in land composition affect coastal and inland aquatic ecosystems?

In addition, minerals such as alunite and minerals produced from the weathering of pyritic waste such as jarosite produce acid runoff (Crowley et al. 2001).

Thus, HypsIRI data will have important implications for the mapping and study of hydrothermal systems, and looking for changes related to anthropogenic and non-anthropogenic drivers such as the environmental monitoring of acid runoff from undisturbed hydrothermal deposits and from active and abandoned mines.

### 2.1.17 CQ6 - Human Health and Urbanization

Over the last 50 years, the world has witnessed a dramatic increase in its urban population. The expansion of cities, both in population and aerial extent, appears to be a relentless process whereby the world's urban population will rise more than 61% by 2030 (UNIS, 2004). Associated with this rapid rise

in worldwide urbanization is a concomitant impact on the local, regional, and even global environment, along with an exacerbation in health problems. HypsIRI measurements will be used to detect, observe, and measure changes in urban growth patterns and provide data that can elucidate how urbanization impacts the environment and human health.

**Table 18: CQ6 Thematic Subquestions**

ID	Question
CQ6a	How do land-surface characteristics (such as vegetation state, temperature, and land cover composition) affect, and how are they affected by, heat stress and drought, vector-borne diseases, and zoonotic diseases?
CQ6b	What changes can be observed and measured in emissivities of urban surfaces, and how do emissivities change for different cities around the world as they impact the urban heat island and associated land-atmosphere energy-balance characteristics?
CQ6c	How does the distribution of urban and peri-urban impervious surfaces affect regional energy-balance fluxes, hydrologic processes, and biogeochemical fluxes; and what is the response of ecosystems to these changes?

HypsIRI data can be used to evaluate multiple factors affecting human health, such as those contributing to environmental health hazards and contagious and infectious diseases. Moreover, HypsIRI data in combination with other data sources can provide spatial information on environmental conditions for understanding distributions of water-borne disease, air quality, soil, and vegetation as they influence community health and livestock.

Because of its enhanced hyperspectral capabilities in the VSWIR bandwidths and its multiple channels in the TIR, HypsIRI will provide much better data to improve modeling of urban characteristics around the world. One of the issues that has been problematic in the past is retrieving accurate measurements of temperature, albedo, and emissivity for specific surfaces across the complex and heterogeneous urban landscape. Because of its bandwidth design, HypsIRI will facilitate

the derivation of temperature, albedo, and emissivities for surfaces that are the “building blocks” of the urban environment. Figure 17 provides an example of detailed temperature and albedo measurements of the urban surface for Atlanta, Georgia. These data were derived from a multispectral VSWIR and TIR (9–12  $\mu\text{m}$ ) aircraft sensor.

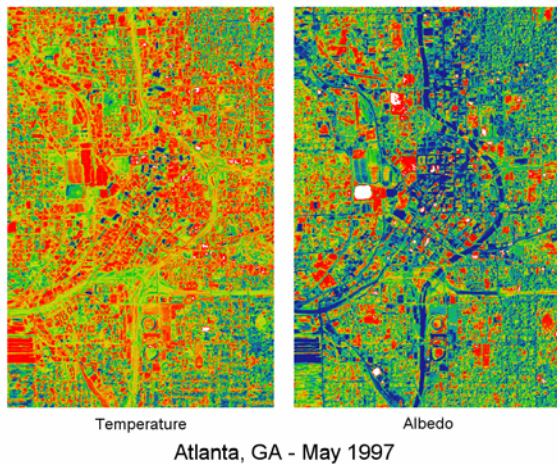


**Figure 17: Temperature and albedo measurements for the Atlanta, GA central business district as derived from multispectral aircraft data (Quattrochi et al. 2009)**

HyspIRI will expand this kind of information by providing hyperspectral data at regular intervals to better characterize the visible, near-IR, and thermal attributes of urban-specific surfaces with more precision to enable better modeling of urban energy balance characteristics, including emissivities.

HyspIRI will also fill the role of the low Earth orbit (LEO) "Special Event Imager" promoted by the NRC Panel on Human Health and Security, providing multispectral thermal infrared image data with a spatial resolution of 60 m and a revisit cycle of 5 days at the Equator. For mid- to high-latitude regions, such as the United States, the revisit times will be shorter than 5 days.

## 2.2 Science Traceability Matrixes

The STMs were developed by determining the initial measurement requirements for each of the science subquestions and overarching questions (see Table 2 – Table 18). All of the individual measurement requirements were grouped together to produce a set of science traceability matrixes that were subsequently used to determine the system-level measurement requirements. This was done in an iterative manner as outlined in Figure 18. At the workshop, breakout sessions reviewed each science-traceability matrix for an associated overarching question. Any updates made are reflected in the science-traceability matrixes presented in Appendix D.

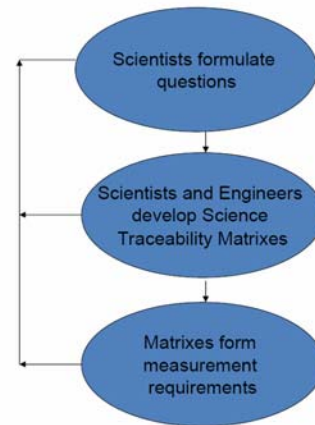


**Figure 18: Process for developing the Science-Traceability Matrixes.**



### 3 Measurement Requirements

The STMs helped determine the system-level requirements for the HypSIRI instruments. The system-level requirements for the VSWIR and TIR instruments are presented in Table 19 and Table 20, respectively.

#### 3.1 VSWIR Instrument

The VSWIR instrument will acquire data between 380 and 2500 nm in 10-nm contiguous bands. The position of these bands will be known to 0.5 nm. The instrument performance was modeled for several different input radiances, and these are shown in Figure 19 for several different benchmark radiances. The instrument will have low polarization sensitivity and low scattered light. One of the most challenging measurement conditions is open water where the signal from the water is very small. In addition, open water can produce sunglint under certain viewing geometries, and this can cause instrument saturation. The effect of sunglint is minimized by pointing the instrument 4 degrees in the backscatter direction. The nominal data collection scenario involves observing the land and coastal zone to a depth of < 50 m at full spatial and spectral resolution and transmitting these data to the ground.

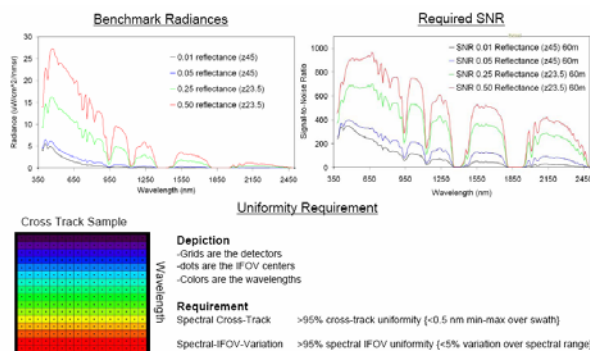


**Figure 19: HypSIRI-VSWIR Key Signal-to-Noise and Uniformity Requirements.**

Over the open ocean, data will be averaged to a spatial resolution of 1 km and be

transmitted to the ground. All data will be quantized at 14 bits. The instrument will have swath width of 145 km with a pixel spatial resolution of 60 m resulting in a temporal revisit of 19 days at the Equator. The nominal overpass time is 11 a.m., but this may be adjusted by as much as  $\pm 30$  minutes to minimize the effects of sunglint.

The absolute radiometric accuracy requirement is greater than 95%, and this will be maintained by using an onboard calibrator as well as monthly lunar views and periodic surface calibration experiments.

#### 3.2 TIR Instrument

The TIR instrument will acquire data in eight spectral bands, seven of these are located in the thermal infrared part of the spectrum between 7 and 13  $\mu\text{m}$ , and the remaining band is located in the mid infrared part of the electromagnetic spectrum around 4  $\mu\text{m}$ . The center position and width of each band is given in Table 20. The exact spectral location of each band was based on the measurement requirements identified in the science-traceability matrices, which included recognition that other sensors were acquiring related data such as ASTER and MODIS. HypSIRI will contribute to maintaining a long time series of these measurements. For example the positions of three of the TIR bands closely match the first three thermal bands of ASTER, and the positions of two of the TIR bands of MODIS typically used for split-window type applications (ASTER bands 12–14 and MODIS bands 31 and 32).

A key science objective for the TIR instrument is the study of hot targets (volcanoes and wildfires), so the saturation temperature for the 4- $\mu\text{m}$  channel is set high (1400 K) whereas the saturation temperatures for the thermal infrared channels are set at 400 K.

Table 19: VSWIR Measurement Characteristics

<b>Visible Shortwave Infrared Measurement Characteristics</b>	
<b>Spectral</b>	
Range	380 to 2500 nm in the solar reflected spectrum
Sampling	10 nm {uniform over range}
Response	<10 nm (full-width-at-half-maximum) {uniform over range}
Accuracy	<0.5 nm
<b>Radiometric</b>	
Range & Sampling	0 to $1.5 \times$ max benchmark radiance, 14 bits measured
Accuracy and stability	>95% absolute radiometric, 98% on-orbit reflectance, 99.5%
Precision (SNR)	See spectral plots at benchmark radiances
Linearity	>99% characterized to 0.1 %
Polarization	<2% sensitivity, characterized to 0.5 %
Scattered Light	<1:200 characterized to 0.1%
<b>Spatial</b>	
Range	>145 km (12 degrees at ~700 km altitude)
Cross-Track Samples	>2400
Sampling	60 m
Response	60 m sampling (FWHM)
<b>Uniformity</b>	
Spectral Cross-Track	>95% cross-track uniformity {<0.5 nm min-max over swath}
Spectral-IFOV-Variation	>95% spectral IFOV uniformity {<5% variation over spectral range}
<b>Temporal</b>	
Orbit Crossing	11 am sun synchronous descending
Global Land Coast Repeat	19 days at equator
Rapid Response Revisit	3 days (cross-track pointing)
<b>Sunlint Avoidance</b>	
Cross Track Pointing	4 degrees in backscatter direction
<b>On Orbit Calibration</b>	
Lunar View	1 per month {radiometric}
Solar Cover Views	1 per week {radiometric}
Surface Cal Experiments	3 per year {spectral & radiometric}
<b>Data Collection</b>	
Land Coverage	Land surface above sea level excluding ice sheets
Water Coverage	Coastal zone –50 m and shallower
Solar Elevation	20 degrees or greater
Open Ocean	Averaged to 1-km spatial sampling
Compression	3:1 lossless

Table 20: TIR Measurement Characteristics

<b>Thermal Infrared Measurement Characteristics</b>	
<b>Spectral</b>	
Bands (8) $\mu\text{m}$	3.98 $\mu\text{m}$ , 7.35 $\mu\text{m}$ , 8.28 $\mu\text{m}$ , 8.63 $\mu\text{m}$ , 9.07 $\mu\text{m}$ , 10.53 $\mu\text{m}$ , 11.33 $\mu\text{m}$ , 12.05 $\mu\text{m}$
Bandwidth	0.084 $\mu\text{m}$ , 0.32 $\mu\text{m}$ , 0.34 $\mu\text{m}$ , 0.35 $\mu\text{m}$ , 0.36 $\mu\text{m}$ , 0.54 $\mu\text{m}$ , 0.54 $\mu\text{m}$ , 0.52 $\mu\text{m}$
Accuracy	<0.01 $\mu\text{m}$
<b>Radiometric</b>	
Range	Bands 2–8 = 200 K – 400 K; Band 1= 1400 K
Resolution	< 0.05 K, linear quantization to 14 bits
Accuracy	< 0.5 K 3-sigma at 250 K
Precision (NEdT)	< 0.2 K
Linearity	>99% characterized to 0.1 %
<b>Spatial</b>	
IFOV	60 m
MTF	>0.65 at FNy
Scan Type	Push-Whisk
Swath Width	600 km ( $\pm 25.5^\circ$ at 623 km altitude)
Cross Track Samples	10,000
Swath Length	15.4 km ( $\pm 0.7$ degrees at 623 km altitude)
Down Track Samples	256
Band to Band Co-Registration	0.2 pixels (12 m)
Pointing Knowledge	1.5 arcsec (0.1 pixels)
<b>Temporal</b>	
Orbit Crossing	11 a.m. Sun synchronous descending
Global Land Repeat	5 days at Equator
<b>On Orbit Calibration</b>	
Lunar views	1 per month {radiometric}
Blackbody views	1 per scan {radiometric}
Deep Space views	1 per scan {radiometric}
Surface Cal Experiments	2 (day/night) every 5 days {radiometric}
Spectral Surface Cal Experiments	1 per year
<b>Data Collection</b>	
Time Coverage	Day and Night
Land Coverage	Land surface above sea level
Water Coverage	Coastal zone minus 50 m and shallower
Open Ocean	Averaged to 1-km spatial sampling
Compression	2:1 lossless

The temperature resolution of the thermal channels is much finer than the mid-infrared channel, which (due to its high saturation temperature) will not detect a strong signal until the target is above typical terrestrial temperatures. All the TIR channels are quantized at 14 bits.

The TIR instrument will have a swath width of 600 km with a pixel spatial resolution of 60 m resulting in a temporal revisit of 5 days at the equator. The instrument will be on both day and night, and it will acquire data over the entire surface of the Earth. Like the VSWIR, the TIR instrument will acquire full spatial resolution data over the land and coastal oceans (to a depth of < 50 m), but over the open oceans the data will be averaged to a

spatial resolution of 1 km. The large swath width of the TIR will enable multiple revisits of any spot on the Earth every week (at least 1 day view and 1 night view). This is necessary to enable monitoring of dynamic or cyclical events such as volcanic hotspots or crop stress associated with water availability.

The radiometric accuracy and precision of the instrument are 0.5 K and 0.2 K, respectively. This radiometric accuracy will be ensured by using an on-board blackbody and view to space included as part of every row of pixels (60 m  $\times$  600 km) observed on the ground. There will also be periodic surface validation experiments and monthly lunar views.

## 4 Mission Concept

The HypsIRI satellite will be put in a Sun synchronous, low Earth orbit. The overpass time is expected to be 11:00 a.m.  $\pm$  30 minutes. As noted in Table 19 and Table 20, the VSWIR has a 19-day revisit at the Equator, and the TIR has a 5-day revisit at the Equator. Since the TIR is on both day and night, it acquires 1 daytime image every 5 days and 1 nighttime image every 5 days. The current altitude for the spacecraft is 626 km at the Equator.

The number of acquisitions for different parts of the Earth in a 19-day cycle is shown in Figure 20. The figure is color-coded such that areas that are green meet the requirement and areas that are light blue, dark blue, and black exceed the requirement. Examination of the TIR map indicates that as one moves poleward the number of acquisitions exceeds the requirements with daily coverage at the poles. No data will be acquired poleward of 83° N and 83° S in the VSWIR since this is an inclined orbit. Similarly no data are acquired poleward of 85° N and 85° S in the TIR. The slightly more poleward extension of the TIR instrument is due to its larger swath width.

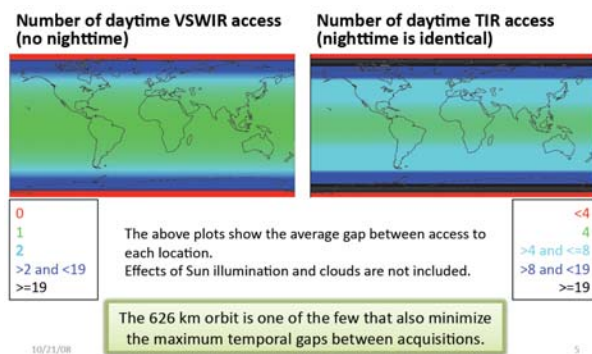


Figure 20: Number of image acquisitions in 19 days.

VSWIR data acquisitions are also limited by the maximum Sun elevation angle with no data being acquired when the Sun elevation angle is less than 20 degrees (Figure 21).

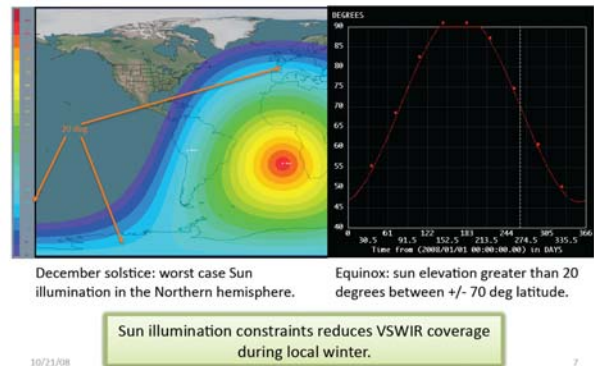


Figure 21: Illustration of the Sun illumination at the winter solstice.

The acquisition scenario for the HypsIRI mission is driven by target maps, with pre-defined maps controlling the acquisition. As noted earlier, the instruments are always on; however, they store data at either high-resolution mode (maximum spatial and spectral) or low-resolution mode. High-resolution mode data are acquired over the land and coastal waters shallower than 50 m. Low-resolution mode data are acquired over the rest of the oceans. The low resolution mode returns data are averaged or sub-sampled to 1 km. This target-map-driven strategy combined with high- and low-resolution modes minimizes the cost of mission operations allowing the instruments to acquire data in a near-autonomous fashion.

The satellite also includes an Intelligent Data Payload (IDP) with a direct broadcast capability that taps into the data feed from the instruments and allows a small subset of the data to be downloaded in real time. The IDP is independent of the onboard data recording and storage system, and it connects to the data stream to pull out the desired wavelengths for direct broadcast. The IDP has no storage capacity. The onboard data recording and storage system takes the data acquired in either low- or high-resolution mode and downlinks them to Earth. These data are then

sent to the appropriate Distributed Active Archive Center (DAAC) for further processing into the different data products.

Table 21 shows the HypsIRI data volume including the rate reduction associated with the VSWIR illumination requirement, compression, and overhead. The continuous averaged data rate is 65 Mbps, which results in a data volume of 372 Gb/orbit and 5.5 Tb/day. Compared to the current Earth Observing System (EOS) missions, the HypsIRI data rates are higher, but they are comparable to other, more recently launched, satellite missions such as WorldView-1 with a data volume of 331 Gb/orbit. The HypsIRI satellite will have an onboard storage capacity of 3 Tb (WorldView-1 has 2.2 Tb of onboard storage).

**Table 21: HypsIRI Data Volume, includes illumination constraints for VSWIR, compression and overhead.**

	VSWIR	TIR
<b>Rate (Mbps)</b>	288.5	59.2
<b>Duty cycle ratio</b>	0.148	0.400
<b>Effective rate</b>	42.700	23.672
<b>Overhead</b>	10%	10%
<b>Average rate with overhead</b>	46.970	26.039
<b>Obstruction ratio</b>	0.2	0
<b>After screening</b>	37.576	26.039

In the current configuration HypsIRI data will be downloaded using Dual X band, which will be capable of download rates of 600 Mbps. Other options, such as Ka band, are also being considered.

## 5 Data Products and Algorithms

The product-level definitions for the HypsIRI mission are identical to those in use by EOS today. These data product levels are briefly summarized below:

- \* Level 0--Reconstructed unprocessed instrument/payload data at full resolution; any and all communications artifacts (e.g., synchronization frames, communications headers) removed.

- \* Level 1A--Reconstructed unprocessed instrument data at full resolution, time-referenced, and annotated with ancillary information, including radiometric and geometric calibration coefficients and georeferencing parameters (i.e., platform ephemeris) computed and appended, but not applied, to the Level 0 data.

- \* Level 1B--Level 1A data that have been processed to sensor units.

- \* Level 2--Derived geophysical variables at the same resolution and location as the Level 1 source data.

- \* Level 3--Variables mapped on uniform space-time grid scales, usually with some completeness and consistency.

- \* Level 4--Model output or results from analyses of lower-level data (i.e., variables derived from multiple measurements).

For the HypsIRI mission, it is anticipated that the project will provide the Level 0 through Level 2 data, whereas the Level 3 and above data will be provided by the scientific community. The Level 1B data for HypsIRI will be geolocated radiance at sensor. Note, the data will not be orthorectified. In other words we will know the latitude and longitude for any given pixel, but the image pixels will not be resampled to be on a defined grid and of equal size. The level 2 data will include surface radiance, surface reflectance, surface

temperature, and surface emissivity. There will also be two cloud masks, one for the VSWIR and the other for the TIR. Two masks are necessary due to the difference in the swath width of the VSWIR and TIR sensors. The size of data granules has not been determined yet, but they will be selected to make it straightforward to work with both the VSWIR and TIR products. The Level 0 though Level 2 products will be treated as standard products (i.e., produced for all scenes), whereas the Level 3 and above products will be considered as special products, i.e., produced for a limited time or region.

It is expected that the Level 0 through Level 2 data will be developed at the Science Data System and will be stored at a Distributed Active Archive Center (DAAC). The Science Data System will be developed later in the project.

The current HypsIRI mission includes a direct broadcast capability, which will allow any user with the appropriate antenna to download a subset of the HypsIRI data stream to a local ground station. It is expected that distributed software will be developed to mimic the software that produces the standard products. This will enable direct broadcast users access to HypsIRI products in near real time. The data latency for the standard products has not been determined, but it is anticipated that it will be on the order of a few days to one week.



## 6 Synergies

### 6.1 VSWIR/TIR Instruments

The combination of a VSWIR imaging spectrometer and a TIR scanner on the same platform offers the opportunity to acquire some unique data sets that will be used to answer the combined science questions. Although the baseline mission concept includes routine acquisition of nighttime data using the TIR scanner, some of the combined science questions will also require the simultaneous acquisition of nighttime VSWIR data (for selected targets and therefore a limited data volume). High-temperature subjects such as vegetation fires and active lavas emit prodigious amounts of spectral radiance at VSWIR wavelengths. Importantly, at night, this self emissive radiance signal is uncontaminated by reflected sunlight. By acquiring nighttime VSWIR and TIR data, HypsIRI will provide thermal radiance spectra for these targets covering the entire wavelength region of 0.4 to 14  $\mu\text{m}$ . This is important for determining, for example, wildfire combustion temperatures, lava flow temperatures, and lava cooling rates. A mission operations concept that allows for the targeted acquisition of VSWIR data at night will also allow HypsIRI to study urban night lights.

The combination of VSWIR imaging spectrometer and TIR scanner data also provides a promising technique to detect and monitor urban heat islands, which have arisen as a serious issue due to urban expansion and rural land conversion. The combined VSWIR and TIR data will be crucial to obtain regional estimates of evapotranspiration (ET) for climate studies, weather forecasts, hydrological surveys, ecological monitoring, and water resource management.

Synergistic applications of optical spectroscopy and thermal emissivity satellite

data are of a key importance among user communities for the development of improved and more effective operational monitoring system of natural resources, including vegetation, soil, water and natural disaster assessments. HypsIRI will provide the critical information for two of the six interdisciplinary NASA Science Focus Areas: Carbon Cycle and Ecosystems, and Water and Energy Cycle. Information regarding these two Science Focus Areas would enable critical understanding and forecasting of a third Science Focus Area, Climate Variability and Change.

### 6.2 Other Missions and Programs

Much of the science that serves as the foundation for the NRC Decadal Survey recommendation for HypsIRI is a result of the use of antecedent data from both aircraft-based and spacecraft-based instruments. In particular, the VSWIR sensor science has benefited significantly by the airborne AVIRIS instrument and the spaceborne Hyperion instrument on the Earth Observing-One (EO-1) platform. Similarly, the TIR instrument benefited from the development of the airborne MODIS/ASTER Airborne Simulator (MASTER) instrument and the spaceborne ASTER instrument on the Terra platform (previously called EOS AM-1).

The AVIRIS program contributed two decades of instrument refinements, image collections over research sites, and development of appropriate imaging spectroscopy processing algorithms. Similarly, the airborne MASTER instrument examined a variety of surfaces, and led to development of techniques for thermal image processing. Both of these aircraft sensors have acquired data over a range of spatial resolutions (2–50 m), depending on the flight altitude. However, the satellite instruments have obtained observations at specified spatial

and temporal scales: for Hyperion, 30 m and potentially  $\leq 16$  day repeats; for ASTER, 90 m collected <weekly. With eight years of Hyperion VSWIR (since 2000) imagery collected at sites around the world, a wide range of science applications have been demonstrated. Likewise, the spaceborne ASTER instrument has provided a number of years of selected late-morning thermal observations at 90-m spatial resolution in conjunction with 8 VSWIR bands at 15–30m spatial resolutions, and also paired with its platform companion, the Moderate Resolution Imaging Spectrometer (MODIS), collecting multispectral VNIR and thermal data at 250–1000 m depending on the bands.

Existing data from all four instruments (ASTER, AVIRIS, Hyperion, and MASTER) are being made freely available for researchers interested in generating precursor datasets for HypsIRI. Also, they can be used for algorithm development. We are also looking forward to the completion of new airborne instruments such as the Hyperspectral thermal emission spectrometer (HyTES) instrument, which is being developed to help prepare for HypsIRI data. Representatives of the Airborne Science Program Airborne Sensor Facility informally presented an analysis of past coincident data collects using AVIRIS and MASTER on the same aircraft at the workshop, and the attendees agreed on the high value of these data and the importance of continued coincident airborne data collects using these instruments over a variety of cover types in order to better assess basic instrument requirements and to provide datasets for development and validation of algorithms for developing the various data products.

The 2009 NASA Research Opportunities in Space and Earth Sciences (ROSES) solicitation calls for proposals using existing spaceborne and airborne imagery for HypsIRI preparatory science.

In addition in 2009, the mission will benefit greatly by already planned AVIRIS and MASTER flights on the NASA ER-2 and Twin Otter aircraft. A much more extensive science campaign encompassing a ridge-to-reef scenario was suggested for 2010, some component of which could be competed through a ROSES solicitation. In the future, synergies with other satellite missions should also be examined, such as NPOESS/VIIRS (launch in 2011), Landsat-8 (the Landsat Data Continuity Mission, LDCM) to be launched in late 2012, and three imaging spectrometers planned for launch in 2011–2013 by Germany, Italy, and India.

## 7 Conclusions and Recommendations

The HypsIRI workshop re-affirmed the importance and desirability of the HypsIRI mission concept to conduct new and unprecedented science targeted at terrestrial and aquatic ecosystems and the interactions between these ecosystems and anthropogenic and natural forcing functions.

The concept would provide high spatial, spectral, and temporal resolution visible through thermal infrared data of the land surface of the Earth and coastal regions (defined by a water depth of < 50m). Data with the same spectral and temporal resolution but lower spatial resolution would be provided for the open ocean with a depth of > 50m. The measurements would be used to extract the surface spectral reflectance, emissivity and temperature that would be used to address a core set of scientific questions related to research, operations, and their associated societal benefits. The study found the mission proposed by the Decadal Survey could be readily implemented with some small modifications, which further enhanced the science return from the mission.

Several key conclusions resulted from the workshop:

- HypsIRI provides a unique capability to address a set of specific scientific questions about global ecosystems, habitats, biodiversity, and hazards, and their response to anthropogenic or natural changes.
- HypsIRI will help integrate terrestrial and aquatic (inland, coastal, and oceanic) ecosystem studies, and allow assessments at spatial scales relevant to resource use by humans.
- The instrument design is capable of meeting the initial science measurement requirements.
- There is an initial set of instrument measurement requirements for

HypsIRI, which are traceable to the early scientific requirements for the mission.

- Significant heritage exists from both a design and risk-reduction standpoint for both instruments. This heritage includes missions such as the Moon Mineralogy Mapper, Hyperion, and the Advanced Spaceborne Thermal Emission and Reflection Radiometer (ASTER), as well as the associated algorithms to deliver the Level 0 through Level 2 data products.
- There are no technology “show stoppers,” and the mission is ready for implementation at the earliest opportunity.
- HypsIRI complements measurements from the DESDynI, ACE, and GEO-CAPE missions, each of which addresses very different spatial scales compared to the local and landscape scales observable with HypsIRI.

Next steps identified by the Science Study Group and affirmed at the workshop include:

- Defining the requirements for *in situ*, tower, and aircraft instrumentation to support HypsIRI
- Developing spectral libraries to support the reduction and analysis of HypsIRI data
- Developing simulated HypsIRI data sets for algorithm development and testing
- Evaluating how data from HypsIRI can be used synergistically with data from other instruments

There was a strong consensus that the HypsIRI mission as recommended by the Decadal Survey would enable the intended science. The mission was seen as being clearly

defined and ready for implementation at the first available opportunity.

## 8 References

- Allen, R. G., M. Tasumi, A. Morse, R. Trezza, J. L. Wright, W. G. M. Bastiaanssen, W. J. Kramber, I. Lorite, and C. W. Robison (2007). Satellite-based energy balance for mapping evapotranspiration with internalized calibration (METRIC). *Applications, J. Irrig. Drainage Eng.*, doi:10.1061/(ASCE) 0733-9437(2007)133:4(395).
- Anderson, G. L., R. I. Carruthers, S. K. Ge, and P. Gong (2005). Monitoring of invasive Tamarix distribution and effects of biological control with airborne hyperspectral remote sensing. *International Journal of Remote Sensing* 26:2487-2489.
- Anderson, M. C., J. M. Norman, J. R. Mecikalski, J. P. Otkin, and W. P. Kustas (2007). A climatological study of evapotranspiration and moisture stress across the continental U.S. based on thermal remote sensing: II. Surface moisture climatology. *J. Geophys. Res.*, 112, D11112, doi:11110.11029/12006JD007507.
- Apan, A., A. Held, S. Phinn, and J. Markley (2004). Detecting sugarcane 'orange rust' disease using EO-1 Hyperion hyperspectral imagery. *International Journal of Remote Sensing* 25:489-498.
- Asner, G.P.,(1998). Biophysical and biochemical sources of variability in canopy reflectance. *Remote Sensing of Environment* 64(3): 234-253.
- Asner, G.P. and P.M. Vitousek (2005). Remote analysis of biological invasion and biogeochemical change. *Proceedings of the National Academy of Sciences* 102(12):4,383-4,386.
- Asner, G. P., R. E. Martin, K. M. Carlson, U. Rascher, and P. M. Vitousek (2006). Vegetation-climate interactions among native and invasive species in Hawaiian rainforest. *Ecosystems* 9:1106-1117.
- Bachmann, C.M., T.F. Donato, G.M. Lamela, W.J. Rhea, M.H. Bettenhausen, R.A. Fusina, K.R. Du Bois, J.H. Porter, B.R. Truitt (2002). Automatic classification of land cover on Smith Island, VA, using HyMAP imagery. *IEEE Interactions on Geoscience and Remote Sensing* 40(10):2313-2330.
- Berg, E.E., J.D. Henry, C.L. Fastie, A.D. De Volder, S.M. Matsuoka, (2006). Spruce beetle outbreaks on the Kenai Peninsula, Alaska, and Kluane National Park and Reserve, Yukon Territory: relationship to summer temperatures and regional differences in disturbance regimes. *For. Ecol. Manage.* 227: 219-232.
- Berthelote, A.R., Prakash, A., and J. Dehn (2008). An empirical function to estimate the depths of linear hot sources: Applied to the Kuhio Lava tube. *Hawaii. Bulletin of Volcanology* 70 (7): 813-824.
- Bidigare, R. R., J. H. Morrow, and D. A. Kiefer (1989). Derivative analysis of spectral absorption by photosynthetic pigments in the western sargasso sea. *Journal of Marine Research* 47(2): 323-341.
- Brando, V. E., and A. G. Dekker (2003). Satellite hyperspectral remote sensing for estimating estuarine and coastal water quality. *IEEE Transactions on*

- Geoscience and Remote Sensing* 41: 1378–1387.
- Carlson, K.M., G.P. Asner, R. Flint Hughes, R., Ostertag, and R.E. Martin, (2007). Hyperspectral Remote Sensing of Canopy Biodiversity in Hawaiian Lowland Rainforests. *Ecosystems* 10: 536–549.
- Castro-Esau, K. L., G. A. Sanchez-Azofeifa, and T. Caelli (2004). Discrimination of lianas and trees with leaf-level hyperspectral data. *Remote Sensing of Environment* 90: 353–372.
- CDC, 2005. Heat-related mortality – Arizona, 1993-2002 and United States, 1979-2002. *MMWR – Morbidity and Mortality Weekly Report*. 54(25): 628–630.
- Claudio H.C., J.A. Gamon, Y. Cheng, D. Fuentes, A.F. Rahman, H.-L. Qiu, D.A. Sims, H. Luo, W.C. Oechel (2006). Monitoring drought effects on vegetation water content and fluxes in chaparral with the 970nm water band index. *Remote Sensing of Environment*. 103:304–311.
- Coops, N., M. Stanford, K. Old, M. Dudzinski, D. Culvenor, and C. Stone (2003). Assessment of dothistroma needle blight of *Pinus radiata* using airborne hyperspectral imagery. *Phytopathology* 93: 1524–1532.
- Craig, S. E., S. E. Lohrenz, Z. P. Lee, K. L. Mahoney, G. J. Kirkpatrick, O. M. Schofield, and R. G. Steward (2006). Use of hyperspectral remote sensing reflectance for detection and assessment of the harmful alga, *Karenia brevis*. *Appl. Opt.* 45:5 414–5425.
- Crowley, J.K., J.C. Mars, and J.M. Hammarstrom (2001). *Airborne Imaging Spectrometer and Field Spectroscopic Studies of Mine Wastes at the Elizabeth Mine, Vermont*. Society of Economic Geologists, Guidebook Series, 35, 249–253.
- Curran, P.J. (1989). Remote sensing of foliar chemistry. *Remote Sens. Environ.* 30(3): 271–278.
- Datt, B., T. R. McVicar, T. G. Van Niel, D. L. B. Jupp, and J. S. Pearlman (2003). Preprocessing EO-1 Hyperion hyperspectral data to support the application of agricultural indexes. *IEEE Transactions on Geoscience and Remote Sensing* 41: 1246–1259.
- Delmelle, P., and Bernard, A. (2000). Volcanic lakes. In: Sigurdsson, Houghton, McNutt, Rymer, Stix (Eds.), *The Encyclopedia of Volcanoes*, Academic Press, London, pp. 877–895.
- Dennison, P.E., and Roberts, D.A. (2003a). Endmember Selection for Multiple Endmember Spectral Mixture Analysis using Endmember Average RMSE. *Remote Sensing of Environment*, 87(2-3): 123–135.
- Dennison, P.E., and Roberts, D.A. (2003b). The Effects of Vegetation Phenology on Endmember Selection and Species Mapping in Southern California Chaparral. *Remote Sens. Environ.*, 87(2-3): 123–135.
- Dennison, P. E., K. Charoensiri, D. A. Roberts, S. H. Peterson, and R. O. Green, (2006). Wildfire temperature and land cover modeling using hyperspectral

- data. *Remote Sensing of Environment* 100: 212–222.
- [DS, Decadal Survey; titles used informally] *Earth Science and Applications from Space: National Imperatives for the Next Decade and Beyond, 2007. Committee on Earth Science and Applications from Space: A Community Assessment and Strategy for the Future (2007)*. National Research Council, National Academies Press. Referred to as the Decadal Survey or NRC 2007.
- EPA (2006). *Excessive Heat Events Guidebook*. Report from the U.S. EPA, EPA 430-B-06-005, 52 pp.
- Foster, J. R., P. A. Townsend, and C. E. Zganjar (2008). Spatial and temporal patterns of gap dominance by low-canopy lianas detected using EO-1 Hyperion and Landsat Thematic Mapper. *Remote Sensing of Environment* 112: 2104–2117.
- Francis, P.W., C. Oppenheimer, and D.S. Stevenson (1993). Endogenous growth of persistently active volcanoes. *Nature*, 366: 554–557.
- Fraser, R. N. (1998). Hyperspectral remote sensing of turbidity and chlorophyll a among Nebraska sand hills lakes. *International Journal of Remote Sensing* 19: 1579–1589.
- Fuentes, D.A., J.A. Gamon, Y. Cheng, H.C. Claudio, H-L Qiub, Z. Mao, D.A. Sims, A.F. Rahman, W. O Luo, and H. Luo (2006). Mapping carbon and water vapor fluxes in a chaparral ecosystem using vegetation indices derived from AVIRIS. *Remote Sensing of the Environment*, 103:312–323.
- Gamon, J.A., C.B. Field, D.A. Roberts, S.L. Ustin, and V. Riccardo (1993). Functional patterns in an annual grassland during an AVIRIS overflight. *Remote Sensing of Environment* 44: 239—253.
- Gamon J.A., K. Kitajima, S.S. Mulkey, L. Serrano, S.J. Wright (2005). Diverse optical and photosynthetic properties in a neotropical forest during the dry season: implications for remote estimation of photosynthesis. *BioTropica* 37(4): 547–560.
- Garcia, M. and Ustin, S.L. (2001). Detection of inter-annual vegetation responses to climatic variability using AVIRIS data in a coastal savanna in California. *IEEE Transactions on GeoScience and Remote Sensing* 39: 1480–1490.
- Gates, D. M., H. J. Keegan, , J. C. Schleter, , and V. R. Weidner,(1965). Spectral properties of plants. *Applied Optics*, 4(1): 11–20.
- GEO (2007). *GEO Inland and Nearshore Coastal Water Quality Remote Sensing Workshop*. Switzerland. [http://www.earthobservations.org/meetings/20070327\\_29\\_water\\_quality\\_workshop\\_report.pdf](http://www.earthobservations.org/meetings/20070327_29_water_quality_workshop_report.pdf)
- Giardino, C., V. E. Brando, A. G. Dekker, N. Strombeck, and G. Candiani (2007). Assessment of water quality in Lake Garda (Italy) using Hyperion. *Remote Sensing of Environment* 109:183–195.
- Giglio, L., I. Csiszar, Á. Restás, , J.T. Morisette, , W. Schroeder, D. Morton, and C.O. Justice, (2008). Active Fire Detection and Characterization with the Advanced Spaceborne Thermal

- Emission and Reflection Radiometer (ASTER). *Remote Sensing of Environment*, doi:10.1016/j.rse.2008.03.003.
- Gitelson, A.A., J. Schalles, C.M. Hladik (2007). Remote chlorophyll-a retrieval in turbid productive estuarine: Chesapeake Bay case study. *Remote Sensing of Environment*, 109: 464–472.
- Glenn, N. F., J. T. Mundt, K. T. Weber, T. S. Prather, L. W. Lass, and J. Pettingill (2005). Hyperspectral data processing for repeat detection of small infestations of leafy spurge. *Remote Sensing of Environment* 95: 399–412.
- Goodin D. G., L. Han, R. N. Fraser, et al. (1993). Analysis of Suspended Solids in Water Using Remotely Sensed High Resolution Derivative Spectra. *Photogrammetric Engineering & Remote Sensing* 59 (4): 505–510.
- Gower, J., C. Hu, G. Borstad, and S. King (2006). Ocean color satellites show extensive lines of floating Sargassum in the Gulf of Mexico. *IEEE Trans. Geosci. Remote Sens.* 44: 3619–3625.
- Green, R. O. (1996). Estimation of biomass fire temperature and areal extent from calibrated AVIRIS spectra. *Summaries of the Sixth Annual JPL Airborne Earth Science Workshop*. JPL Publication 96-4, 1, Jet Propulsion Laboratory, Pasadena, California, 105–113.
- Haboudane, D., J. R. Miller, N. Tremblay, P. J. Zarco-Tejada, and L. Dextraze (2002). Integrated narrow-band vegetation indices for prediction of crop chlorophyll content for application to precision agriculture. *Remote Sensing of Environment* 81: 416–426.
- Hansen, J. (2008). Tipping point: Perspective of a climatologist. In *State of the Wild 2008-2009: A Global Portrait of Wildlife, Wildlands, and Oceans*. W. Woods, Ed. Wildlife Conservation Society/Island Press, Washington, DC, pp. 6–15.
- Hirano, A., M. Madden, and R. Welch (2003). Hyperspectral image data for mapping wetland vegetation. *Wetlands* 23: 436–448.
- Hochberg, E. J., and Atkinson, M. J. (2003). Capabilities of remote sensors to classify coral, algae, and sand as pure and mixed spectra. *Remote Sens. Environ.* 85: 174–189.
- Hochberg E.J, A.M. Apprill, M.J. Atkinson, R.R. Bidigare (2006). Bio-optical modeling of photosynthetic pigments in corals. *Coral Reefs* 25: 99–109.
- Hochberg E.J., and Atkinson, M.J. (2008). Coral reef benthic productivity based on optical absorptance and light-use efficiency. *Coral Reefs* 27: 49–59
- Hook, S. J., J. E. Dmochowski, K. A. Howard, L. C. Rowan, K. E. Karlstrom, and J. M. Stock (2005). Mapping variations in weight percent silica measured from multispectral thermal infrared imagery - Examples from the Hiller Mountains, Nevada, USA and Tres Virgenes-La Reforma, Baja California Sur, Mexico. *Remote Sensing of Environment*, 95: 273–289.
- Hu, C., K. L. Carder, and F. E. Muller-Karger, (2000). Atmospheric correction of SeaWiFS imagery: assessment of the use

- of alternative bands. *Appl. Opt.* 39: 3573-3581.
- Hu, C., F. E. Muller-Karger, C. Taylor, K. L. Carder, C. Kelble, E. Johns, and C. Heil (2005). Red tide detection and tracing using MODIS fluorescence data: A regional example in SW Florida coastal waters. *Remote Sens. Environ.* 97: 311–321.
- Hunt, G.R.,= (1977). Spectral signatures of particulate minerals in the visible and near infrared. *Geophysics* 42(3): 501–513.
- Hunt, G. R. (1980). Electromagnetic radiation: The communication link in remote sensing, in *Remote Sensing in Geology*, edited by B. S. Siegal and A. R. Gillespie, John Wiley, New York, pp. 5–45.
- Ichoku, C., and Kaufman, Y. J. (2005). A method to derive smoke emission rates from MODIS fire radiative energy measurements. I 43: 2636–2649.
- Ip, F., J. M. Dohm, V. R. Baker, T. Doggett, A. G. Davies, R. Castano, S. Chien, B. Cichy, R. Greeley, R. Sherwood, D. Tran, and G. Rabideau (2006). Flood detection and monitoring with the autonomous sciencecraft experiment onboard EO-1. *Remote Sensing of Environment* 101: 463–481.
- John Heinz Center (2007). *The State of the Nation's Ecosystems 2007: Measuring the Land, Waters, and Living Resources of the United States*. John Heinz III Center for Science, Economics and the Environment, Washington, DC.
- Jollineau, M. Y., and Howarth, P.J. (2008). Mapping an inland wetland complex using hyperspectral imagery, *International Journal of Remote Sensing*. 29(12):3609–3631.
- Judd, C., S. Steinberg, F. Shaughnessy, and G. Crawford (2007). Mapping salt marsh vegetation using aerial and hyperspectral imagery and linear unmixing in Humboldt Bay, California. *Wetlands* 27(4): 1144–1152.
- Kalacska, M., S. Bohman, G. A. Sanchez-Azofeifa, K. Castro-Esau, and T. Caelli. (2007). Hyperspectral discrimination of tropical dry forest lianas and trees: Comparative data reduction approaches at the leaf and canopy levels. *Remote Sensing of Environment* 109: 406–415.
- Kallio, K., T. Kutser, T. Hannonen, S. Koponen, J. Pulliainen, J. Vepsalainen, T. Pyhalahti (2001). Retrieval of water quality from airborne imaging spectrometry of various lake types in different seasons. *Science of the Total Environment* 268: 59–77.
- Kalma, J. D., T. R. McVicar, and M. F. McCabe (2008). Estimating land surface evaporation: A review of methods using remotely sensing surface temperature data. *Survey Geophys.*, DOI 10.1007/s10712-008-9037-z.
- Kasischke, E.S., and Stocks, B.J. (2000).. *Fire, Climate Change, and Carbon Cycling in the Boreal Forest. Ecological Studies*, Vol. 138, Springer, New York.
- Kaufman, Y. J., C. O. Justice, L. P. Flynn, J. D. Kendall, E. M. Prins, L. Giglio, D. E. Ward, W. P. Menzel, and A. W. Setzer, (1998). Potential global fire monitoring from EOS-MODIS. *Journal*

- of Geophysical Research* 103: 32215–32238.
- Kim, M. S., Y. R. Chen, and P. M. Mehl (2001). Hyperspectral reflectance and fluorescence imaging system for food quality and safety. *Transactions of the ASAE* 44: 721–729.
- Kutser, T. (2004). Quantitative detection of chlorophyll in cyanobacterial blooms by satellite remote sensing. *Limnology and Oceanography* 49: 2179–2189.
- Kutser, T., L. Metsamaa, N. Strombeck, and E. Vahtmae (2006). Monitoring cyanobacterial blooms by satellite remote sensing. *Estuarine Coastal and Shelf Science* 67: 303–312.
- LeBauer D.S., K.K. Treseder (2008). Nitrogen limitation of net primary productivity in terrestrial ecosystems is globally distributed. *Ecology* 89: 371–379.
- Lee, Z.P., B. Casey, R. Arnone, A. Weidemann, R. Parsons, M.J. Montes, B.C. Gao, W. Goode, C.O. Davis, and J. Dye (2007). Water and bottom properties of a coastal environment derived from Hyperion data measured from the EO-1 spacecraft platform. *Journal of Applied Remote Sensing* 1: DOI: 10.1117/1111.2822610
- Lowell, J.D., and Guilbert, J.M. (1970). Lateral and vertical alteration-mineralization zoning in porphyry ore deposits. *Economic Geology and the Bulletin of the Society of Economic Geologists* 65(4): 373–408.
- MacDonald, G.M. (2002). *Biogeography: Space, Time and Life*. John Wiley and Sons, New York. 518 p.
- McNeil, B. E., K. M. de Beurs, K. N. Eshleman, J. R. Foster, and P. A. Townsend. 2007. Maintenance of ecosystem nitrogen limitation by ephemeral forest disturbance: An assessment using MODIS, Hyperion, and Landsat ETM. *Geophysical Research Letters* 34, Art no. L19406, 5 pp.
- Marks, M., B. Lapin, and J. Randall (1994). *Phragmites australis (P. communis): Threats, management, and monitoring. Natural Areas Journal* 14: 285–294.
- Martin, M. E., L. C. Plourde, S. V. Ollinge, M. L. Smith, and B. E. McNeil (2008). A generalizable method for remote sensing of canopy nitrogen across a wide range of forest ecosystems. *Remote Sensing of Environment* 112: 3511–3519.
- Matthews, S. J., M. C. Gardeweg, and R.S.J. Sparks (1997). The 1984 to 1996 cyclic activity of Lascar volcano, northern Chile: Cycles of dome growth, dome subsidence, degassing, and explosive eruptions. *Bulletin of Volcanology* 59: 72–82.
- Melillo, J.M., C.B. Field, and B. Moldan (2003). *Interactions of the Major Biogeochemical Cycles: Global Change and Human Impacts. Scientific Committee on Problems of the Environment (SCOPE)*. Island Press Publishers, Washington, DC.
- Myneni, R.B., C.D. Keeling, C.J. Tucker, G. Asrar, and R.R. Nemani, (1997), Increased plant growth in the northern high latitudes from 1981 to 1991. *Nature* 386: 698–702.

- Noujdina, N., and Ustin, S.L. (2008). Mapping downy brome (*Bromus tectorum*) using multi-date AVIRIS data. *Weed Science* 56: 173-179.
- NRC 2007 (see DS or *Decadal Survey*)
- Ollinger, S.V., M.L. Smith, M.E. Martin, R.A. Hallett, C.L. Goodale, and J.D. Aber (2002). Regional variation in foliar chemistry and soil nitrogen status among forests of diverse history and composition. *Ecology*, 83, 339–355.
- Ollinger, S.V., O. Sala, G. Ågren, B. Berg, E. Davidson, C. Field, M. Lerdau, J. Neff, M. Scholes, R. Sterner (2003). New Frontiers in the Study of Element Interactions. In: Melillo and Field (Eds.), *Interactions of the Major Biogeochemical Cycles*, Scientific Committee on Problems of the Environment (SCOPE), Island Press Publishers, Washington, DC.
- Ollinger, S.V., and Smith, M-L. (2005). Net primary production and canopy nitrogen in a temperate forest landscape: An analysis using imaging spectroscopy, modeling and field data. *Ecosystems* 8: 760–778.
- Ollinger, S.V., A.D. Richardson, M.E. Martin, D.Y. Hollinger, S.E. Frolking, P.B. Reich, L.C. Plourde, G.G. Katul, J.W. Munger, R. Oren, M-L. Smith, K.T. Paw U, P.V. Bolstad, B.D. Cook, M.C. Day, T.A. Martin, R.K. Monson, H.P. Schmid. 2008. Canopy nitrogen, carbon assimilation and albedo in temperate and boreal forests: Functional relations and potential climate feedbacks. Proceedings of the National Academy of Sciences. 105(49): 19335–19340.
- Oppenheimer, C., P.W. Francis, D.A. Rothery, R.W.T. Carlton, and L.S. Glaze (1993). Infrared image analysis of volcanic thermal features: Lascar Volcano, Chile, 1984–1992. *Journal of Geophysical Research* 98: 4269–4286.
- Ouzounov, D., and Freund, F. (2004). Mid-infrared emission prior to strong earthquakes analyzed by remote sensing, *Adv. Space. Res.* 33: 268–273.
- Pengra, B. W., C. A. Johnston, and T. R. Loveland (2007). Mapping an invasive plant, *Phragmites australis*, in coastal wetlands using the EO-1 Hyperion hyperspectral sensor. *Remote Sensing of Environment* 108: 74–81.
- Phillips, O.L., R.V. Martinez, L. Arroyo, T.R. Baker, T. Killeen, S.L. Lewis, Y. Malhi, A.M. Mendoza, D. Neill, P.N. Vargas M. Alexiades, C. Ceron, A. Di Fiore, T. Erwin, A. Jardim, W. Palacios, M. Saldias, and B. Vinceti (2002). Increasing dominance of large lianas in Amazonian forests. *Nature* 418(6899): 770–774.
- Pontius, J., R. Hallett, and M. Martin (2005). Using AVIRIS to assess hemlock abundance and early decline in the Catskills, New York. *Remote Sensing of Environment* 97: 163–173.
- Pontius, J., M. Martin, L. Plourde, and R. Hallett (2008). Ash decline assessment in emerald ash borer-infested regions: A test of tree-level, hyperspectral technologies. *Remote Sensing of Environment* 112: 2665–2676.

- Pu, R., P. Gong, Y. Tian, X. Miao, R. I. Carruthers, and G. L. Anderson (2008). Invasive species change detection using artificial neural networks and CASI hyperspectral imagery. *Environmental Monitoring and Assessment* 140: 15–32.
- Quattrochi, D.A., Anupma Prakash, Mariana Eneva, Robert Wright, Dorothy K. Hall, Martha Anderson, William P. Kustas, Richard G. Allen, Thomas Pagano, and Mark F. Coolbaugh, 2009. Thermal Remote Sensing: Theory, Sensors, and Applications (Chapter 3). In *Manual of Remote Sensing, American Society for Photogrammetry and Remote Sensing*, (Jackson, Mark W., ed.), Falls Church, VA, (In Press).
- Ramsey, E., A. Rangoonwala, G. Nelson, R. Ehrlich, and K. Martella (2005a). Generation and validation of characteristic spectra from EO1 Hyperion image data for detecting the occurrence of the invasive species, Chinese tallow, *International Journal of Remote Sensing*, 26(8): 1611–1636.
- Ramsey, E., A. Rangoonwala, G. Nelson, and R. Ehrlich (2005b). Mapping the invasive species, Chinese tallow, with EO1 satellite Hyperion hyperspectral image data and relating tallow occurrences to a classified Landsat Thematic Mapper land cover map, *International Journal of Remote Sensing* 26(8): 1637–1657.
- Reich, P.B., B.A. Hungate, and Y. Luo (2006). Carbon-nitrogen interactions in terrestrial ecosystems in response to rising atmospheric carbon dioxide. *Ann. Rev. Ecol. Evol. System.* 37: 611–636.
- Ritchie, J.C., P.V. Zimba, and J.H. Everitt (2003). Remote Sensing Techniques to Assess Water Quality. *Photogrammetric Engineering and Remote Sensing* 69(6): 695–704.
- Roberts, D. A., R.O. Green, and J.B. Adams (1997). Temporal and spatial patterns in vegetation and atmospheric properties from AVIRIS. *Remote Sensing of Environment* 62: 223–240.
- Roberts, D. A., M. Gardner, R. Church, S. Ustin, G. Scheer, and R.O. Green (1998). Mapping chaparral in the Santa Monica mountains using multiple endmember spectral mixture models. *Remote Sensing of Environment* 65: 267–279.
- Roberts, D.A., S.L. Ustin, S. Ogunjemiyo, J. Greenberg, S.Z. Dobrowski, J. Chen, and T.M. Hinckley, (2004). Spectral and structural measures of Northwest forest vegetation at leaf to landscape scales, *Ecosystems* 7: 545–562.
- Rosso, P.H., S.L. Ustin, and A. Hastings, 2005. Mapping marshland vegetation of San Francisco Bay, California, using hyperspectral data. *International Journal of Remote Sensing* 26(23): 5169–5191.
- Sadro, S., M. Gastil-Buhl, J. Melack (2007). Characterizing patterns of plant distribution in a southern Californian salt marsh using remotely sensed topographic and hyperspectral data and local tidal fluctuations. *Remote Sensing of Environment* 110: 226–239.

- Sanchez-Azofeifa, G. A., and Castro-Esau, K. (2006). Canopy observations on the hyperspectral properties of a community of tropical dry forest lianas and their host trees. *International Journal of Remote Sensing* 27: 2101–2109.
- Saraf, Arun K., Vineeta Rawat, Priyanka Banerjee, Swapnamita Choudhury, Santosh K. Panda, Sudipta Dasgupta, and J. D. Das (2008), Satellite detection of earthquake thermal precursors in Iran, *Natural Hazards*, DOI DOI 10.1007/s11069-007-9201-7.
- Serrano, L., S. L. Ustin, D. A. Roberts, J. A. Gamon, , and J. Penuelas (2002). Deriving water content of chaparral vegetation from AVIRIS data. *Remote Sensing of Environment* 74(3): 570–581.
- Smith, L.C., G.M. MacDonald, A.A. Velichko, , D.W. Beilman, O.K. Borisova, , K.E. Frey, K.V. Kremenetski, and Y. Sheng (2004). Siberian peatlands, a net carbon sink and global methane source since the early Holocene. *I* 303: 353–356.
- Stone, C., L. Chisholm, and N. Coops (2001). Spectral reflectance characteristics of eucalypt foliage damaged by insects. *Australian Journal of Botany* 49: 687–698.
- Strachan, I. B., E. Pattey, and J. B. Boisvert (2002). Impact of nitrogen and environmental conditions on corn as detected by hyperspectral reflectance. *Remote Sensing of Environment* 80:213–224.
- Swayze, G. A., R. N. Clark, A. F. Goetz, T. G. Chrien, and N. S. Gorelick (2003). Effects of spectrometer band pass, sampling, and signal-to-noise ratio on spectral identification using the Tetracorder algorithm. *Journal of Geophysical Research-Planets* 108(E9), 5105. doi:10.1029/2002JE001975
- Thiemann, S., and Kaufmann, H. (2002). Lake water quality monitoring using hyperspectral airborne data - a semi-empirical multisensor and multitemporal approach for the Mecklenburg Lake District, Germany. *Remote Sensing of Environment* 81: 228–237.
- Thomas, V.; J. H. Treitz,;T. McCaughey, T. Noland, and L. Rich (2008). Canopy chlorophyll concentration estimation using hyperspectral and lidar data for a boreal mixed wood forest in northern Ontario, Canada. *International Journal of Remote Sensing* 29(4): 1029–1052.
- Treitz, P.M., and P. J. Howarth, P.J. (1999). Hyperspectral remote sensing for estimating biophysical parameters of forest ecosystems. *Progress in Physical Geography* 23: 359–390.
- Underwood, E., S. Ustin, and D. DiPietro (2003). Mapping nonnative plants using hyperspectral imagery. *Remote Sensing of Environment* 86: 150–161.
- Underwood, E.C., M.J. Mulitsch, J.A. Greenberg, M.L. Whiting, S.L. Ustin, S.C. Kefauver (2006). Mapping invasive aquatic vegetation in the Sacramento-San Joaquin Delta using hyperspectral imagery. *Environmental*

- Monitoring and Assessment* 121: 47–64. <http://www.westgov.org/wga/publicat/Water06.pdf>
- UNIS (2004). UN report says world urban population of 3 billion today expected to reach 5 billion by 2030, URL: <http://www.unis.unvienna.org/unis/pre/ssrels/2004/pop899.html>, United Nations Information Service, Vienna, Austria.
- USCOP (2004). U.S. Commission on Ocean Policy. 2004. An Ocean Blueprint for the 21st Century. Final Report of the U.S. Commission on Ocean Policy. Washington, DC, pp. 345, 404.
- Ustin S.L., D.A. Roberts, J.A. Gamon, G.P. Asner, and R.O. Green (2004). Using imaging spectroscopy to study ecosystem processes and properties. *Bioscience*, 54: 523–534.
- Vitousek, P.M., H.A. Mooney, J. Lubchenco, and J.M. Melillo (1997). Human Domination of Earth's Ecosystems. *Science* 277(5325): 494–499.
- Wang, M., and Shi, W. (2005). Estimation of ocean contribution at the MODIS near-infrared wavelengths along the east coast of the U.S.: Two case studies. *Geophys. Res. Lett.* 32: L13606, doi:10.1029/2005GL022917, 2005
- Wessman C. A., J.D. Aber, D.L. Peterson, and J.M. Melillo (1988). Remote sensing of canopy chemistry and nitrogen cycling in temperate forest ecosystems. *Nature* 333: 154–156.
- WGA (2006). Water Needs and Strategies for a Sustainable Future, 2006 report of the Western Governors Association (WGA). Available from <http://www.westgov.org/wga/publicat/Water08.pdf>
- WGA (2008). Water Needs and Strategies for a Sustainable Future: Next Steps, 2008 report of the Western Governors Association. Available from <http://www.westgov.org/wga/publicat/Water08.pdf>
- Wright I.J., P. K. Groom, B. B. Lamont, P. Poot, L. D. Prior, P. B. Reich, E.D. Schulze, E. J. Veneklaas and M. Westoby 2004. The worldwide leaf economics spectrum. *Nature* 428: 821–827.
- Wright, R., and Flynn, L.P. (2003). On the retrieval of lava flow surface temperatures from infrared satellite data. *Geology* 31: 893–896.
- Zarco-Tejada, P.J., S.L. Ustin, and M.L. Whiting, (2005a). Temporal and spatial relationships between within-field yield variability in cotton and high-spatial hyperspectral remote sensing imagery. *Agronomy Journal* 97: 641–653.
- Zarco-Tejada, P. J., A. Berjon, R. Lopez-Lozano, J. R. Miller, P. Martin, V. Cachorro, M. R. Gonzalez, and A. de Frutos (2005b). Assessing vineyard condition with hyperspectral indices: Leaf and canopy reflectance simulation in a row-structured discontinuous canopy. *Remote Sensing of Environment* 99: 271–287.

## 9 Appendices

### Appendix A – Acronyms

**abs cal:** Absolute Calibration

**AC:** Coastal Aquatic

**ACE:** Aerosol-Cloud-Ecosystems (Mission)

**ALEXI/DisALEXI:** Atmosphere-Land Exchange Inverse / Disaggregated Atmosphere-Land Exchange Inverse

**ASTER:** Advanced Spaceborne Thermal Emission and Reflection Radiometer

**AVHRR:** Advanced Very High Resolution Radiometer

**AVIRIS:** Airborne Visible Infrared Imaging Spectrometer

**cal/val:** Calibration/Validation

**CCSP:** Climate Change Science Program

**CDOM:** Colored Dissolved Organic Matter

**CQ:** Combined Question(s)

**DAAC:** Distributed Active Archive Center

**DesDynI:** Deformation, Ecosystems Structure, and Dynamics of Ice

**DS:** Decadal Survey

**EO-1** Earth Observing-1

**EOS :** Earth Observing System

**ET:** Evapotranspiration

**FG:** Functional Group

**FRP:** Fire Radiative Power

**FWHM:** Full Width at Half Maximum

**GDP:** Gross Domestic Product

**GEO:** Group on Earth Observations

**GEO-CAPE:** Geostationary Coastal and Air Pollution Events

**GEOS:** Global Earth Observation System of Systems

**GOES:** Geostationary Operational Environmental Satellite

**HAB:** Harmful Algal Bloom

**HyspIRI:** Hyperspectral Infrared Imager

**HyTES:** Hyperspectral thermal emission spectrometer

**ICESat-II:** Ice, Cloud, and Land Elevation Satellite II

**IDP :** Intelligent Data Payload

**IFOV:** Instantaneous Field of View

**InSAR:** Interferometric Synthetic Aperture Radar

**IOOS** : Integrated Ocean Observing System  
**IR**: Infrared  
**IOOS**: Integrated Ocean Observing System  
**LDCM**: Landsat Data Continuity Mission  
**LEO**: Low Earth Orbit  
**LST**: Land Surface Temperature  
**M3**: Moon Mineralogy Mapper  
**MASTER**: MODIS/ASTER Airborne Simulator  
**MCR**: Mission Concept Review  
**MODIS**: Moderate Resolution Imaging Spectroradiometer  
**NAS**: National Academy of Sciences  
**NASA**: National Aeronautics and Space Administration  
**NDVI**: Normalized Difference Vegetation Index  
**NE**: Noise-Equivalent  
**NEAT**: Noise-Equivalent Delta Temperature  
**NPOESS/VIIRS**: National Polar-orbiting Operational Environmental Satellite System / Visible Infrared Imaging Radiometer Suite  
**NOAA**: National Oceanographic and Atmospheric Administration  
**NPV**: Non-Photosynthetic Vegetation  
**NRC**: National Research Council  
**PET**: Potential Evapotranspiration  
**PFT**: Plant Functional Type  
**PV**: Photosynthetic Vegetation  
**NPV**: Non photosynthetic vegetation  
**ROSES**: Research Opportunities in Space and Earth Sciences  
**SAV**: Submerged Aquatic Vegetation  
**SCOPE**: Scientific Organization on Problems of the Environment  
**SEVIRI**: Spinning Enhanced Visible and InfraRed Imager  
**SNR**: Signal-to-Noise Ratio  
**SSG**: (HyspIRI) Science Study Group  
**STM**: Science Traceability Matrix  
**SWIR**: Short-Wave Infrared  
**T-E Separation**: Temperature-Emissivity Separation  
**TIR**: Thermal Infrared  
**TM**: (Landsat) Thematic Mapper  
**TQ**: Thermal Infrared Question(s)  
**UHI**: Urban Heat Island  
**UNIS**: United Nations Information Service

**USCOP:** U.S. Commission on Ocean Policy

**VIIRS:** Visible Infrared Imager Radiometer Suite

**VNIR :** Visible and Near Infrared

**VQ :** Visible Shortwave Infrared Question(s)

**VSWIR:** Visible Shortwave Infrared

**WGA:** Western Governors Association

## Appendix B - Workshop Agenda

### HyspIRI Workshop Agenda

Oct 21st-23rd, Courtyard Marriott (Monrovia)

#### Oct 21st

Start Time	Length	Title	Speaker
7:30:00 AM	00:30:00	Registration	
		Welcome and Overview of HyspIRI Science	
8:00:00 AM	00:15:00	Workshop	Woody Turner
		Overview of Decadal Survey Mission and	
8:15:00 AM	00:30:00	HyspIRI Plans and Status	Steve Neeck
8:45:00 AM	00:00:00	Review of Current Baseline HyspIRI Science Measurements Characteristics	
8:45:00 AM	00:30:00	VSWIR Science Measurement Specifications	Rob Green
9:15:00 AM	00:30:00	TIR Science Measurement Specifications	Simon Hook
9:45:00 AM	00:30:00	Review of HyspIRI Mission Characteristics	Francois Rogez
10:15:00 AM	00:30:00	BREAK	
		VQ1 – Pattern and Spatial Distribution of	
10:45:00 AM	00:15:00	Ecosystems and their Components	Dar Roberts
		VQ2 – Ecosystem Function, Physiology and	
11:00:00 AM	00:15:00	Seasonal Activity	Susan Ustin
11:15:00 AM	00:15:00	VQ3 - Biogeochemical Cycles	John Gamon
11:30:00 AM	00:15:00	VQ4 - Ecosystem Response to Disturbance	Greg Asner
11:45:00 AM	00:15:00	VQ5 – Ecosystems and Human Well-being	Betsy Middleton
		VQ6. Earth Surface and Shallow Water Bottom	
12:00:00 PM	00:15:00	Composition	Rob Green
12:15:00 PM	01:00:00	LUNCH	
1:15:00 PM	00:15:00	Science Traceability Matrices 101	Simon Hook
1:30:00 PM	01:15:00	VSWIR Breakout Session 1 (see tab)	Breakout leads
2:45:00 PM	00:30:00	BREAK	
3:15:00 PM	01:15:00	VSWIR Breakout Session 2 (see tab)	Breakout leads
		BREAK (lead and rapporteur prepare for	
4:30:00 PM	00:15:00	plenary)	
4:45:00 PM	01:00:00	Breakout reports in Plenary	Breakout leads
5:45:00 PM		Close	

#### Oct 22nd

		Potential HyspIRI Mission precursor Airborne	
8:00:00 AM	01:00:00	Campaign	Woody Turner
9:00:00 AM	00:15:00	TQ1 – Volcanoes	Mike Abrams
9:15:00 AM	00:15:00	TQ2 – Wildfires	Rob Wright
9:30:00 AM	00:15:00	TQ3 – Water Use and Availability	Martha Anderson
9:45:00 AM	00:15:00	TQ4 – Human Health and Urbanization	Dale Quattrochi
10:00:00 AM	00:30:00	BREAK	
10:30:00 AM	00:15:00	TQ5 – Earth surface composition and Change	Anupma Prakash
10:45:00 AM	01:15:00	TIR Breakout Session 1 (see tab)	Breakout leads
12:00:00 PM	01:00:00	LUNCH	
1:00:00 PM	01:15:00	TIR Breakout Session 2 (see tab)	Breakout leads
		BREAK (lead and rapporteur prepare for	
2:15:00 PM	00:15:00	plenary)	
2:30:00 PM	00:50:00	Breakout reports in Plenary	Breakout leads
3:20:00 PM	00:30:00	BREAK	

2008 HYSPIRI WHITEPAPER AND SCIENCE WORKSHOP REPORT

---

3:50:00 PM	01:30:00	Using advanced technologies to optimize the HyspIRI Mission	Steve Ungar
5:20:00 PM	01:00:00	Open Discussion	All
6:20:00 PM		Close	

**Oct 23rd**

8:00:00 AM	00:15:00	CQ1 – Coastal, ocean, and inland aquatic environments	Dave Siegel
8:15:00 AM	00:15:00	CQ2 – Wildfires	Simon Hook
8:30:00 AM	00:15:00	CQ3 – Volcanoes	Rob Wright
8:45:00 AM	00:15:00	CQ4 – Ecosystem Function and Diversity	Dar Roberts
9:00:00 AM	00:15:00	CQ5 – Land surface composition and change	Lyle Mars
9:15:00 AM	00:15:00	CQ6 – Human Health and Urbanization	Greg Glass
9:30:00 AM	00:30:00	BREAK	
10:00:00 AM	01:15:00	Combined Breakout Session 1 (see tab)	Breakout leads
11:15:00 AM	01:00:00	LUNCH	
12:15:00 PM	01:15:00	Combined Breakout Session 2 (see tab)	Breakout leads
1:30:00 PM	00:15:00	BREAK (lead and rapporteur prepare for plenary)	
1:45:00 PM	01:00:00	Breakout reports in Plenary	Breakout leads
2:45:00 PM	00:30:00	Discussion of VSWIR Measurement Baseline with respect to. Science Questions	Rob Green
3:15:00 PM	00:30:00	BREAK	
3:45:00 PM	00:30:00	Discussion of TIR Measurement Baseline w.r.t. Science Questions	Simon Hook
4:15:00 PM	00:30:00	International and Domestic Partnerships	Rob Green
4:45:00 PM	00:45:00	Review of Workshop and Next Steps	Woody Turner et al.
5:30:00 PM		Close	

**Appendix C – List of Participants**

<b>Last</b>	<b>First</b>	<b>Last</b>	<b>First</b>
Abrams	Michael	Luvall	Jeffrey
Abuelgasim	Abdel	Mace	Tom
Allen	Richard	Mamo	Tadesse
Anderson	Martha	Mandl	Dan
Armstrong	Ed	MARION	Rodolphe
Asner	Greg	Mars	John
Baldauf	Brian	Mars	John
Baranoski	Gladimir	Matsunago	Tsuneo
Baxter	Jan	McCarthy	John
Berthiaume	Gregory	Mcubbin	Ian
Biradar	Chandrashekhar	Mehall	Greg
Bissett	Paul	Meyer	David
Block	Gary	Middletone	Elizabeth
Boardman	Joseph	Miller	Charles
Brown	Linda	Minnett	Peter
Buckner	Janice	Moersch	Jeffrey
Buermann	Wolfgang	Mouroulis	Pantazis
Campbell	Petya	Muller-Karger	Frank
Cecere	Thomas	Myers	Jeffrey
Chao	Yi	Myneni	Ranga
Chekalyuk	Alexander	Neeck	Steven
Cheng	Yen-Ben	Nemani	Ramakrishna
Chrien	Thomas	Newman	Timothy
Corlett	Gary	Nightingale	Joanne
Corp	Lawrence	Norton	Charles
Crawford	Melba	Oaida	Bogdan
Cwik	Tom	Ogawa	Kenta
Daughtry	Craig	Okin	Gregory
Dennison	Philip	Ong	Lawrence
DiMiceli	Charlene	Pagano	Tom
Driese	Ken	Paine	Christopher
Dobson	Craig	Painter	Thomas

<b>Last</b>	<b>First</b>	<b>Last</b>	<b>First</b>
Dungan	Jennifer	pereira	john
Dwyer	John	Petheram	John
Eastwood	Michael	Petroy	Shelley
Eng	Bjorn	Pieri	David
Enright	Richard	Powell	Dylan
Fladeland	Matthew	Prakash	Anupma
Foote	Marc	Prasad	Saurabh
Francois	Rogez	Procino	Wes
Freeman	Tony	Quattrochi	Dale
French	Andy	Quetin	Gregory
Freund	Friedemann	Quirk	Bruce
Gamon	John	Radelhoff	Volker
Gao	Bo-Cai	Rahman	Abdullah
Giglio	Louis	Ramsey	Michael
Glass	Gregory	Realmuto	Vince
Gould	Richard	Reuter	Dennis
Greb	Steve	Roberts	Dar
Green	Robert	Rodolphe	Marion
Guanter	Luis	Rogez	Francois
Gubbels	Timothy	Russ	Mary
Guess	Abigail	Sarture	Charles
Hall	Jeffrey	Schoenung	Susan
Halligan	Kerry	Shakir	Safwat
Held	Alex	Sheffner	Ed
Helmlinger	Mark	Shu	Peter
Henebry	Geoffrey	Siegel	Dave
Hepner	George	Sikorski	Richard
Hill	Michael	Small	Christopher
Hollinger	Allan	Smith	Robert
Holt	Ben	Spiers	Gary
Hook	Simon	Staehele	Robert
Hosford	Steven	Staenz	Karl
Hu	Steven	Thome	Kurt
Huemmrlich	Karl	Thompson	Patrick

<b>Last</b>	<b>First</b>	<b>Last</b>	<b>First</b>
Hulley	Glynn	Townsend	Phil
Hyon	Jason	Tratt	David
Irons	James	Turmon	Michael
Jacob	Joseph	Turner	Woody
Johnson	Brian	Ungar	Steve
Johnson	William	Ustin	Susan
Kalkhan	Mohammed	Ustin	Susan
Kampe	Thomas	Valle	Tim
Kaufmann	Hermann	van Aardt	Jan
Kavanau	Maria	Vande Castle	John
Knox	Robert	Vannan	Suresh
Knyazikhin	Yuri	Vasudevan	Gopal
Koch	Timothy	Walton	Amy
Kokaly	Raymond	Wang	Le
Kruse	Fred	Wang	Weile
LaBrecque	John	Westberg	Karl
Lau	Gary	Wright	Robert
Lipschultz	Fred	Wright	Conrad
Lodhi	Mahtab	Xiao	Xiangming
		Zhang	Ying

## Appendix D – Science-Traceability Matrices

The DS cross-references in the Science Objectives column (first column refer to page numbers in the 2007 Decadal

Science Objectives	Measurement Objectives	Measurement Requirements	Instrument Requirements	Other Mission and Measurement Requirements
<b>VQ1. Pattern and Spatial Distribution of Ecosystems and their Components: What is the pattern of ecosystem distribution and how do ecosystems differ in their composition or biodiversity? [DS 195]</b>				
How are ecosystems organized within different biomes associated with temperate, tropical, and boreal zones, and how are these changing? [DS 191, 203]	Fractional Cover of Plant Functional Types and Species where possible (terrestrial): e.g. tree, shrub, herbaceous, cryptogam; thick/thin leaves; broad/needle leaves; deciduous/evergreen; nitrogen-fixer/non-fixer; C3/C4 physiology.	Measure diagnostic spectral signature to derive plant functional type and species: Measure seasonally through several years: Measure patch scales of <100 m: Measure regionally important PFT. Requires frequent (at least 20 per day) sampling.	Spectral measurement from 400 to 2500 nm at 10 nm (terrestrial): 380 to 900 nm at 10 nm with additional SWIR for AC (coastal aquatic): > 95% Spectral cal uniformity: SNR 600 VNIR, 300 SWIR (23.5ZA 0.25R); 14 bit precision: >95% abs cal: > 98% on-orbit stability: no saturation of ecosystem targets: <2% polarization sensitivity 380 to 700 nm: >99% linearity 2 to 98% saturation: ≤60 m spatial sampling: >95% Spectral IFOV uniformity: <20 day revisit to minimize cloud obscuration:	Surface reflectance in the solar reflected spectrum for elevation angles >20: Rigorous calibration/validation program: Monthly lunar calcs: Daily solar calcs: 6 per year vicarious calibrations ~700 mbs downlink: >3X zero loss compression: ~11 a.m. Sun sync LEO orbit: Radiometric calibration: Atmospheric Correction: AC validation: Geolocation: Pointing strategy to minimize Sun glint: Avoid terrestrial hot spot: Ground processing: Seasonal latency.
How do similar ecosystems differ in size, species composition, fractional cover, and biodiversity across terrestrial and aquatic biomes? [DS 195]	Measure fraction of dominant Plant Functional Types and Species where possible (terrestrial): e.g. tree, shrub, herbaceous, cryptogam; thick/thin leaves; broad/needle leaves; deciduous/evergreen; nitrogen-fixer/non-fixer; C3/C4 physiology. Dominant aquatic phytoplankton functional types; e.g., phytoplankton (diatoms, dinoflagellates, coccolithophores, N-fixers) Dominant submerged aquatic communities (i.e., coral, sea grass, kelp). Aquatic biogeochemical constituent: (phytoplankton, sediment, CDOM, benthos)	Measure diagnostic spectral signature to derive functional groups, species (terrestrial and aquatic), and critical measurable abiotic components. <ul style="list-style-type: none"> <li>• Measure seasonally through several years to capture baseline:</li> <li>• Measure patch scales of &lt;100 m.</li> <li>• Measure regionally important PFT.</li> <li>• Requires frequent (at least every 20 days) sampling.</li> </ul>	Spectral measurement from 400 to 2500 nm at 10 nm (terrestrial): 380 to 900 nm at 10 nm with additional SWIR for AC (coastal aquatic): > 95% Spectral cal uniformity: Terrestrial: SNR 600 VNIR, 300 SWIR (23.5ZA 0.25R); Aquatic: ~SNR 300 (45ZA 0.01R) 14-bit precision: >95% abs cal: > 98% on-orbit stability: no saturation of ecosystem targets: <2% polarization sensitivity 380 to 700 nm: >99% linearity 2 to 98% saturation: ≥ 60 sampling: >95% Spectral IFOV uniformity: <20 day revisit to minimize cloud obscuration:	Surface reflectance in the solar reflected spectrum for elevation angles >20: Rigorous cal/val program: Monthly lunar calcs: Daily solar calcs: 6 per year vcalcs: ~700-mbs downlink: >3X zero loss compression: ~11 a.m. Sun sync LEO: Radiometric calibration: Atmospheric Correction: AC validation: Geolocation: Pointing strategy to minimize Sun glint: Avoid terrestrial hot spot: Ground processing: Seasonal latency:
What is the current spatial distribution of ecosystems, functional groups, or key species within major biomes including agriculture, and how are these being altered by climate variability, human uses, and other factors? [DS 191, 203]	Fractional Cover of Plant Functional Types and Species where possible (terrestrial): e.g. tree, shrub, herbaceous, cryptogam; thick/thin leaves; broad/needle leaves; deciduous/evergreen; nitrogen-fixer/non-fixer; C3/C4 physiology.	Measure diagnostic spectral signature to derive plant functional type and species: Measure seasonally through several years: Measure patch scales of <100 m: Measure regionally important PFT. Requires frequent (at least every 20 days) sampling.	Spectral measurement from 400 to 2500 nm at 10 nm (terrestrial): 380 to 900 nm at 10 nm with additional SWIR for AC (coastal aquatic): > 95% Spectral cal uniformity: SNR 600 VNIR, 300 SWIR (23.5ZA 0.25R); 14 bit precision: >95% abs cal: > 98% on-orbit stability: no saturation of ecosystem targets: <2% polarization sensitivity 380 to 700 nm: >99% linearity 2 to 98% saturation: ≤ 60 sampling: >95% Spectral IFOV uniformity: <20 day revisit to minimize cloud obscuration:	Surface reflectance in the solar reflected spectrum for elevation angles >20: Rigorous cal/val program: Monthly lunar calcs: Daily solar calcs: 6 per year vcalcs: ~700-mbs downlink: >3X zero loss compression: ~11 am sun sync LEO: Radiometric calibration: Atmospheric Correction: AC validation: Geolocation: Pointing strategy to minimize Sun glint: Avoid terrestrial hot spot: Ground processing: Seasonal latency:
What are the extent and impact of invasive species in terrestrial and aquatic ecosystems? [DS 192, 194, 196, 203, 204, 214]	Species-type measurements in terrestrial and coastal aquatic regions.	Measure diagnostic spectral signature to derive plant species: Measure seasonally through several years: Measure patch scales of <100 m: Measure regionally important PFT. Requires frequent (at least 20 per day) sampling. Measure diagnostic spectral signature of aquatic vegetation in coastal regions with < 100 m spatial resolution and temporal repeat to observe the seasonal regional occurrence and trends in the coastal regions. Requires frequent (at least 20 per day) repeat.	Spectral measurement from 400 to 2500 nm at 10 nm (terrestrial): 380 to 900 nm at 10 nm with additional SWIR for AC (coastal aquatic): > 95% Spectral cal uniformity: SNR 600 VNIR, 300 SWIR (23.5ZA 0.25R); 14-bit precision: >95% abs cal: > 98% on-orbit stability: no saturation of ecosystem targets: <2% polarization sensitivity 380 to 700 nm (aquatic): >99% linearity 2 to 98% saturation: ≥ 60 sampling: >95% Spectral IFOV uniformity: <20 day revisit to minimize cloud obscuration:	Surface reflectance in the solar reflected spectrum for elevation angles >20: Rigorous cal/val program: Monthly lunar calcs: Daily solar calcs: 6 per year vcalcs: ~700 mbs downlink: >3X zero loss compression: ~11 a.m. Sun sync LEO: Radiometric calibration: Atmospheric Correction: AC validation: Geolocation: Pointing strategy to minimize Sun glint: Avoid terrestrial hot spot: Ground processing: Seasonal latency:
What is the spatial structure and species distribution in a phytoplankton bloom? [DS 201, 208]	Characterize algal bloom (including harmful) species and spatial structure	Measure diagnostic spectral signature of aquatic vegetation in coastal regions with < 100 m spatial resolution and temporal repeat to observe the seasonal regional occurrence and trends in the coastal regions.	Spectral measurement from 380 to 900 nm at 10 nm with additional SWIR for AC (coastal aquatic): > 95% Spectral cal uniformity: SNR 600 VNIR, 300 SWIR (23.5ZA 0.25R); 14-bit digitization: >95% abs cal: > 98% on-orbit stability: no saturation of ecosystem targets: <2% polarization sensitivity 380 to 700 nm (aquatic): >99% linearity 2 to 98% saturation: ≤ 60 sampling: >95% Spectral IFOV uniformity: <20 day revisit to minimize cloud obscuration:	Surface reflectance in the solar reflected spectrum for elevation angles >20: Rigorous cal/val program: Monthly lunar calcs: Daily solar calcs: 6 per year vcalcs: ~700 mbs downlink: >3X zero loss compression: ~11 a.m. Sun sync LEO: Radiometric calibration: Atmospheric Correction: AC validation: Geolocation: Pointing strategy to minimize sun glint: Avoid terrestrial hot spot: Ground processing: Seasonal latency:
How do changes in coastal morphology and surface composition impact coastal ecosystem composition, diversity and function [DS 41]?	Measure coastal ecosystem functional characteristics and diversity at the seasonal and multiyear time scale.	Measure diagnostic spectral signature of aquatic vegetation in coastal regions with < 100 m spatial resolution and temporal repeat to observe the seasonal regional occurrence and trends in the coastal regions. Requires frequent (at least 20 per day) sampling.	Spectral measurement from 400 to 2500 nm at 10 nm (terrestrial): 380 to 900 nm at 10 nm with additional SWIR for AC (coastal aquatic): > 95% Spectral cal uniformity: SNR 600 VNIR, 300 SWIR (23.5ZA 0.25R); 14-bit precision: >95% abs cal: > 98% on-orbit stability: no saturation of ecosystem targets: <2% polarization sensitivity 380 to 700 nm: >99% linearity 2 to 98% saturation: ≤60 sampling: >95% Spectral IFOV uniformity: <20 day revisit to minimize cloud obscuration:	Surface reflectance in the solar reflected spectrum for elevation angles >20: Rigorous cal/val program: Monthly lunar calcs: Daily solar calcs: 6 per year vcalcs: ~700 mbs downlink: >3X zero loss compression: ~11 a.m. Sun sync LEO: Radiometric calibration: Atmospheric Correction: AC validation: Geolocation: Pointing strategy to minimize Sun glint: Avoid terrestrial hot spot: Ground processing: Seasonal latency:

VQ1

Science Objectives	Measurement Objectives	Measurement Requirements	Instrument Requirements	Other Mission and Measurement Requirements
<b>VQ2. Ecosystem Function, Physiology, and Seasonal Activity: What are the seasonal expressions and cycles for terrestrial and aquatic ecosystems, functional groups and diagnostic species? How are these being altered by changes in climate, land use, and disturbances? [DS 191, 195, 203]</b>				
How does the seasonal activity of ecosystems and functional types vary across biomes, geographic zones, or environmental gradients between the Equator and the poles? How are seasonal patterns of ecosystem function being affected by climate change? [DS 205, 206, 210] (include agriculture?)	Measure the functional type composition of ecosystems globally. Measure these at the spatial scale and temporal scale to address regional to global distributions. Measure these at temporal scale to answer seasonal and several-year trends.	Measure surface reflectance in the VSWIR region at high precision and accuracy. Measure globally at spatial resolution patch scale relevant for ecosystem 10 <sup>4</sup> to 10 <sup>6</sup> m <sup>2</sup> . Measure temporally to have high probability to achieve seasonal measurements. (consider replace measure to retrieve)	Spectral measurement from 400 to 2500 nm at 10 nm (terrestrial): 380 to 900 nm at 10 nm with additional SWIR for AC (coastal aquatic): > 95% Spectral cal uniformity (include spectral and spatial stray light?): SNR 600 VNIR, 300 SWIR (23.5ZA 0.25R): 14-bit precision: >95% abs cal: > 98% on-orbit stability: no saturation of ecosystem targets: <2% polarization sensitivity 380 to 700 nm: >99% linearity 2 to 98% saturation: ≤60 sampling: >95% Spectral IFOV uniformity: <20 day revisit to minimize cloud obscuration: (possibly provide Noise Equivalent delta radiance?) (be specific about wavelength)	Surface reflectance in the solar reflected spectrum for elevation angles >20: Rigorous cal/val program: Monthly lunar cal: Daily solar cal: 6 per year vcal: ~700-mbs downlink: >3X zero loss compression: ~11 am sun sync LEO: Radiometric calibration: Atmospheric Correction: AC validation: Geolocation: Pointing strategy to minimize Sun glint: Avoid terrestrial hot spot: Ground processing: Seasonal latency:
How do seasonal changes affect productivity, carbon sequestration, and hydrological processes across ecosystems and agriculture? [DS 195, 205, 210]	Measure seasonal changes and status of natural ecosystem and agricultural lands over the seasonal and multiyear scale.	Measure surface reflectance spectral reflectance in the VSWIR region at high repeatable accuracy.  Measure globally at spatial resolution patch scale relevant for ecosystem 10 <sup>4</sup> to 10 <sup>6</sup> m <sup>2</sup> .  Measure temporally to have high probability to achieve seasonal measurements.	Spectral measurement from 400 to 2500 nm at 10 nm (terrestrial): 380 to 900 nm at 10 nm with additional SWIR for AC (coastal aquatic): >95% Spectral cal uniformity: SNR 600 VNIR, 300 SWIR (23.5ZA 0.25R): 14-bit precision: >95% abs cal: > 98% on-orbit stability: no saturation of ecosystem targets: <2% polarization sensitivity 380 to 700 nm: >99% linearity 2 to 98% saturation: ≤60 sampling: >95% Spectral IFOV uniformity: <20 day revisit to minimize cloud obscuration:	Surface reflectance in the solar reflected spectrum for elevation angles >20: Rigorous cal/val program: Monthly lunar cal: Daily solar cal: 6 per year vcal: ~700-mbs downlink: >3X zero loss compression: ~11 a.m. Sun sync LEO: Radiometric calibration: Atmospheric Correction: AC validation: Geolocation: Pointing strategy to minimize Sun glint: Avoid terrestrial hot spot: Ground processing: Seasonal latency:
How do environmental stresses affect the physiological function of water and carbon exchanges at the seasonal time scale within ecosystems (including agriculture)? [DS 203, 206, 210]	Measure the physiological function indicators of ecosystems related to water and carbon exchange over the seasonal and multiyear time frame.	Measure spectral signature in the VSWIR region at high precision and accuracy. Special focus on precision and accuracy in the pigment region of vegetation in the visible portion of the spectrum. Water: 980±50 nm, 1180±50 nm, and broad SWIR water signatures to 2500 nm. Measure globally at spatial resolution patch scale relevant for ecosystem 10 <sup>4</sup> to 10 <sup>6</sup> m <sup>2</sup> . Measure temporally to have high probability to achieve seasonal measurements.	Spectral measurement from 400 to 2500 nm at 10 nm (terrestrial): 380 to 900 nm at 10 nm with additional SWIR for AC (coastal aquatic): >95% Spectral cal uniformity: SNR 600 VNIR, 300 SWIR (23.5ZA 0.25R): 14-bit precision: >95% abs cal: >98% on-orbit stability: no saturation of ecosystem targets: <2% polarization sensitivity 380 to 700 nm: >99% linearity 2 to 98% saturation: ≤60 sampling: >95% Spectral IFOV uniformity: <20 day revisit to minimize cloud obscuration:	Surface reflectance in the solar reflected spectrum for elevation angles >20: Rigorous cal/val program: Monthly lunar cal: Daily solar cal: 6 per year vcal: ~700-mbs downlink: >3X zero loss compression: ~11 a.m. Sun sync LEO: Radiometric calibration: Atmospheric Correction: AC validation: Geolocation: Pointing strategy to minimize sun glint: Avoid terrestrial hot spot: Ground processing: Seasonal latency:
What is the environmental impact of aquatic plants and coral on inland and coastal water environments at the seasonal time scale? [DS 201, 208]	Measure the distribution and type of algal bloom in a sampling sense globally over the seasonal and multiyear timescale.	Measure diagnostic spectral signature of in coastal regions with <100 m spatial resolution and temporal repeat to observe the seasonal regional occurrence and trends in the coastal regions. Measure globally at spatial resolution patch scale relevant for ecosystem 10 <sup>4</sup> to 10 <sup>6</sup> m <sup>2</sup> . Measure temporally to have high probability to achieve seasonal measurements.	Spectral measurement from 380 to 900 nm at 10 nm with additional SWIR for AC (coastal aquatic): > 95% Spectral cal uniformity: SNR 600 VNIR, 300 SWIR (23.5ZA 0.25R): 14-bit digitization: >95% abs cal: > 98% on-orbit stability: no saturation of ecosystem targets: <2% polarization sensitivity 380 to 700 nm: >99% linearity 2 to 98% saturation: ≤60 sampling: >95% Spectral IFOV uniformity: <20 day revisit to minimize cloud obscuration:	Surface reflectance in the solar reflected spectrum for elevation angles >20: Rigorous cal/val program: Monthly lunar cal: Daily solar cal: 6 per year vcal: ~700-mbs downlink: >3X zero loss compression: ~11 a.m. Sun sync LEO: Radiometric calibration: Atmospheric Correction: AC validation: Geolocation: Pointing strategy to minimize Sun glint: Avoid terrestrial hot spot: Ground processing: Seasonal latency:

VQ2

Science Objectives	Measurement Objectives	Measurement Requirements	Instrument Requirements	Other Mission and Measurement Requirements
<b>VQ3. Biogeochemical Cycles: How are the biogeochemical cycles that sustain life on Earth being altered/disrupted by natural and human-induced environmental change? How do these changes affect the composition and health of ecosystems, and what are the feedbacks with other components of the Earth system?</b>				
How do changes in climate and atmospheric processes affect the physiology and biogeochemistry of ecosystems? [DS 194, 201]	Measure the biogeochemistry of both photosynthetic vegetation and non-photosynthetic vegetation.	Measure at high accuracy and precision the spectral signature that is shown to be sensitive to vegetation canopy chemistry. -Pigments: Visible spectral region. -Water: 980 ±50 nm, 1180±50 nm, and broad SWIR water signatures to 2500 nm. -Nitrogen and other components: Spectral region 1300 to 2500 nm at 10 nm. Measure globally at spatial resolution patch scale relevant for ecosystem 10 <sup>4</sup> to 10 <sup>6</sup> m <sup>2</sup> . Measure temporally to have high probability to achieve seasonal measurements.	Spectral measurement from 400 to 2500 nm at 10 nm (terrestrial): 380 to 900 nm at 10 nm with additional SWIR for AC (coastal aquatic): > 95% Spectral cal uniformity: SNR 600 VNIR, 300 SWIR (23.5ZA 0.25R): 14-bit precision: >95% abs cal: > 98% on-orbit stability; no saturation of ecosystem targets: <2% polarization sensitivity 380 to 700 nm: >99% linearity 2 to 98% saturation: ≥60 sampling: >95% Spectral IFOV uniformity: <20 day revisit to minimize cloud obscuration:	Surface reflectance in the solar reflected spectrum for elevation angles >20: Rigorous cal/val program: Monthly lunar calcs: Daily solar calcs: 6 per year vcalcs: ~700-mbs downlink: >3X zero loss compression: ~11 a.m. Sun sync LEO orbit: Radiometric calibration: Atmospheric Correction: AC validation: Geolocation: Pointing strategy to minimize Sun glint: Avoid terrestrial hot spot: Ground processing: Seasonal latency:
What are the consequences of uses of land and coastal systems, such as urbanization, agriculture, and resource extraction, for the carbon cycle, hydrological cycle, nutrient fluxes, and functional composition [DS 196, 197]	Measure biological component and state of land and coastal ecosystems globally at the seasonal to several-year time scales. Relate these to sources, conduits and sinks of relevant elements.	Measure at high accuracy and precision the spectral signature that allows mapping of coastal and land ecosystem elements. Measure globally at spatial resolution patch scale relevant for ecosystem 10 <sup>4</sup> to 10 <sup>6</sup> m <sup>2</sup> . Measure temporally to have high probability to achieve seasonal measurements.	Spectral measurement from 400 to 2500 nm at 10 nm (terrestrial): 380 to 900 nm at 10 nm with additional SWIR for AC (coastal aquatic): > 95% Spectral cal uniformity: SNR 600 VNIR, 300 SWIR (23.5ZA 0.25R): 14-bit precision: >95% abs cal: > 98% on-orbit stability; no saturation of ecosystem targets: <2% polarization sensitivity 380 to 700 nm: >99% linearity 2 to 98% saturation: ≥60 sampling: >95% Spectral IFOV uniformity: <20 day revisit to minimize cloud obscuration:	Surface reflectance in the solar reflected spectrum for elevation angles >20: Rigorous cal/val program: Monthly lunar calcs: Daily solar calcs: 6 per year vcalcs: ~700 mbs downlink: >3X zero loss compression: ~11 a.m. Sun sync LEO: Radiometric calibration: Atmospheric Correction: AC validation: Geolocation: Pointing strategy to minimize Sun glint: Avoid terrestrial hot spot: Ground processing: Seasonal latency:
What are the consequences of increasing nitrogen deposition for carbon cycling and biodiversity in terrestrial and coastal ecosystems? [DS 195, 196]	Measure ecological components of terrestrial and coastal ecosystem including elements of biodiversity. Measure ecological signatures closely tied to nitrogen deposition.	Measure at high accuracy and precision the spectral signatures that allow mapping of aquatic, coastal, and land ecosystem elements. Measure globally at spatial resolution patch scale relevant for ecosystem 10 <sup>4</sup> to 10 <sup>6</sup> m <sup>2</sup> . Measure temporally to have high probability to achieve seasonal measurements	Spectral measurement from 400 to 2500 nm at 10 nm (terrestrial): 380 to 900 nm at 10 nm with additional SWIR for AC (coastal aquatic): > 95% Spectral cal uniformity: SNR 600 VNIR, 300 SWIR (23.5ZA 0.25R): 14-bit precision: >95% abs cal: > 98% on-orbit stability; no saturation of ecosystem targets: <2% polarization sensitivity 380 to 700 nm: >99% linearity 2 to 98% saturation: ≥60 sampling: >95% Spectral IFOV uniformity: <20 day revisit to minimize cloud obscuration:	Surface reflectance in the solar reflected spectrum for elevation angles >20: Rigorous cal/val program: Monthly lunar calcs: Daily solar calcs: 6 per year vcalcs: ~700 mbs downlink: >3X zero loss compression: ~11 a.m. Sun sync LEO: Radiometric calibration: Atmospheric Correction: AC validation: Geolocation: Pointing strategy to minimize Sun glint: Avoid terrestrial hot spot: Ground processing: Seasonal latency:
How do changes in hydrology, pollutant inputs, and sediment transport affect freshwater and coastal marine ecosystems? [DS 196]	Measure diagnostic elements of freshwater and coastal marine ecosystem including sediments, chlorophyll, algal communities, and CDOM.	Measure at high accuracy and precision the spectral signatures that allow derivation of key elements of freshwater and coastal marine ecosystems. Measure spectral region where sediments, chlorophyll, algae, CDOM, etc. provide a usable signal. Measure globally at spatial resolution patch scale relevant for ecosystem 10 <sup>4</sup> to 10 <sup>6</sup> m <sup>2</sup> . Measure temporally to have high probability to achieve seasonal measurements.	Spectral measurement from 400 to 2500 nm at 10 nm (terrestrial): 380 to 900 nm at 10 nm with additional SWIR for AC (coastal aquatic): > 95% Spectral cal uniformity: SNR 600 VNIR, 300 SWIR (23.5ZA 0.25R): 14-bit precision: >95% abs cal: > 98% on-orbit stability; no saturation of ecosystem targets: <2% polarization sensitivity 380 to 700 nm: >99% linearity 2 to 98% saturation: ≥60 sampling: >95% Spectral IFOV uniformity: <20 day revisit to minimize cloud obscuration:	Surface reflectance in the solar reflected spectrum for elevation angles >20: Rigorous cal/val program: Monthly lunar calcs: Daily solar calcs: 6 per year vcalcs: ~700 mbs downlink: >3X zero loss compression: ~11 a.m. Sun sync LEO: Radiometric calibration: Atmospheric Correction: AC validation: Geolocation: Pointing strategy to minimize Sun glint: Avoid terrestrial hot spot: Ground processing: Seasonal latency:
How do changing water balances affect carbon storage by terrestrial ecosystems? [DS 196]	Measure water content of canopies. Measure signals of evapotranspiration.	Measure at high accuracy and precision the spectral signatures that allow derivation of canopy liquid water. Also measure canopy associated water vapor. Measure spectral region where liquid water and water vapor are expressed. Water: 980 ±50 nm, 1180±50 nm, and broad SWIR water signatures to 2500 nm. Measure globally at spatial resolution patch scale relevant for ecosystem 10 <sup>4</sup> to 10 <sup>6</sup> m <sup>2</sup> . Measure temporally to have high probability to achieve seasonal measurements.	Spectral measurement from 900 to 2500 nm at 10 nm (terrestrial): >95% Spectral cal uniformity: SNR 600 VNIR, 300 SWIR (23.5ZA 0.25R): 14-bit precision: >95% abs cal: > 98% on-orbit stability; no saturation of ecosystem targets: <2% polarization sensitivity 380 to 700 nm: >99% linearity 2 to 98% saturation: ≥60 sampling: >95% Spectral IFOV uniformity: <20 day revisit to minimize cloud obscuration:	Surface reflectance in the solar reflected spectrum for elevation angles >20: Rigorous cal/val program: Monthly lunar calcs: Daily solar calcs: 6 per year vcalcs: ~700-mbs downlink: >3X zero loss compression: ~11 a.m. Sun sync LEO: Radiometric calibration: Atmospheric Correction: AC validation: Geolocation: Pointing strategy to minimize Sun glint: Avoid terrestrial hot spot: Ground processing: Seasonal latency:
What are the key interactions between biogeochemical cycles and the composition and diversity of ecosystems? [195, 196]	Measure biogeochemistry elements as well as composition and diversity of ecosystems.	Measure at high accuracy and precision the spectral signature that is shown to be sensitive to vegetation canopy chemistry. -Pigments: Visible spectral region. -Water: 980 ±50 nm, 1180±50 nm, and broad SWIR water signatures to 2500 nm. -Nitrogen and other components: Spectral region 1300 to 2500 nm at 10 nm. Measure spectral signatures across the VSWIR region at high precision and accuracy to derive ecosystem composition and diversity. Measure globally at spatial resolution patch scale relevant for ecosystem 10 <sup>4</sup> to 10 <sup>6</sup> m <sup>2</sup> . Measure temporally to have high probability to achieve seasonal measurements.	Spectral measurement from 400 to 2500 nm at 10 nm (terrestrial): 380 to 900 nm at 10 nm with additional SWIR for AC (coastal aquatic): > 95% Spectral cal uniformity: SNR 600 VNIR, 300 SWIR (23.5ZA 0.25R): 14-bit precision: >95% abs cal: > 98% on-orbit stability; no saturation of ecosystem targets: <2% polarization sensitivity 380 to 700 nm: >99% linearity 2 to 98% saturation: ≥60 sampling: >95% Spectral IFOV uniformity: <20 day revisit to minimize cloud obscuration:	Surface reflectance in the solar reflected spectrum for elevation angles >20: Rigorous cal/val program: Monthly lunar calcs: Daily solar calcs: 6 per year vcalcs: ~700-mbs downlink: >3X zero loss compression: ~11 a.m. Sun sync LEO: Radiometric calibration: Atmospheric Correction: AC validation: Geolocation: Pointing strategy to minimize Sun glint: Avoid terrestrial hot spot: Ground processing: Seasonal latency:
How do changes in biogeochemical processes feed back to climate and other components of the Earth system? [DS 190, 192, 195]	Measure global biogeochemical constituents related to processes involved in feedback to climate and other environmental factors.	Measure at high accuracy and precision the spectral signature that is shown to be sensitive to vegetation canopy chemistry. -Pigments: Visible spectral region. -Water: 980 ±50 nm, 1180±50 nm, and broad SWIR water signatures to 2500 nm. -Nitrogen and other components: Spectral region 1300 to 2500 nm at 10 nm. Measure globally at spatial resolution patch scale relevant for ecosystem 10 <sup>4</sup> to 10 <sup>6</sup> m <sup>2</sup> . Measure temporally to have high probability to achieve seasonal measurements.	Spectral measurement from 400 to 2500 nm at 10 nm (terrestrial): 380 to 900 nm at 10 nm with additional SWIR for AC (coastal aquatic): >95% Spectral cal uniformity: SNR 600 VNIR, 300 SWIR (23.5ZA 0.25R): 14-bit precision: >95% abs cal: > 98% on-orbit stability; no saturation of ecosystem targets: <2% polarization sensitivity 380 to 700 nm: >99% linearity 2 to 98% saturation: ≥60 sampling: >95% Spectral IFOV uniformity: <20 day revisit to minimize cloud obscuration:	Surface reflectance in the solar reflected spectrum for elevation angles >20: Rigorous cal/val program: Monthly lunar calcs: Daily solar calcs: 6 per year vcalcs: ~700-mbs downlink: >3X zero loss compression: ~11 a.m. Sun sync LEO: Radiometric calibration: Atmospheric Correction: AC validation: Geolocation: Pointing strategy to minimize Sun glint: Avoid terrestrial hot spot: Ground processing: Seasonal latency:

VQ3

Science Objectives	Measurement Objectives	Measurement Requirements	Instrument Requirements	Other Mission and Measurement Requirements
<b>VQ4. Changes in Disturbance Activity: How are disturbance regimes changing and how do these changes affect the ecosystem processes that support life on Earth?</b>				
How do patterns of abrupt (pulse) disturbance vary and change over time within and across ecosystems?	Measure changes in fractional cover (from clearing, logging, wetland drainage, fire, weather related, etc.) at the seasonal and multiyear time scales, to characterize disturbance regimes in global ecosystems (e.g., conditional frequencies and/or return intervals for VQ1 ecosystem classes).	Measure spectral signature in the VSWIR region at high precision and accuracy. - Detect fractional surface cover changes > 10%. - Sufficient precision and accuracy for spectral mixture algorithms to give insight to subpixel events. Measure globally at spatial resolution patch scale relevant for ecosystem 10 <sup>4</sup> to 10 <sup>6</sup> m <sup>2</sup> . Cloud-free measurement at least once per season.	Spectral measurement from 400 to 2500 nm at 10 nm (terrestrial): 380 to 900 nm at 10 nm with additional SWIR for AC (coastal aquatic): > 95% Spectral cal uniformity: SNR 600 VNIR, 300 SWIR (23.52A 0.25R): 14-bit precision: >95% abs cal: > 98% on-orbit stability; no saturation of ecosystem targets: <2% polarization sensitivity 380 to 700 nm: >99% linearity 2 to 98% saturation: <60 m spatial sampling: >95% Spectral IFOV uniformity: <20 day revisit to minimize cloud obscuration:	Surface reflectance in the solar reflected spectrum for elevation angles >20: Rigorous cal/val program: Monthly lunar calis: Daily solar calis: 6 per year vcalis: ~700-mbs downlink: >3X zero loss compression: ~11 a.m. Sun sync LEO: Radiometric calibration: accurate enough to simulate historical satellite data through band synthesis. Atmospheric Correction: AC validation: Geolocation: 10 m (1 sigma). Ground processing: Seasonal latency:
How do climate changes affect disturbances such as fire and insect damage? [DS 196]	Measure changes in vegetation canopy cover, pigments, and water content in ecosystems globally at the seasonal and multiyear time scale. Make measurements in such a way that they are backward compatible with pre-existing estimates and algorithms (e.g., band synthesis for historical vegetation indexes), as well as allowing more advanced algorithmic approaches.	Measure characteristic changes or differences in plant pigments (10% changes in total chlorophyll, carotenoids, anthocyanins) and water content. Measure PV, NPV and Soil (+/- 5%) using full VSWIR and SWIR algorithms. Measure globally at spatial resolution patch scale relevant for ecosystem 10 <sup>4</sup> to 10 <sup>6</sup> m <sup>2</sup> . Cloud-free measurement at least once per season. VNIR-SWIR spectra suitable for band synthesis consistent with historical data.	Spectral measurement from 400 to 2500 nm at 10 nm (terrestrial): > 95% Spectral cal uniformity: SNR 600 VNIR, 300 SWIR (23.52A 0.25R): 14-bit precision: >95% abs cal: > 98% on-orbit stability; no saturation of ecosystem targets: <2% polarization sensitivity 380 to 700 nm: >99% linearity 2 to 98% saturation: <60 m spatial sampling: >95% Spectral IFOV uniformity: <20 day revisit to minimize cloud obscuration:	Surface reflectance in the solar reflected spectrum for elevation angles >20: Rigorous cal/val program: Monthly lunar calis: Daily solar calis: 6 per year vcalis: ~700-mbs downlink: >3X zero loss compression: ~11 a.m. Sun sync LEO: Radiometric calibration: Atmospheric Correction: AC validation: Geolocation: Pointing strategy to minimize Sun glint: Avoid terrestrial hot spot: Ground processing: Seasonal latency:
What are the interactions between invasive species and other types of disturbance?	Measure the distribution and cover of key invasive species that introduce novel life histories or functional types, in concert with disturbance measurements. Measure (disturbance related) changes in vegetation canopy cover, pigments, and water content in ecosystems globally at the seasonal and multiyear time scale.	Measure spectral signature in the VSWIR region at high precision and accuracy. -Sufficient precision and accuracy for spectral mixture algorithms to give insight to subpixel events. -Measure species-type and functional type using full spectrum. -Measure PV, NPV, and Soil using full VSWIR and SWIR algorithms. Measure globally at spatial resolution patch scale relevant for ecosystem 10 <sup>4</sup> to 10 <sup>6</sup> m <sup>2</sup> . Cloud-free measurement at least once per season.	Spectral measurement from 400 to 2500 nm at 10 nm (terrestrial): > 95% Spectral cal uniformity: SNR 600 VNIR, 300 SWIR (23.52A 0.25R): 14-bit precision: >95% abs cal: > 98% on-orbit stability; no saturation of ecosystem targets: <2% polarization sensitivity 380 to 700 nm: >99% linearity 2 to 98% saturation: <60 m spatial sampling: >95% Spectral IFOV uniformity: <20 day revisit to minimize cloud obscuration:	Surface reflectance in the solar reflected spectrum for elevation angles >20: Rigorous cal/val program: Monthly lunar calis: Daily solar calis: 6 per year vcalis: ~700-mbs downlink: >3X zero loss compression: ~11 a.m. Sun sync LEO: Radiometric calibration: Atmospheric Correction: AC validation: Geolocation: Pointing strategy to minimize sun glint: Avoid terrestrial hot spot: Ground processing: Seasonal latency:
How are human-caused and natural disturbances changing the biodiversity composition of ecosystems, e.g.: through changes in the distribution and abundance of organisms, communities, and ecosystems?	Measure the composition of ecosystems and ecological diversity indicators globally and at the seasonal and multiyear time scale.	Measure spectral signature in the VSWIR region at high precision and accuracy. -Sufficient precision and accuracy for spectral mixture algorithms to give insight to subpixel events. -Measure species-type and functional type using full spectrum. -Measure PV, NPV, and Soil using full VSWIR and SWIR algorithms. Measure globally at spatial resolution patch scale relevant for ecosystem 10 <sup>4</sup> to 10 <sup>6</sup> m <sup>2</sup> . Measure temporally to have high probability to achieve seasonal measurements.	Spectral measurement from 400 to 2500 nm at 10 nm (terrestrial): > 95% Spectral cal uniformity: SNR 600 VNIR, 300 SWIR (23.52A 0.25R): 14-bit precision: >95% abs cal: > 98% on-orbit stability; no saturation of ecosystem targets: <2% polarization sensitivity 380 to 700 nm: >99% linearity 2 to 98% saturation: <60 m spatial sampling: >95% Spectral IFOV uniformity: <20 day revisit to minimize cloud obscuration:	Surface reflectance in the solar reflected spectrum for elevation angles >20: Rigorous cal/val program: Monthly lunar calis: Daily solar calis: 6 per year vcalis: ~700-mbs downlink: >3X zero loss compression: ~11 a.m. Sun sync LEO: Radiometric calibration: Atmospheric Correction: AC validation: Geolocation: Pointing strategy to minimize sun glint: Avoid terrestrial hot spot: Ground processing: Seasonal latency:
How do climate change, pollution and disturbance augment the vulnerability of ecosystems to invasive species? [DS 114,196]	Measure disturbances and ecosystem status. Measure invasive trends. Measure at the seasonal to multiyear time scale.	Measure spectral signature in the VSWIR region at high precision and accuracy. -Sufficient precision and accuracy for spectral mixture algorithms to give insight to subpixel events. -Measure species-type and functional type using full spectrum. -Measure PV, NPV, and Soil using full VSWIR and SWIR algorithms. Measure globally at spatial resolution patch scale relevant for ecosystem 10 <sup>4</sup> to 10 <sup>6</sup> m <sup>2</sup> . Measure temporally to have high probability to achieve seasonal measurements.	Spectral measurement from 400 to 2500 nm at 10 nm (terrestrial): > 95% Spectral cal uniformity: SNR 600 VNIR, 300 SWIR (23.52A 0.25R): 14-bit precision: >95% abs cal: > 98% on-orbit stability; no saturation of ecosystem targets: <2% polarization sensitivity 380 to 700 nm: >99% linearity 2 to 98% saturation: <60 m spatial sampling: >95% Spectral IFOV uniformity: <20 day revisit to minimize cloud obscuration:	Surface reflectance in the solar reflected spectrum for elevation angles >20: Rigorous cal/val program: Monthly lunar calis: Daily solar calis: 6 per year vcalis: ~700-mbs downlink: >3X zero loss compression: ~11 a.m. Sun sync LEO: Radiometric calibration: Atmospheric Correction: AC validation: Geolocation: Pointing strategy to minimize sun glint: Avoid terrestrial hot spot: Ground processing: Seasonal latency:
What are the effects of disturbances on productivity, water resources, and other ecosystem functions and services? [DS 196]	Measure disturbances and productivity indicators including ecosystem function and services on the seasonal to multiyear time scale	Measure spectral signature in the VSWIR region at high precision and accuracy. -Sufficient precision and accuracy for spectral mixture algorithms to give insight to subpixel events. -Measure species-type and functional type using full spectrum. -Measure PV, NPV, and Soil using full VSWIR and SWIR algorithms. Measure globally at spatial resolution patch scale relevant for ecosystem 10 <sup>4</sup> to 10 <sup>6</sup> m <sup>2</sup> . Measure temporally to have high probability to achieve seasonal measurements.	Spectral measurement from 400 to 2500 nm at 10 nm (terrestrial): > 95% Spectral cal uniformity: SNR 600 VNIR, 300 SWIR (23.52A 0.25R): 14-bit precision: >95% abs cal: > 98% on-orbit stability; no saturation of ecosystem targets: <2% polarization sensitivity 380 to 700 nm: >99% linearity 2 to 98% saturation: <60 m spatial sampling: >95% Spectral IFOV uniformity: <20 day revisit to minimize cloud obscuration:	Surface reflectance in the solar reflected spectrum for elevation angles >20: Rigorous cal/val program: Monthly lunar calis: Daily solar calis: 6 per year vcalis: ~700-mbs downlink: >3X zero loss compression: ~11 a.m. Sun sync LEO: Radiometric calibration: Atmospheric Correction: AC validation: Geolocation: Pointing strategy to minimize sun glint: Avoid terrestrial hot spot: Ground processing: Seasonal latency:
How do changes in human uses of ecosystems affect their vulnerability to disturbance and extreme events? [DS 196]	Measure status of ecosystems globally and relation to disturbances and major events at the seasonal to multiyear time scale.	Measure spectral signature in the VSWIR region at high precision and accuracy. -Sufficient precision and accuracy for spectral mixture algorithms to give insight to subpixel events. -Measure species-type and functional type using full spectrum. -Measure PV, NPV, and Soil using full VSWIR and SWIR algorithms. Measure globally at spatial resolution patch scale relevant for ecosystem 10 <sup>4</sup> to 10 <sup>6</sup> m <sup>2</sup> . Measure temporally to have high probability to achieve seasonal measurements.	Spectral measurement from 400 to 2500 nm at 10 nm (terrestrial): > 95% Spectral cal uniformity: SNR 600 VNIR, 300 SWIR (23.52A 0.25R): 1-bit precision: >95% abs cal: > 98% on-orbit stability; no saturation of ecosystem targets: <2% polarization sensitivity 380 to 700 nm: >99% linearity 2 to 98% saturation: <60 m spatial sampling: >95% Spectral IFOV uniformity: <20 day revisit to minimize cloud obscuration:	Surface reflectance in the solar reflected spectrum for elevation angles >20: Rigorous cal/val program: Monthly lunar calis: Daily solar calis: 6 per year vcalis: ~700-mbs downlink: >3X zero loss compression: ~11 a.m. Sun sync LEO: Radiometric calibration: Atmospheric Correction: AC validation: Geolocation: Pointing strategy to minimize sun glint: Avoid terrestrial hot spot: Ground processing: Seasonal latency:

VQ4

2008 HYSPIRI WHITEPAPER AND SCIENCE WORKSHOP REPORT

Science Objectives	Measurement Objectives	Measurement Requirements	Instrument Requirements	Other Mission and Measurement Requirements
<b>VQ5. Ecosystem and Human Health: How do changes in ecosystem composition and function affect human health, resource use, and resource management?</b>				
How do changes in ecosystem composition and function affect the spread of infectious diseases and the organisms that transmit them [DS155, 160, 161] for example, tracking malaria by water fraction, Hantavirus?	Measure the ecosystem composition and function globally at the seasonal and multiyear timescale. Relate these to measures of infectious diseases and organisms that transmit them. Understand the impact of climate change on the disease vectors environments and interaction with human settlement changes	Measures species/functional type and function through the VSWIR spectral signature acquired at high precision and accuracy. Measure globally at spatial resolution patch scale relevant for ecosystem 10 <sup>4</sup> to 10 <sup>6</sup> m <sup>2</sup> . Measure temporally to have high probability to achieve seasonal measurements.	Spectral measurement from 400 to 2500 nm at 10 nm (terrestrial): 380 to 900 nm at 10 nm with additional SWIR for AC (coastal aquatic): > 95% Spectral cal uniformity: SNR 600 VNIR, 300 SWIR (23.5ZA 0.25R): 14 bit precision: >95% abs cal: > 98% on-orbit stability: no saturation of ecosystem targets: <2% polarization sensitivity 380 to 700 nm: >99% linearity 2 to 98% saturation: <= 60 sampling: >95% Spectral IFOV uniformity: <20 day revisit to minimize cloud obscuration:	Surface reflectance in the solar reflected spectrum for elevation angles >20: Rigorous cal/val program: Monthly lunar cal: Daily solar cal: 6 per year vcal: ~700-mbs downlink: >3X zero loss compression: ~11 a.m. Sun sync LEO orbit: Radiometric calibration: Atmospheric Correction: AC validation: Geolocation: Pointing strategy to minimize sun glint: Avoid terrestrial hot spot: Ground processing: Seasonal latency:
How will changes in pollution and biogeochemical cycling alter water quality?	Measure biogeochemical, pollution, and water quality indicators globally at the seasonal and multiyear time scale.	Measure vegetation biogeochemical signatures in the VSWIR spectral signature acquired at high precision and accuracy. Measure water quality and pollution indicators in the visible portion of the spectrum. Measure globally at spatial resolution patch scale relevant for ecosystem 10 <sup>4</sup> to 10 <sup>6</sup> m <sup>2</sup> . Measure temporally to have high probability to achieve seasonal measurements. Measure turbidity and water clarity, algal and cyanobacterial growth. Measure size and health (biodiversity) of wetlands	Spectral measurement from 400 to 2500 nm at 10 nm (terrestrial): 380 to 900 nm at 10 nm with additional SWIR for AC (coastal aquatic): > 95% Spectral cal uniformity: SNR 600 VNIR, 300 SWIR (23.5ZA 0.25R): 14 bit precision: >95% abs cal: > 98% on-orbit stability: no saturation of ecosystem targets: <2% polarization sensitivity 380 to 700 nm: >99% linearity 2 to 98% saturation: <= 60 sampling: >95% Spectral IFOV uniformity: <20 day revisit to minimize cloud obscuration:	Surface reflectance in the solar reflected spectrum for elevation angles >20: Rigorous cal/val program: Monthly lunar cal: Daily solar cal: 6 per year vcal: ~700-mbs downlink: >3X zero loss compression: ~11 a.m. Sun sync LEO orbit: Radiometric calibration: Atmospheric Correction: AC validation: Geolocation: Pointing strategy to minimize sun glint: Avoid terrestrial hot spot: Ground processing: Seasonal latency:
How are changes in ecosystem distribution and productivity linked to resource use, and resource management such as forestry management, fire effects, biofuels, and agricultural management?	Measure ecosystem composition, productivity and distribution globally at the seasonal and multiyear time scale. Relate these to measures of resource use and management. Map the function types (communities) of the forestry resources, biofuel (corn, sugar cane, etc.) regionally and locally.	Measure vegetation composition, function and production in the VSWIR spectral signature acquired at high precision and accuracy. Measure globally at spatial resolution patch scale relevant for ecosystem 10 <sup>4</sup> to 10 <sup>6</sup> m <sup>2</sup> . Measure temporally to have high probability to achieve seasonal measurements. Measure seasonal changes in productivity	Spectral measurement from 400 to 2500 nm at 10 nm (terrestrial): 380 to 900 nm at 10 nm with additional SWIR for AC (coastal aquatic): > 95% Spectral cal uniformity: SNR 600 VNIR, 300 SWIR (23.5ZA 0.25R): 14 bit precision: >95% abs cal: > 98% on-orbit stability: no saturation of ecosystem targets: <2% polarization sensitivity 380 to 700 nm: >99% linearity 2 to 98% saturation: <= 60 sampling: >95% Spectral IFOV uniformity: <20 day revisit to minimize cloud obscuration: vnr -swir spectra required, polarization requirement may be looser for this application.	Surface reflectance in the solar reflected spectrum for elevation angles >20: Rigorous cal/val program: Monthly lunar cal: Daily solar cal: 6 per year vcal: ~700-mbs downlink: >3X zero loss compression: ~11 a.m. Sun sync LEO orbit: Radiometric calibration: Atmospheric Correction: AC validation: Geolocation: Pointing strategy to minimize sun glint: Avoid terrestrial hot spot: Ground processing: Seasonal latency: validation ground test sites related to the resources to be managed
How will changes in climate and pollution affect the health and productivity of aquatic and agricultural resources?	Measure aquatic and agricultural resource systems globally and through the seasonal and multiyear time frame. Relate these to measures of climate and pollution to detect trends and make predictions.	Measure the composition and productivity of agricultural and aquatic resource ecosystems using the VSWIR spectral signature acquired at high precision and accuracy. Measure globally at spatial resolution patch scale relevant for ecosystem 10 <sup>4</sup> to 10 <sup>6</sup> m <sup>2</sup> . Measure temporally to have high probability to achieve seasonal measurements. Measure surface spectral reflectivity and water spectral absorption sufficient to get at water turbidity for example	Spectral measurement from 400 to 2500 nm at 10 nm (terrestrial): 380 to 900 nm at 10 nm with additional SWIR for AC (coastal aquatic): > 95% Spectral cal uniformity: SNR 600 VNIR, 300 SWIR (23.5ZA 0.25R): 14 bit precision: >95% abs cal: > 98% on-orbit stability: no saturation of ecosystem targets: <2% polarization sensitivity 380 to 700 nm: >99% linearity 2 to 98% saturation: <= 60 sampling: >95% Spectral IFOV uniformity: <20 day revisit to minimize cloud obscuration:	Surface reflectance in the solar reflected spectrum for elevation angles >20: Rigorous cal/val program: Monthly lunar cal: Daily solar cal: 6 per year vcal: ~700-mbs downlink: >3X zero loss compression: ~11 a.m. Sun sync LEO orbit: Radiometric calibration: Atmospheric Correction: AC validation: Geolocation: Pointing strategy to minimize sun glint: Avoid terrestrial hot spot: Ground processing: Seasonal latency:
What are the economic and human health consequences associated with the spread of invasive species?	Measure the global distribution and seasonal variation of invasive species from one to several years. Relate this to economic and human health factors to support both direct assessment and future trend prediction. Distinguish the invasive species from the natural species	Measure the distribution of invasive species using the VSWIR spectral signature acquired at high precision and accuracy. Measure globally at spatial resolution patch scale relevant for ecosystem 10 <sup>4</sup> to 10 <sup>6</sup> m <sup>2</sup> . Measure temporally to have high probability to achieve seasonal measurements. Observe over the growing season with enough temporal resolution to catch the growth cycle points where the likelihood of distinction is maximized.	Spectral measurement from 400 to 2500 nm at 10 nm (terrestrial): 380 to 900 nm at 10 nm with additional SWIR for AC (coastal aquatic): > 95% Spectral cal uniformity: SNR 600 VNIR, 300 SWIR (23.5ZA 0.25R): 14 bit precision: >95% abs cal: > 98% on-orbit stability: no saturation of ecosystem targets: <2% polarization sensitivity 380 to 700 nm: >99% linearity 2 to 98% saturation: <= 60 sampling: >95% Spectral IFOV uniformity: <20 day revisit to minimize cloud obscuration:	Surface reflectance in the solar reflected spectrum for elevation angles >20: Rigorous cal/val program: Monthly lunar cal: Daily solar cal: 6 per year vcal: ~700-mbs downlink: >3X zero loss compression: ~11 a.m. Sun sync LEO orbit: Radiometric calibration: Atmospheric Correction: AC validation: Geolocation: Pointing strategy to minimize sun glint: Avoid terrestrial hot spot: Ground processing: Seasonal latency. Knowledge of local situation vis-à-vis active invasive species of import. Local spectral databases of natural and invasive species.
How does the spatial pattern of policy, environmental management, and economic conditions correlate with the state and changes in ecosystem function and composition? (DS 155 [5-5?], 230 [8-7])	Measure ecosystem composition, function, and distribution globally and seasonal and multiyear time scale. Relate this to the spatial pattern of environmental management and economic conditions for direct assessment and future prognostication.	Measure ecosystem vegetation composition, function and distribution using the VSWIR spectral signature acquired at high precision and accuracy. Measure globally at spatial resolution patch scale relevant for ecosystem 10 <sup>4</sup> to 10 <sup>6</sup> m <sup>2</sup> . Measure temporally to have high probability to achieve seasonal measurements.	Spectral measurement from 400 to 2500 nm at 10 nm (terrestrial): 380 to 900 nm at 10 nm with additional SWIR for AC (coastal aquatic): > 95% Spectral cal uniformity: SNR 600 VNIR, 300 SWIR (23.5ZA 0.25R): 14 bit precision: >95% abs cal: > 98% on-orbit stability: no saturation of ecosystem targets: <2% polarization sensitivity 380 to 700 nm: >99% linearity 2 to 98% saturation: <= 60 sampling: >95% Spectral IFOV uniformity: <20 day revisit to minimize cloud obscuration:	Surface reflectance in the solar reflected spectrum for elevation angles >20: Rigorous cal/val program: Monthly lunar cal: Daily solar cal: 6 per year vcal: ~700-mbs downlink: >3X zero loss compression: ~11 a.m. Sun sync LEO orbit: Radiometric calibration: Atmospheric Correction: AC validation: Geolocation: Pointing strategy to minimize sun glint: Avoid terrestrial hot spot: Ground processing: Seasonal latency:
What are the impacts of flooding and sea-level rise on ecosystems, human health, and security? [DS 195, 224, 227, 348, 357]	Measure ecosystem composition, function and distribution in the coastal regions globally at the seasonal and multiyear timescale. Relate these measurements to the status of coastal ecosystem and the human health and security implications.	Measure coastal ecosystem vegetation composition, function and distribution in both the terrestrial and aquatic domains using the VSWIR spectral signature acquired at high precision and accuracy. Measure globally at spatial resolution patch scale relevant for ecosystem 10 <sup>4</sup> to 10 <sup>6</sup> m <sup>2</sup> . Measure temporally to have high probability to achieve seasonal measurements. Surface reflectance over the vis-swir, and water spectral absorption over the visible spectrum	Spectral measurement from 400 to 2500 nm at 10 nm (terrestrial): 380 to 900 nm at 10 nm with additional SWIR for AC (coastal aquatic): > 95% Spectral cal uniformity: SNR 600 VNIR, 300 SWIR (23.5ZA 0.25R): 14 bit precision: >95% abs cal: > 98% on-orbit stability: no saturation of ecosystem targets: <2% polarization sensitivity 380 to 700 nm: >99% linearity 2 to 98% saturation: <= 60 sampling: >95% Spectral IFOV uniformity: <20 day revisit to minimize cloud obscuration:	Surface reflectance in the solar reflected spectrum for elevation angles >20: Rigorous cal/val program: Monthly lunar cal: Daily solar cal: 6 per year vcal: ~700-mbs downlink: >3X zero loss compression: ~11 a.m. Sun sync LEO orbit: Radiometric calibration: Atmospheric Correction: AC validation: Geolocation: Pointing strategy to minimize sun glint: Avoid terrestrial hot spot: Ground processing: Seasonal latency:

VQ5

Science Objectives	Measurement Objectives	Measurement Requirements	Instrument Requirements	Other Mission and Measurement Requirements
<b>VQ6. Earth Surface and Coastal Benthic Composition: What is the land surface soil/rock and shallow coastal benthic compositions?</b>				
What is the distribution of the primary minerals and mineral groups on the exposed terrestrial surface? [DS 218]	Measure the exposed surface rock and soil compositions globally. Measure the available rock forming and alteration minerals and subtle changes in composition via spectral absorption position and shape. Derive fractional abundance through spectral mixture analysis and related approaches.	Spectral signature in the visible to short wavelength infrared to capture the diagnostic absorptions features of clay, iron, carbonate, and other rock/soil forming minerals.	Spectral measurement from 400 to 2500 nm at 10 nm (terrestrial): > 95% Spectral cal uniformity: SNR >600 VNIR, SNR >300 SWIR (23.5ZA 0.25R): 12-bit precision: >95% abs cal: > 98% on-orbit stability: no saturation of ecosystem targets: >99% linearity 2 to 98% saturation: ≤60 sampling: >95% Spectral IFOV uniformity: <90 day revisit to minimize cloud obscuration globally.	Surface reflectance in the solar reflected spectrum for elevation angles >20: Rigorous cal/val program: Monthly lunar calcs: Daily solar calcs: 6 per year vcalcs: ~700-mbs downlink: >3X zero loss compression: ~11 a.m. Sun sync LEO: Radiometric calibration: Atmospheric Correction: AC validation: Geolocation: Ground processing: Seasonal latency:
What is the bottom composition (sand, rock, mud, coral, algae, SAV, etc.) of the shallow-water regions of the Earth?	Measure the composition of the optically available shallow-water bottom regions of the coastal oceans and inland waters.	High precision and accurate spectral signatures in the visible to near infrared to capture the bottom composition interaction with light. Selected wavelengths in the short wavelength infrared to allow atmospheric correction. Measurements at a spatial scale to resolve material patches at <100 m. Temporal measurements high probability of several tides optimized and clear observations.	Spectral measurement from 380 to 900 nm at 10 nm with additional SWIR for AC (coastal aquatic): >95% Spectral cal uniformity: SNR—violet/blue/green: 400:1, yellow/orange/red: 300:1, wavelength >900 nm: ≥100:1; 14-bit digitization: >95% abs cal: > 98% on-orbit stability: no saturation of ecosystem targets: <2% polarization sensitivity 380 to 700 nm: >99% linearity 2 to 98% saturation: ≤60 sampling: >95% Spectral IFOV uniformity: <20 day revisit to minimize cloud obscuration:	Surface reflectance in the solar reflected spectrum for elevation angles >20: Rigorous cal/val program: Monthly lunar calcs: Daily solar calcs: 6 per year vcalcs: ~700-mbs downlink: >3X zero loss compression: ~11 a.m. Sun sync LEO: Radiometric calibration: Atmospheric Correction: AC validation: Geolocation: Pointing strategy to minimize Sun glint: Avoid terrestrial hot spot: Ground processing: Seasonal latency:
What fundamentally new concepts for mineral and hydrocarbon research will arise from uniform and detailed global geochemistry of the exposed rock/soil surface? [DS227]	Measure the exposed surface rock and soil compositions globally. Derive geochemical information. Ion substitution expressed as spectral signature shifts.	Spectral signature in the visible to short wavelength infrared to capture the diagnostic absorptions features of clay, iron, carbonate, and other rock/soil forming minerals. Spectral regions of absorption features that are sensitive to subtle geochemical changes in composition.	Spectral measurement from 400 to 2500 nm at 10 nm (terrestrial): > 95% Spectral cal uniformity: SNR >600 VNIR, SNR >300 SWIR (23.5ZA 0.25R): 12-bit precision: >95% abs cal: > 98% on-orbit stability: no saturation of ecosystem targets: >99% linearity 2 to 98% saturation: ≤60 sampling: >95% Spectral IFOV uniformity: <90 day revisit to minimize cloud obscuration globally.	Surface reflectance in the solar reflected spectrum for elevation angles >20: Rigorous cal/val program: Monthly lunar calcs: Daily solar calcs: 6 per year vcalcs: ~700-mbs downlink: >3X zero loss compression: ~11 a.m. Sun sync LEO: Radiometric calibration: Atmospheric Correction: AC validation: Geolocation: Ground processing: Seasonal latency:
What changes in bottom substrate occur in shallow coastal and inland aquatic environments? [DS 25]	Measure the composition of the optically available shallow-water bottom regions of the coastal oceans and inland waters. Bottom substrate composition of sand, coral, mud, SAV, etc. More detailed specificity as possible with the available signal.	High precision and accurate spectral signatures in the visible to near infrared to capture the bottom composition interaction with light. Selected wavelengths in the short wavelength infrared to allow atmospheric correction. Measurements at a spatial scale to resolve material patches at <100m. Temporal measurements high probability of several tides optimized and clear observations.	Spectral measurement from 380 to 900 nm at 10 nm with additional SWIR for AC (coastal aquatic): >95% Spectral cal uniformity: SNR—violet/blue/green: 400:1, yellow/orange/red: 300:1, wavelength >900 nm: ≥100:1; 14-bit digitization: >95% abs cal: > 98% on-orbit stability: no saturation of ecosystem targets: <2% polarization sensitivity 380 to 700 nm: >99% linearity 2 to 98% saturation: ≤60 sampling: >95% Spectral IFOV uniformity: <20 day revisit to minimize cloud obscuration:	Surface reflectance in the solar reflected spectrum for elevation angles >20: Rigorous cal/val program: Monthly lunar calcs: Daily solar calcs: 6 per year vcalcs: ~700-mbs downlink: >3X zero loss compression: ~11 a.m. Sun sync LEO: Radiometric calibration: Atmospheric Correction: AC validation: Geolocation: Pointing strategy to minimize sun glint: Avoid terrestrial hot spot: Ground processing: Seasonal latency:
Can measurements of rock and soil composition be used to understand and mitigate hazards? [DS 114,227]	Measure the exposed surface rock and soil compositions globally to determine the occurrence of hazard-associated minerals. For example, Acid-generating minerals, Asbestos, etc.	Spectral signature in the visible to short wavelength infrared to capture the diagnostic absorptions features of acid-generating (sulfates), asbestos, minerals.	Spectral measurement from 400 to 2500 nm at 10 nm (terrestrial): > 95% Spectral cal uniformity: SNR >600 VNIR, SNR >300 SWIR (23.5ZA 0.25R): 12-bit precision: >95% abs cal: > 98% on-orbit stability: no saturation of ecosystem targets: >99% linearity 2 to 98% saturation: ≤60 sampling: >95% Spectral IFOV uniformity: <90 day revisit to minimize cloud obscuration globally.	Surface reflectance in the solar reflected spectrum for elevation angles >20: Rigorous cal/val program: Monthly lunar calcs: Daily solar calcs: 6 per year vcalcs: ~700-mbs downlink: >3X zero loss compression: ~11 a.m. Sun sync LEO: Radiometric calibration: Atmospheric Correction: AC validation: Geolocation: Ground processing: Seasonal latency:

VQ6

Science Objectives	Measurement Objectives	Measurement Requirements	Instrument Requirements	Other Mission and Measurement Requirements
<b>TQ1. Volcanoes and Earthquakes: How can we help predict and mitigate earthquake and volcanic hazards through detection of transient thermal phenomena?</b>				
Do volcanoes signal impending eruptions through changes in surface temperature or gas emission rates and are such changes unique to specific types of eruptions? [DS 227]	Detect, quantify, and monitor subtle variations in: 1) surface temperatures; 2) surface emissivity; and 3) sulfur dioxide concentrations at low, non-eruptive, flux background levels. Compilation of long-term baseline data sets.	Temperature measurements in the range -30 to 200°C. TIR radiance measurements at ~8 µm; 5 sufficient other TIR bands for use in SO <sub>2</sub> retrieval algorithm; 7-day repeat.	4 TIR channels, 7.3 µm, 8.5 µm, 2 bands between 9-12 µm Pixel size ≤60 m NEΔT ~0.02 K. 0.2 >95% abs. radiometric calibration	Nighttime data acquisitions.
What do changes in the rate of lava effusion tell us about the maximum lengths that lava flows can attain, and the likely duration of lava flow-forming eruptions? [DS 226]	Area covered by active lava flows; Lava flow surface temperatures; Radiant flux from lava flow surfaces.	Temperature measurements in the range 0 to 1200°C (active lava), and 0-50°C (ambient background). 5 day repeat.	1 low gain channel at ~4 µm (NEΔT ~ 1-2 K). 2 nominal gain channels at 10-12 µm Pixel size ≤90 Rapid bright-target recovery at 4 µm (<2 pixels), bands saturate at 1200°C	Nighttime data acquisitions. NIR/SWIR hyperspectral data is beneficial. Rapid response off-nadir pointing capability. Rapid re-tasking for acquisition of targets of opportunity.
What are the characteristic dispersal patterns and residence times for volcanic ash clouds, and how long do such clouds remain a threat to aviation? [DS 224]	Discrimination of volcanic ash clouds from meteorological clouds (both water and ice), in both wet and dry air masses. Day and night measurements	Four spectral channels at 8.5, 10, 11, and 12 µm; NEΔT of 0.2 K, Max. repeat cycle of 5 days. Temperature measurements in the range -20 to 200°C. Multispectral radiance measurements between 8.5 and 12 µm. NEDT>0.5 K. 5-day repeat	4 channels, 8-14 µm. 50 nm at 8.5, 100 nm other bands Pixel size ≤90 m >95% abs. radiometric calibration	NIR/SWIR hyperspectral data valuable to assist in recognition of meteorological clouds and estimation of plume height. Nighttime data acquisitions to increase the frequency of observation.
What do the transient thermal anomalies that may precede earthquakes tell us about changes in the geophysical properties of the crust? [DS 227, 229]	Detect and monitor increases in TIR surface radiance surface temperatures along potentially active faults.	Temperature measurements in range -25C to 50°C. 5-day repeat (or better); nighttime data	1 band at 8-8.5 µm; 1 band 7.3-8 µm ,1 band >10 µm; pixel size 100 m; NEDT = 0.2 K; nighttime data	
Can the energy released by the periodic recharge of magma chambers be used to predict future eruptions? [DS 227] How can the release of energy at the surface of volcanic edifices be used to understand magma processes at depth and over time?	Detect and monitor temperature changes of volcanic edifices	Temperature measurements in range of -25°C to 1200°C; 5-day repeat	1 low-gain channel at ~4 µm (NEΔT ~ 1-2 K) 2 nominal gain channels at 10-12 µm Pixel size ≤90 m	Nighttime data acquisitions.

TQ1

TQ2. Wildfires: What is the impact of global biomass burning on the terrestrial biosphere and atmosphere, and how is this impact changing over time?				
Science Objectives	Measurement Objectives	Measurement Requirements	Instrument Requirements	Other Mission and Measurement Requirements
How are global fire regimes (fire location, type, frequency, and intensity) changing in response to changing climate and land use practices? [DS 198] (feedbacks?)	Fire monitoring, fire intensity	Detect flaming and smoldering fires as small as ~10 sq. m in size, fire radiative power, fire temperature and area, 4–10 day repeat cycle	Low and normal gain channels at 4 and 11 $\mu\text{m}$ (possible dual gain for 11 $\mu\text{m}$ ). Low-gain saturation at 1400 K and 1100 K, respectively, with 2–3 K NE $\Delta$ T; normal-gain NE $\Delta$ T < 0.2 K. Stable behavior in the event of saturation. 50–100 m spatial resolution. Accurate inter-band coregistration (< 0.25 pixel). Opportunistic use of additional bands in 8–14 $\mu\text{m}$ region.	Daytime and nighttime data acquisition, direct broadcast, and onboard processing, pre-fire and post-fire thematic maps, opportunistic validation. Low Earth Orbit.
Is regional and local fire frequency changing? [DS 196]	Fire detection	Detect smoldering fires as small as ~10 sq. m in size, 4–10 day repeat cycle over the duration of the mission	8–12 $\mu\text{m}$ normal gain. normal-gain NE $\Delta$ T < 0.2 K. Stable behavior in the event of saturation. 50–100 m spatial resolution. Accurate inter-band coregistration (< 0.25 pixel)	Daytime and nighttime data acquisition. Requires an historical context from other sensors with measurement intercalibration, establishes a baseline. Low Earth Orbit. Daytime and nighttime data acquisition (Thermal inertia)
What is the role of fire in global biogeochemical cycling, particularly trace gas emissions? [DS 195]	Fire detection, fire intensity, fire monitoring, burn severity, delineate burned area	Detect flaming and smoldering fires as small as ~10 sq. m in size, fire radiative power, 4–10 day repeat cycle; fire temperature and area.	Low and normal gain channels at 4 and 11 $\mu\text{m}$ (possible dual gain for 11 $\mu\text{m}$ ). Low-gain saturation at 1400 K and 1100 K, respectively, with 2–3 K NE $\Delta$ T; normal-gain NE $\Delta$ T < 0.2 K. Stable behavior in the event of saturation. 50–100 m spatial resolution. Accurate inter-band coregistration (< 0.25 pixel). Opportunistic use of additional bands in 8–14 $\mu\text{m}$ region.	Daytime and nighttime data acquisition, pre-fire vegetation cover, condition and loads for fuel potential. Requires fuel fire modeling element.
Are there regional feedbacks between fire and climate change?	Extent of fire front and confirmation of burn scars	Detect flaming and smoldering fires as small as ~10 sq. m in size, fire radiative power, 4–10 day repeat cycle; fire temperature and area.	Low and normal gain channels at 4 and 11 $\mu\text{m}$ . Low-gain saturation at 1400 K, 1100 K, respectively, with 2–3 K NE $\Delta$ T; normal-gain NE $\Delta$ T < 0.2 K. Stable behavior in the event of saturation. 50–100 m spatial resolution. Accurate inter-band coregistration (< 0.25 pixel).	Daytime and nighttime data acquisition, pre-fire vegetation cover, condition and loads for fuel potential. Requires fuel-fire modeling element.

TQ2

Science Objectives	Measurement Objectives	Measurement Requirements	Instrument Requirements	Other Mission and Measurement Requirements
<b>TQ3. Water Use and Availability: How is consumptive use of global freshwater supplies responding to changes in climate and demand, and what are the implications for sustaining water resources?</b>				
How is climate variability impacting the evaporative component of the global water cycle over natural and managed landscapes? (DS 166, 196, 203, 257, 368; WGA)	Evapotranspiration (surface energy balance) at scales resolving the typical length scales of land-surface moisture heterogeneity	Global coverage of surface radiometric temperature; ~weekly to monthly revisit; resolving land-use components; LST accurate to 1 K; ~10–11 A.M. local overpass	<100-m resolution; 3+ bands in the 8–12 micron region (for atmospheric and emissivity correction); Min/Max T 250/360 K; ~weekly revisit; Maximum view angle 20–30 deg from nadir	Maps of vegetation index; coincident broadband albedo retrievals (from integrated VSWIR or 3 or more wide bands in green, red, nearIR); landuse; insolation data; Landsat-like mid-morning Sun-synchronous overpass. Cloud detection mechanism, (including cirrus); Ancillary meteorological data (varies with process)
How can information about evapotranspiration and its relationship to land-use/land-cover be used to facilitate better management of freshwater resources? (DS 196, 203, 368; WGA)	Evapotranspiration at scales resolving the typical length scales of land surface moisture and vegetation heterogeneity	Global coverage; ~weekly revisit; resolving e.g., field, riparian patches, reservoirs, water rights (agricultural field-sized) polygons; LST accurate to 1 K; ~10-11 A.M. overpass	<100-m resolution; 3+ bands as above; Min/Max T 270/360 K	Maps of vegetation index; land use; insolation data; coincident broadband albedo retrievals; Landsat-like mid-morning sun-synchronous overpass
How can we improve early detection, mitigation, and impact assessment of droughts at local to global scales? (DS 166, 196, 203, 368; WGA)	Moisture stress index at field scales	Global coverage; ~weekly revisit; resolving field-scale (1 ha) patches; LST accurate to 1 K; ~10–11 A.M. overpass	<100-m resolution; 3+ bands as above; Min/Max T 270/360 K	As above; some methods require potential evapotranspiration (based on meteorological data and/or satellite-based insolation); hyperspectral stress signatures will provide supplemental stress info
What is the current global irrigated acreage, how is it changing with time, and are these changes in a sustainable balance with regional water availability? (DS 196, 368)	Robust detection of pixels with water consumption in excess of rainfall	Global coverage; ~weekly to monthly revisit; resolving irrigation patches; ~10–11 A.M. overpass	<100-m resolution; 3+ bands as above; Min/Max T 270/360 K	Detailed land cover classification (can be improved using hyperspectral); vegetation indices; coincident broadband albedo retrievals; regional hydrologic water balances and stores
Can we increase food production in water-scarce agricultural regions while improving or sustaining water available for ecosystem function and other human uses? (DS 196, 368; WGA)	Accurate evapotranspiration at sub-field scales	Global coverage, < weekly revisit, irrigation patches well resolved; LST accurate to 1 K; ~10–11 A.M. overpass	<100-m resolution; 3+ bands as above; Min/Max T 270/360 K	Vegetation indices; accurate local meteorological forcing conditions; coincident broadband albedo retrievals; hyperspectral data may improve partitioning of ET into E & T.
How can improved accuracy in evapotranspiration imaging drive advances in science and understanding of the water cycle and hydrologic processes?	Evapotranspiration at scales resolving the typical length scales of land surface moisture and vegetation heterogeneity and across all climate regimes	Global coverage; ~weekly revisit; resolving e.g., fields, riparian patches, reservoirs; LST accurate to 1 K; ~10-11 A.M. overpass	<100-m resolution; 3+ bands as above; Min/Max T 270/360 K	Vegetation indices; coincident broadband albedo retrievals; hyperspectral data may improve partitioning of ET into E and T. Soil moisture retrievals via microwave will improve description of water flow in soils

TQ3

Science Objectives	Measurement Objectives	Measurement Requirements	Instrument Requirements	Other Mission and Measurement Requirements
<b>TQ4. Urbanization and Human Health: How does urbanization affect the local, regional and global environment? Can we characterize this effect to help mitigate its impact on human health and welfare?</b>				
How do changes in local and regional land cover and land use, in particular urbanization, affect surface energy balance characteristics that impact human welfare? [DS: 160-161, 166-167, 196, 198]	Surface temperature, Surface energy fluxes, Surface emissivity, terrestrial coverage	NEΔT 0.2–0.3 greater than 4 bands distributed between 8 and 12 μm High spatial resolution (≤ 60 m) Accuracy 1.0 K	260–360 K NEdT 0.1 K Acc 0.5 K	High temporal resolution (weekly) Long term validation sites (incl. emissivity targets) and periodic urban campaigns
What are the dynamics, magnitude, and spatial form of the urban heat island effect (UHI); how does it change from city to city; what are its temporal, diurnal, and nocturnal characteristics; and what are the regional impacts of the UHI on biophysical, climatic, and environmental processes? [DS: 158, 166-168]	Day and night surface temperature Urban coverage Intra-seasonal measurements	High spatial resolution (≤ 60 m) Day/night observations Acc 1 K Coregistration 0.2 pix NEdT 0.2–0.3	>4 bands for accurate t-e separation Do we need more bands for cloud masking at night? High spatial resolution (≤ 60 m) NEdT 0.1 Min T/Max T 260-360K for diurnal observations	High temporal resolution (weekly) Accuracy of 1 deg.K/NEΔT 0.2–0.3
How can the factors influencing heat stress on humans be better resolved and measured. [DS: 156, 158, 160, 183–184]	Surface temperature Urban coverage	Acc. 1K Nedt 0.2-0.3K Daytime/nighttime observations Vegetated/non-vegetated surfaces	>4 bands for T-E separation Diurnal and nocturnal observations Low temperature and high temperature targets (NEΔT 0.2-0.3 K) Acc 0.5 K	High temporal resolution (weekly) High spatial resolution (≤ 60 m) Accuracy of 1 deg.K/NEΔT 0.2-0.3 Air temperature
How can the characteristics associated with environmentally related health effects, that affect vector-borne and animal-borne diseases, be better resolved and measured? [DS: 156, 158, 160, 183–184]	Surface temperature Terrestrial coverage	Detection of wet/dry surfaces Daytime/nighttime observations Vegetated/non-vegetated surfaces	Multispectral thermal bands for surface temperature measurements (3–6 bands) Diurnal and nocturnal observations Low temperature and high temperature targets (NEΔT 0.2–0.3 K)	High temporal resolution (weekly) High spatial resolution (≤ 60 m) Accuracy of 1 deg.K/NEΔT 0.2–0.3 Soil moisture or precipitation Air temperature water inundation
How do horizontal and temporal scales of variation in heat flux and mixing relate to human health, human ecosystems, and urbanization? [DS: 156, 160-161, 166-167, 179,184]	Surface temperature Surface energy balance Surface energy fluxes Global coverage	Daytime/nighttime observations Multispectral thermal measurements (3–6 bands) High spatial resolution High temporal resolution	Multiple spectral bands (3–6) for surface temperature and energy balance flux measurements Diurnal and nocturnal observations Low-temperature and high-temperature target discrimination	High-temporal resolution (weekly) High spatial resolution (≤ 60 m) Accuracy of 1 deg.K/NEΔT 0.2–0.3

TQ4

Science Objectives	Measurement Objectives	Measurement Requirements	Instrument Requirements	Other Mission and Measurement Requirements
<b>Earth Surface Composition and Change: What are the composition and thermal properties of the exposed surface of the Earth? How do these factors change over time and affect land use and habitability?</b>				
What is the spectrally observable mineralogy of the Earth's surface, and how does this relate to geochemical and surficial processes? [DS 114]	<i>Mapping spectral emissivity variations associated with mineralogy and rock type in exposed terrains</i>	Variation in silica content and non-silicate <i>minerals</i> based on 8–12 $\mu\text{m}$ band shape. (Spectral emissivities to within 0.5%)	7 bands in 8–12 $\mu\text{m}$ range with NE $\Delta$ T < 0.2 K; spatial resolution < 60 m; temporal repeat quarterly	<i>Geolocation to subpixel accuracy</i> Band to band calibration must be validated, in-flight <i>and radiometric calibration</i>
What is the nature and extent of man-made disturbance of the Earth's surface associated with exploitation of <i>renewable</i> and non-renewable resources? How do these vary over time? [DS 227]	<i>Surface temperature and emissivity variations associated with hydrocarbon and mineral extraction (dumps and pits)</i>	Variation in mineral content based on 8–12 $\mu\text{m}$ band shape including detection of sulfate spectral features. <i>At scale of mining activities.</i>	<i>At least 5 bands in 8–12 <math>\mu\text{m}</math> range with NE<math>\Delta</math>T &lt; 0.2 K; spatial resolution &lt; 60 m; temporal repeat monthly</i>	<i>Geolocation to subpixel accuracy</i> Band to band calibration must be validated, preferably in-flight <i>and radiometric calibration</i>
How do surface temperature anomalies relate to deeper thermal sources, such as <i>hydrothermal systems</i> , buried lava tubes, underground coal fires and engineering structures? How do changes in the surface temperatures relate to changing nature of the deep seated hot source? [DS 243]	Surface temperatures corrected for emissivity variations <i>for temperature anomalies</i>	<i>Measure variations in temperature with high accuracy and precision and spatial resolution</i>	3+ bands in 8-12 $\mu\text{m}$ range with NE $\Delta$ T < 0.2 K; Spatial resolution < 60 m; temporal repeat weekly	Nighttime data necessary to minimize radiant interference due to solar heating
What is the spatial distribution pattern of surface temperatures and emissivities, and how do these influence the Earth's heat budget?	Surface emissivity variations and temperatures of all surficial cover materials	Complex surface emissivity properties based on 8–12 $\mu\text{m}$ band shape	<i>1 band at 3.98 <math>\mu\text{m}</math> and 7 bands in 8–12 <math>\mu\text{m}</math> range with NE<math>\Delta</math>T &lt; 0.2 K; spatial resolution 60–500 m; temporal repeat weekly</i>	Accurate methods of temperature emissivity separation applicable to wide range of materials needed.
What are the water-surface temperature <i>distributions</i> in coastal, ocean, and <i>inland water bodies</i> how do they change; and how do they influence <i>aquatic ecosystems</i> ? [DS 378]	Spatial and temporal variation in <i>surface temperatures</i>	<i>Measure variations in temperature with high accuracy (&lt;0.5 K) and precision and good to moderate spatial resolution</i>	<i>1 band at 3.98 <math>\mu\text{m}</math> and 3+ bands in 8-12 <math>\mu\text{m}</math> range with NE<math>\Delta</math>T &lt; 0.2 K; Spatial resolution 50 to 100 m; temporal repeat weekly</i>	Day and night measurements preferable

TQ5